2017

ROLE OF INTRACELLULAR GROWTH DURING THE GASTROINTESTINAL STAGE OF *LISTERIA MONOCYTOGENES* INFECTION

Grant Steven Jones

University of Kentucky, grantjones@uky.edu

Author ORCID Identifier:

https://orcid.org/0000-0001-7945-8038

Digital Object Identifier: https://doi.org/10.13023/ETD.2017.242

STUDENT AGREEMENT:

I represent that my thesis or dissertation and abstract are my original work. Proper attribution has been given to all outside sources. I understand that I am solely responsible for obtaining any needed copyright permissions. I have obtained needed written permission statement(s) from the owner(s) of each third-party copyrighted matter to be included in my work, allowing electronic distribution (if such use is not permitted by the fair use doctrine) which will be submitted to UKnowledge as Additional File.

I hereby grant to The University of Kentucky and its agents the irrevocable, non-exclusive, and royalty-free license to archive and make accessible my work in whole or in part in all forms of media, now or hereafter known. I agree that the document mentioned above may be made available immediately for worldwide access unless an embargo applies.

I retain all other ownership rights to the copyright of my work. I also retain the right to use in future works (such as articles or books) all or part of my work. I understand that I am free to register the copyright to my work.

REVIEW, APPROVAL AND ACCEPTANCE

The document mentioned above has been reviewed and accepted by the student's advisor, on behalf of the advisory committee, and by the Director of Graduate Studies (DGS), on behalf of the program; we verify that this is the final, approved version of the student's thesis including all changes required by the advisory committee. The undersigned agree to abide by the statements above.

Grant Steven Jones, Student

Dr. Sarah E.F. D'Orazio, Major Professor

Dr. Ken Fields, Director of Graduate Studies

ROLE OF INTRACELLULAR GROWTH DURING THE GASTROINTESTINAL STAGE OF *LISTERIA MONOCYTOGENES* INFECTION

DISSERTATION

A dissertation submitted in partial fulfillment of
the requirements for the degree of Doctor of Philosophy in the
College of Medicine at the University of Kentucky

By
Grant Steven Jones

Lexington, Kentucky

Director: Dr. Sarah D'Orazio, Associate Professor of

Microbiology, Immunology, and Molecular Genetics

Lexington, Kentucky

2017

ABSTRACT OF DISSERTATION

ROLE OF INTRACELLULAR GROWTH DURING THE GASTROINTESTINAL STAGE OF *LISTERIA MONOCYTOGENES* INFECTION

Listeria monocytogenes is a facultative intracellular bacterium that causes foodborne disease in humans. *L. monocytogenes* invade the gut mucosa and then disseminate, causing systemic infections associated with high mortality rates in immunocompromised individuals. It is unknown how *L. monocytogenes* traffic to the mesenteric lymph nodes, which represent an important bottleneck for systemic spread. In addition, little is known about the gastrointestinal stage of infection due to the general resistance of mice to oral infection with *L. monocytogenes.* Our laboratory developed a novel foodborne mouse model of listeriosis utilizing a murinized strain of *L. monocytogenes* to investigate the gastrointestinal stage of infection. First, we found that the majority of *L. monocytogenes* isolated from the intestinal tissue and MLN were extracellular; however, the minimal fraction of intracellular *L. monocytogenes* was vital for persistence in the gut and spread to the MLN. The vast majority of cell-associated *L. monocytogenes* in the MLN were adhered to inflammatory monocytes, but these cells did not support the intracellular growth of *L. monocytogenes*. A minor proportion of *L. monocytogenes* were associated with migratory dendritic cells in the intestinal lamina propria and MLN, but like monocytes, these cells did not appear to serve as an intracellular growth niche for *L. monocytogenes.* Lastly, extracellular *L. monocytogenes* were observed migrating in mesenteric lymphatic vessels that drain from the intestine to the MLN, suggesting that *L. monocytogenes* can spread beyond the intestinal mucosa independent of migratory immune cells. Overall, these studies are the first to characterize the interaction of *L. monocytogenes* with immune cells in the intestine and MLN following foodborne infection and suggest that extracellular, and not cytosolic *L. monocytogenes*, primarily drive innate immune responses in the gut.

KEYWORDS: *Listeria monocytogenes,* bacteria, foodborne infection, extracellular, monocytes, mesenteric lymph nodes

Grant S. Jones

June 22, 2017

Date

ROLE OF INTRACELLULAR GROWTH
DURING THE GASTROINTESTINAL STAGE OF
LISTERIA MONOCYTOGENES INFECTION

By

Grant Steven Jones

Dr. Sarah E.F. D'Orazio
Director of Dissertation

Dr. Ken Fields
Director of Graduate Studies

June 22, 2017
Date

ACKNOWLEDGEMENTS

First, I would like to thank my dissertation advisor Dr. Sarah D'Orazio for her guidance and mentorship that has fostered my independence since first joining the lab. Her patience and willingness to listen has motivated me to be a thoughtful scientist with a passion to seek truth inside and outside of the lab. I am lucky that she was willing to take me on as an undergraduate in her lab even though I practically knew nothing about true research. Her passion for teaching has rubbed off on me, and her trust in allowing me to freely mentor undergraduates in the lab has empowered me and instilled self-confidence. I have gained an invaluable skill set under the mentorship of Dr. D'Orazio that I know has prepared me for a successful future in science.

Next, I would like to thank the members of my dissertation committee including Dr. Sue Straley for her thoughtful discussions and interest in my project that motivated me at the beginning of my graduate career; Dr. Don Cohen for serving as my mentor for my second year seminar and discussions related to phagocytes in the gut; Dr. Jerry Woodward for being the first to teach me about immunology during my first year rotation in his lab; Dr. Becky Dutch for her mentorship during my rotation in her lab and thoughtful suggestions in committee meetings; and Dr. Ken Fields for his willingness to join my committee after the retirement of Dr. Straley. I would also like to thank Dr. David Feola for agreeing to be my outside examiner and teaching my wife in pharmacy school.

I would also like to express my gratitude towards other members of the department who I have closely worked with during organization of the departmental retreat including Ms. Kate Fresca for her encouragement and always having my back; Dr. Beth Garvy, our department chair, for her advice and support throughout my graduate career; and Dr. Joe McGillis for his kindness and willingness to listen to my honest opinions.

I have been fortunate to have worked with members of the D'Orazio lab that have contributed in one way or another to my project as well as making every day at work more enjoyable. These past and present members include Pooja Patil, Achmad Hidayatullah, Hilary Denney, and Travis Combs. I would like to especially thank the follow members specifically: Elsa Bou Ghanem, who first taught me general lab techniques and provided me with honest advice; Tanya Myers-Morales for her assistance with anything and everything in the lab as well as teaching me cloning; Michelle Pitts, for willingness to provide an extra set of hands whenever; and Jakob Schardt, for his willingness to come work in the lab as a visiting scholar and being such fun to work with every day. I would also like to thank Kate Bussell who directly contributed to the studies in this dissertation by generating the data presented in Figures 3.5 and 3.6, as well as Victoria Smith for technical assistance with the data shown in chapter 5.

I would also like to thank other members of the department that have directly contributed to my studies including Jennifer Strange and Greg Bauman for sharing their flow cytometry expertise and providing technical assistance, and members of the Bondada lab including Sara Alhakeem, Katie McKenna, and Karine Oben for their generous sharing of lab equipment, ideas, and technical assistance.

Lastly, I would like to thank my parents, Dave and Deena Jones, for supporting my love for science by answering my endless and persistent "why" and "what if" questions throughout my childhood. Most importantly, I have to thank my wife, Alexis, for her support that primarily encouraged me to attend graduate school to pursue science as a career.

TABLE OF CONTENTS

LIST OF TABLES

LIST OF FIGURES

Chapter 1: Introduction

I. Listeriosis

A. Saprophytic bacterium

Listeria monocytogenes (*L. monocytogenes* or *Lm*) are Gram-positive bacteria that are ubiquitous in the environment and thrive on decaying plant matter (Freitag et al., 2009; Welshimer and Donker-Voet, 1971). *L. monocytogenes* have been isolated from farm animals, soil, stagnant water, and sewage (Vivant et al., 2013). This leads to the contamination of a wide variety of foods such as raw fruits and vegetables, soft cheeses made with unpasteurized milk, cold-smoked seafood, and processed prepackaged meats (Farber and Peterkin, 1991). Pre-harvest foods are thought to be primarily contaminated by the use of *L. monocytogenes*-contaminated water (Strawn et al., 2013; Watkins and Sleath, 1981; Weller et al., 2015). *L. monocytogenes* can adhere to a variety of surfaces used in food processing equipment and form biofilms which are resistant to common sanitizers (Mullapudi et al., 2008; Renier et al., 2011; Somers and Wong, 2004). *L. monocytogenes* can tolerate and grow in a combination of stresses commonly used for food preservation such as high salts and cold temperatures, largely due to the expression of stress response genes under control of the alternative sigma factor, sigma B (σ^B) (NicAogain and O'Byrne, 2016; Sue et al., 2004; van der Veen et al., 2008). In fact, *L. monocytogenes* are capable of growing at refrigeration temperature over long periods of time, which may induce sub-lethal damage (Dykes and Withers, 1999). This poses a considerable health risk if *L. monocytogenes* remain undetected on food products that are later consumed without being heated (Dykes and Withers, 1999). Consequently, the USDA-FSIS has a “zero tolerance” policy for any number of *L. monocytogenes* found in processed, “ready-to-eat” foods due to the risk of bacterial growth during food storage.

B. Foodborne disease

1. Gastroenteritis

L. monocytogenes is occasionally consumed by healthy individuals without causing disease and was found in ~1% of fecal samples collected over the course of a year (Grif et al., 2003; MacGowan et al., 1994). For example, a study following three healthy Austrian volunteers found that *L. monocytogenes* could be recovered from stool samples five to nine times throughout the year per person, none of which were associated with any gastrointestinal symptoms (Grif et al., 2003). The acquisition of foodborne listeriosis is likely dependent on the amount of *L. monocytogenes* ingested and susceptibility in terms of immune competence. When gastroenteritis does occur, the incubation period varies after the consumption of contaminated food. An analysis of 37 documented cases of human listeriosis from 1988 to 2012 resulted in a median incubation period of 24 hours for gastroenteritis cases (Goulet et al., 2013). Foodborne disease can range from self-limiting to severe gastroenteritis due to the ability of *L. monocytogenes* to cross the intestinal barrier. Gastrointestinal symptoms such as diarrhea typically last 1-3 days, but may last up to a week (Ooi and Lorber, 2005). Fever and fatigue commonly accompany gastrointestinal symptoms; however, relatively few of these patients (2-19%) require hospitalization during foodborne outbreaks (Aureli et al., 2000; Dalton et al., 1997).

2. Invasive infections

Life-threatening systemic infections can occur when *L. monocytogenes* disseminate beyond the gastrointestinal tract and cause systemic infection. Interestingly, the incubation period for invasive cases of listeriosis can be somewhat delayed relative to gastrointestinal symptoms. For example, central nervous system involvement and pregnancy-associated cases were 9 days and 27.5 days, respectively (Goulet et al., 2013). Central nervous system infections primarily manifest as meningoencephalitis or septicemia in populations such as the elderly and patients receiving immunosuppressive agents (Allerberger and Wagner, 2010). The case-fatality rate from 2009-2011 was 24% for patients ≥65 years old (CDC, 2013). Rhombencephalitis is a relatively rare form of invasive listeriosis that mainly affects healthy individuals and can cause permanent neurological sequelae with an estimated overall mortality rate of 51% (Allerberger and

Wagner, 2010; Armstrong and Fung, 1993; Kayaaslan et al., 2009; Zapata et al., 2009). In addition to the blood-brain barrier, *L. monocytogenes* are capable of crossing the fetoplacental barrier and therefore pose risk to the mother and fetus in perinatal cases. Pregnancy-associated cases had a 21% rate of neonatal death or fetal loss from 2009-2011 (CDC, 2013).

3. Incidence

In the United States, there were 24 confirmed listeriosis outbreaks from 1998-2008 which resulted in 359 illnesses, 215 hospitalizations, and 38 deaths (Cartwright et al., 2013). In 2011, the second deadliest listeriosis outbreak in U.S. history occurred, which resulted in a total of 147 illnesses, 33 deaths, and 1 miscarriage due to the consumption of contaminated cantaloupes (CDC, 2012). There are ~1600 documented *L. monocytogenes* infections and ~260 deaths annually, which makes *L. monocytogenes* the third leading cause of death among common foodborne pathogens (CDC, 2013; Scallan et al., 2011).

II. Facultative intracellular pathogen

In this section, I will outline the bacterial factors shown to be involved in intracellular infection *in vitro*. Later, I will discuss the role of these factors during the gastrointestinal stage of infection.

A. Regulation of virulence

The ability of *L. monocytogenes* to switch from an extracellular life cycle in the environment to an intracellular pathogen is facilitated by the expression of genes under the control of the alternative sigma factor, σ^B and the positive regulatory factor A protein, PrfA. Transcription of the σ^B promoter is induced by general environmental stresses such as osmotic shock, heat shock, entry into stationary phase, or growth at cold temperatures (Becker et al., 1998; Becker et al., 2000; Wiedmann et al., 1998). σ^B expression is induced in the gastrointestinal tract and is thought to be important for survival via osmoregulation and bile acid resistance (Sue et al., 2004; Toledo-Arana et al., 2009; Wiedmann et al., 1998). Lastly, σ^B positively regulates *prfA* expression, which

is thought of as the global regulator of *L. monocytogenes* virulence genes (Nadon et al., 2002).

The *Listeria* pathogenicity island 1 (LIP-1) contains six genes that support the intracellular life cycle of *L. monocytogenes* including the pore-forming toxin listeriolysin O (*hly)*, phospholipases (*plcA* and *plcB*), metalloprotease, actin assembly-inducing protein (*actA*), and *prfA*, which auto-regulates the PrfA gene cluster in a positive manner (Chakraborty et al., 1992; de las Heras et al., 2011). In addition, PrfA regulates the expression of genes important during mammalian infection including internalins (*inlA* and *inlB*) that trigger the invasion of non-phagocytic cells, as well as a hexose phosphate transporter important for intracellular growth (Chico-Calero et al., 2002; Lingnau et al., 1995; Toledo-Arana et al., 2009). Translation of the PrfA regulon is partially controlled by an RNA thermosensor that obscures translation at ≤30°C due to an RNA hairpin, which is destabilized at 37°C, thus allowing PrfA-dependent genes to be expressed (Johansson et al., 2002). In addition, glutathione is a recently identified co-factor required for the transcriptional activation of PrfA (Reniere et al., 2015).

B. Adherence

Approximately 5% of the wild type *L. monocytogenes* genome encodes surface proteins responsible for adherence and invasion of mammalian cells, while nearly a quarter of these genes are absent from *L. innocua*, which lacks LIP-1 and is considered nonpathogenic (Cabanes et al., 2002). Modification of the Gram-positive cell wall components and the expression of adhesins mediate attachment to host cells and promote overall virulence. Adherence to the intestinal wall and subsequent invasion of the intestinal mucosa are important for establishing intestinal infection. *L. monocytogenes* express multiple membrane-anchored adhesins that mediate attachment to epithelial cells including *Ami*, an autolytic amidase, (Milohanic et al., 2001; Milohanic et al., 2000), as well as another autolysin, IspC, (Wang and Lin, 2007). *Listeria* adhesion protein B (LapB) is a LPTXG surface protein positively regulated by PrfA (Reis et al., 2010). Although the host-cell receptor for LapB is unknown, expression of LapB was important for invasion of Caco-2 cells and was crucial for colonization of the spleen and liver after either intravenous or oral infection of mice (Reis et al., 2010). Fibronectin-binding protein A (FbpA) is exposed on the surface of *L. monocytogenes* and contributes to overall virulence by promoting colonization of the intestine and liver following oral infection (Dramsi et al., 2004). Lastly, *L. monocytogenes* express *Listeria* adhesion

protein (LAP), which binds human heat shock protein 60, and was shown to mediate adhesion to epithelial cells (Wampler et al., 2004). LAP is proposed to mediate translocation across the intestinal epithelium and will be discussed later in the context of intestinal infection (Burkholder and Bhunia, 2010).

C. Cell Invasion

1. Phagocytosis

L. monocytogenes can invade mammalian cells after being taken up by professional phagocytes such as monocytes, macrophages, dendritic cells, and granulocytes. Opsonization enhances, but is not required for *L. monocytogenes* uptake, which is attributed primarily to the deposition of C1q and C3b complement components on the surface of the bacteria (Alvarez-Dominguez et al., 1993; Drevets and Campbell, 1991). Likewise, expression of complement receptor type 3 mediates the internalization and killing of *L. monocytogenes* by inflammatory peritoneal macrophages (Drevets and Campbell, 1991; Drevets et al., 1993). Other surface receptors expressed by macrophage-like cells that are associated with the uptake of *L. monocytogenes* including scavenger receptors type A (SRA) and FcγR1 (CD64). SRA are correlated with protection against *L. monocytogenes* by enhancing the ability of macrophages to limit the escape of *L. monocytogenes* from the phagocytic vacuole (Ishiguro et al., 2001). Whereas, CD64 expression was associated with the invasion of *L. monocytogenes* through an unknown mechanism that was IgG-independent (Perelman et al., 2016). The expression of CD64 did not affect the internalization of *L. innocua*, and was only associated with *L. monocytogenes* uptake via the interaction with human or rabbit CD64, and not mouse or sheep, suggesting a specific ligand is expressed by *L. monocytogenes* with a host tropism (Perelman et al., 2016).

2. Internalin-mediated endocytosis

The invasion of non-phagocytic cells is thought to be mediated primarily by the expression of *L. monocytogenes* surface proteins known as internalins, which promote a “zipper-like” mechanism of internalization after binding host ligands. Twenty-seven internalin family members have been identified in *L. monocytogenes*, all of which contain tandem leucine-rich repeats and most are covalently anchored in cell wall peptidoglycan

via a LPXTG motif (Pizarro-Cerda et al., 2012). Internalin A (InlA) and InlB were the first two internalin family members identified to promote the invasion of mammalian cells.

Internalin A (InlA) independently promotes the adhesion and internalization of *L. monocytogenes* into intestinal epithelial cells (Gaillard et al., 1991; Lecuit et al., 1997). Hence, it is considered one of the mechanisms used by *L. monocytogenes* to cross the intestinal barrier. InlA interacts with the transmembrane adhesion protein, E-cadherin, which is expressed on the basolateral surface of enterocytes (Mengaud et al., 1996). Pentecost *et al.* showed that E-cadherin is accessible to luminal *L. monocytogenes* during the extrusion of senescent epithelial cells located at the tips of intestinal villi and also near goblet cells (Nikitas et al., 2011; Pentecost et al., 2006). The clustering of InlA bound to E-cadherin promotes a series of signaling cascades involving clathrin-associated endocytic machinery that eventually recruits the Arp2/3 complex and actin cytoskeletal polymerization, resulting in bacterial internalization (Pizarro-Cerda et al., 2012). In addition to promoting invasion of the intestinal epithelium, InlA has been shown to be important for crossing the fetoplacental barrier (Disson et al., 2008), as well as dissemination from the gut to the mesenteric lymph nodes and systemic organs (Bergmann et al., 2013; Bou Ghanem et al., 2012).

In contrast to the LPXTG motif of InlA and most other internalins, the carboxy-terminal region of InlB consists of dipeptide Gly-Trp modules that non-covalently anchor it to lipoteichoic acids in the *L. monocytogenes* cell wall (Pizarro-Cerda et al., 2012). Surface-bound InlB interacts with its host-cell receptor, c-Met (hepatocyte growth factor receptor), and promotes the invasion of non-professional phagocytes as well as membrane ruffling (Gaillard et al., 1991; Shen et al., 2000). Binding of InlB with c-Met promotes actin cytoskeletal rearrangements eventually resulting in *L. monocytogenes* internalization, but unlike InlA-mediated invasion, recruitment of PI 3-kinase and the actin depolymerizing factor, cofilin, are also important during InlB-mediated internalization (Seveau et al., 2007). Due to its non-covalent anchorage in the cell wall, soluble InlB can be released into the extracellular environment via heparin, allowing it to interact with gC1q-R and glycosaminoglycans, which enhance internalization of *L. monocytogenes* (Braun et al., 2000; Jonquieres et al., 2001). In addition to cytoskeletal rearrangements, InlB induces signaling pathways such as PLCγ and NF-κB that promote growth and survival, which are thought to promote cell survival following bacterial invasion (Bierne and Cossart, 2002). InlB is thought to promote internalization into hepatocytes and endothelial cells (Braun et al., 1998; Dramsi et al., 1995). Furthermore,

InlB is thought to be involved in crossing the blood-brain barrier, as the invasion of human brain microvascular endothelial cells has been shown to be InlB-dependent. Lastly, InlB may synergize with InlA to promote transcytosis across the fetoplacental barrier as well as the intestinal epithelium, which is thought to be due to accelerating the rate of bacterial internalization (Pentecost et al., 2010).

3. Other routes of invasion

L. monocytogenes express multiple other proteins that are associated with cell invasion including virulence protein (Vip), listeriolysin O (LLO), and ActA, the latter two of which were first identified as virulence factors involved in the intracellular life cycle of *L. monocytogenes* (discussed below). Similar to InlA, Vip is also a LPXTG surface protein positively regulated by PrfA, but is not a member of the internalin family (Cabanes et al., 2005). Vip promotes the invasion of cells that express the endoplasmic reticulum resident chaperone Gp96 at the cell surface and enhances intestinal infection and systemic spread following oral infection of mice (Cabanes et al., 2005). ActA was named for its role of inducing actin polymerization and cell-to-cell spread of *L. monocytogenes*, but it also promotes the invasion of epithelial cell lines through a mechanism that may involve the induction of small pseudopods that engulf *L. monocytogenes* (Suarez et al., 2001). Lastly, the secretion of listeriolysin O (LLO), which is thought to be one of the main mechanisms used by *L. monocytogenes* to escape from the phagocytic vacuole, is also associated with the invasion of hepatocytes (Vadia et al., 2011). Vadia *et al.* showed that LLO-mediated internalization occurred due to actin rearrangements during host cell repair of LLO-induced pore formation (Vadia et al., 2011).

D. Phagosomal escape

To survive intracellularly, facultative intracellular pathogens can either grow in the phagocytic vacuole after inhibiting fusion with the phagolysosome, or escape before acidification of the phagosome. *L. monocytogenes* is able to perform the latter by means of the pore-forming cholesterol-dependent cytolysin, LLO, and two types of phospholipase C. LLO is encoded by *hly* on LIP-1 and early studies showed that deletion of *hly* resulted in *L. monocytogenes* that were trapped in the phagocytic vacuole and were essentially nonvirulent *in vivo* (Gaillard et al., 1986; Geoffroy et al., 1987; Leimeister-Wachter et al., 1990; Mengaud et al., 1987). LLO secretion is upregulated

during intracellular growth and maturation of the phagosome is thought to be required for optimum LLO activity, as LLO has a pH optimum of 5.5 (Geoffroy et al., 1987; Glomski et al., 2002). Three other effectors encoded on LIP-1 mediate escape from the phagocytic vacuole including phosphatidylinositol-specific (PI-PLC) phospholipase (*plcA*) and phosphatidylcholine-specific (PC-PLC) phospholipase (*plcB*) (Marquis et al., 1995; Smith et al., 1995a). Classical activation of macrophages due to LPS, TNF-α, or IFN-γ impairs escape of *L. monocytogenes* from the phagocytic vacuole (Davis et al., 2012; Myers et al., 2003), while neutrophils are bactericidal against *L. monocytogenes* due to the their ability to efficiently degrade LLO via metalloproteinase-8 (Arnett et al., 2014).

E. Cell-to-cell spread

Cytoplasmic motility is a unique strategy developed by intracellular bacterial pathogens including *L. monocytogenes, Shigella flexneri,* multiple *Rickettsia* species, and *Burkholderia pseudomallei* to spread from cell-to-cell without having to leave the intracellular environment (Gouin et al., 2005). After escape from the phagocytic vacuole, cytosolic *L. monocytogenes* become surrounded by an “actin cloud” followed by the formation of an actin “comet tail”, which were first observed in macrophages *in vitro* using electron microscopy (Tilney and Portnoy, 1989). The polar expression of ActA (encoded by *actA* on LIP-1) enables *L. monocytogenes* to polymerize F-actin by mimicking host cell nucleation-promoting factors of the WASP/WAVE family proteins, thereby activating the Arp2/3 complex (Chong et al., 2009; Domann et al., 1992; Kocks et al., 1992; Kocks et al., 1993; Welch et al., 1997). ActA-mediated cell-to-cell spread of *L. monocytogenes* is induced by the protrusion of a “pseudopodal projection” containing *L. monocytogenes* that is engulfed by the neighboring cell (Tilney and Portnoy, 1989). An additional internalin, InlC, is thought to enhance the intercellular spread of *L. monocytogenes* by reducing the surface tension of the host cell plasma membrane (Rajabian et al., 2009). After *L. monocytogenes* is taken up by the neighboring cell, it is found inside a double-membrane vacuole, in which PI-PLC and PC-PLC allow *L. monocytogenes* to escape the inner membrane while LLO mediates escape from the outer membrane to restart the intracellular life cycle of *L. monocytogenes* (Alberti-Segui et al., 2007; Smith et al., 1995a).

III. Gastrointestinal stage of infection

The intracellular life cycle of *L. monocytogenes* has been used as a tool by cell biologists to investigate actin polymerization machinery, endocytic vacuole dynamics, and cell signaling pathways following the interaction of *L. monocytogenes* proteins with host ligands (Hamon et al., 2006). Immunologists have taken advantage of the fact that systemic infection with *L. monocytogenes* induces robust antigen-specific CD8 T cell responses (Pamer, 2004). Thus, most of what is known regarding *L. monocytogenes* pathogenesis and host response to infection is derived from either *in vitro* infection or systemic (i.e., intravenous or intraperitoneal) infection studies in mice. There is relatively little known about the gastrointestinal phase of infection.

A. Infectious dose

The estimated infectious dose of *L. monocytogenes* is 10^6-10^7 CFU in primates and humans (Farber et al., 1996; Smith et al., 2008), but as few as 10^4 organisms could have caused listeriosis in immunocompromised patients in a foodborne outbreak involving contaminated butter (Maijala et al., 2001). Rodents including mice, rats, and guinea pigs are highly resistant to oral infection with *L. monocytogenes*, requiring inocula as high as 10^9-10^{10} CFU to establish intestinal infection (D'Orazio, 2014). The relatively high dose required for mouse infections has been mainly attributed to a species specificity of the *L. monocytogenes* surface protein, InlA, as well as the use of relatively resistant mouse strains.

B. Species specificity

InlA strongly interacts with guinea pig, rabbit, and gerbil E-cadherin, but not with mouse or rat E-cadherin (Lecuit et al., 1999b). In contrast, InlB recognizes mouse, rat, and gerbil c-Met, but not with the rabbit or guinea pig proteins (Khelef et al., 2006). The small size of mice and the extensive catalog of commercial reagents makes them an ideal model organism for studying human disease. To overcome the species barrier of InlA, investigators could either generate mice that express human E-cadherin, or modify the bacterial InlA protein to interact with murine E-cadherin. The Lecuit group generated two different knock-in mice; one that specifically expresses mutagenized E-cadherin in enterocytes of the small intestine (Lecuit et al., 2001), and the other expressing

"humanized" E-cadherin in all cell types (Disson et al., 2008). However, both of these mice have the caveat of being on a relatively resistant strain background (C57BL/6) that is relatively resistant to infection with *L. monocytogenes*. Instead of modifying the host receptor, Wollert *et al.* engineered wild type *L. monocytogenes* InlA to have a higher affinity for mouse E-cadherin by creating two specific amino acid substitutions, termed $InlA^m$ (Wollert et al., 2007). This modified $InlA^m$ protein has a similar affinity for mouse E-cadherin that InlA has for human E-cadherin (Wollert et al., 2007).

C. Foodborne infection of mice

Our group developed a natural feeding model of listeriosis in mice utilizing the mouse-adapted $InlA^m$-expressing *L. monocytogenes* strain (Bou Ghanem et al., 2012; Bou Ghanem et al., 2013a; Bou Ghanem et al., 2013b). This model recapitulates human listeriosis by the ingestion of contaminated food, a reproducible delay in spread of *L. monocytogenes* to systemic organs, and late stage spread to the brain (Bou Ghanem et al., 2012). We showed that a relatively lower inoculum (10^8) of *L. monocytogenes* $InlA^m$ elicits a similar course of infection as 10^9 wild type *L. monocytogenes* while avoiding rapid spread and colonization of systemic organs (Bou Ghanem et al., 2012; Jones et al., 2015). This feature of the foodborne model allows us to investigate the mechanisms used by *L. monocytogenes* to cause systemic disease following the consumption of contaminated food, which remains a mystery during human disease.

D. Intestinal infection

1. Survival in the lumen

The survival of foodborne pathogens in the intestinal lumen is crucial for repeated infection of the gut tissue and ability to be shed back into the environment. First, *L. monocytogenes* must survive the acidic environment of the stomach in which 90% of the bacteria were killed within 15 minutes after inoculation of mice (Saklani-Jusforgues et al., 2000). This was supported by a foodborne outbreak in which antacid therapy was associated with the acquisition of listeriosis (Ho et al., 1986). However, the small proportion of bacteria that survive passage through the stomach undergo changes in gene transcription mediated by σ^B, which induce the expression of genes responsible for invasion of enterocytes and acid tolerance (Kim et al., 2004; Sue et al., 2004). *L.*

monocytogenes express three different PrfA and σ^B-dependent systems that promote resistance against bile salts including bile salt hydrolase, bile acid dehydratase, and a bile exclusion factor (Begley et al., 2005; Dussurget et al., 2002; Sleator et al., 2005). Recently, Listeriolysin S, a hemolytic factor secreted by *L. monocytogenes,* was shown to function as a bacteriocin in the gut lumen, thereby enhancing persistence in the lumen by reducing competition with the host microbiota (Quereda et al., 2016).

2. Transcytosis across the gut barrier

In a guinea pig model of listeriosis, it was calculated that ~1 in 10^6 *L. monocytogenes* invade any part of the intestinal villi after oral inoculation (Melton-Witt et al., 2012). There are at least four proposed mechanisms used by *L. monocytogenes* to invade the intestinal barrier. One of the first routes identified was the InlA-mediated invasion of enterocytes after binding E-cadherin, which is most accessible to luminal *L. monocytogenes* near the tips of intestinal villi when apoptotic cells are extruded from the epithelium, or near mucus-secreting goblet cells (Nikitas et al., 2011; Pentecost et al., 2006). Interestingly, InlA-mediated invasion near goblet cells allows *L. monocytogenes* to be released directly into the underlying lamina propria (LP) without escaping the vacuole or having to replicate inside epithelial cells (Nikitas et al., 2011). Instead of directly invading epithelial cells, *L. monocytogenes* may also invade the intestinal epithelium using a paracellular route of entry via the secretion of LAP as evidenced by translocation across Caco-2 monolayers (Burkholder and Bhunia, 2010; Burkholder et al., 2009; Kim and Bhunia, 2013). LAP is upregulated during anaerobic conditions, suggesting its expression plays an important role during infection of the lower gastrointestinal tract (Burkholder et al., 2009).

Uptake of luminal *L. monocytogenes* by specialized phagocytes may also be a mechanism to colonize the intestinal mucosa. Microfold (M) cells are unique phagocytes that continually sample luminal contents and are located within intestinal villi above either isolated lymphoid follicles or aggregated lymphoid follicles known as Peyer's patches (Sansonetti and Phalipon, 1999). Using microscopy approaches, *L. monocytogenes* and other foodborne pathogens have been shown to adhere and invade M cells (Jang et al., 2004; Jensen et al., 1998; Sansonetti and Phalipon, 1999). It is also possible that luminal *L. monocytogenes* are engulfed by tissue-resident mononuclear phagocytes defined by the high expression of fractalkine receptor (CX_3CR1), which

reside in the intestinal lamina propria and have been shown to extend processes into the lumen to sample luminal contents (Niess et al., 2005). However, luminal sampling by transepithelial dendrites has only been observed in the ileum of the small intestine and may not occur in all mouse strains (Vallon-Eberhard et al., 2006). These cells share characteristics of both dendritic cells and macrophages and make up the majority of mononuclear phagocytes in the colon (Bain et al., 2013).

3. Colonization of the intestinal lamina propria

There is increasing evidence that *L. monocytogenes* colonize the large intestine more efficiently than the small intestine. Disson *et al.* found that higher numbers of wild type *L. monocytogenes* could be recovered from the large intestine compared to the small intestine after oral infection of mice that expressed human E-cadherin (Disson et al., 2008). Indeed, we showed that after foodborne infection with mouse-adapted *L. monocytogenes,* the colon harbored approximately 10-fold higher bacterial burdens compared to the ileum, which was reflected in both the lamina propria and epithelium of fractionated tissue (Bou Ghanem et al., 2012). InlA may be more important in invading or crossing the colon epithelium compared to the small intestine. InlA-mediated uptake was shown to occur preferentially near goblet cells (Nikitas et al., 2011), which increase in abundance from the small intestine to the rectum (Specian and Oliver, 1991). Anaerobic conditions (mimicking anoxic conditions in the large intestine) triggered the expression of InlA and InlB using a *L. monocytogenes* mutant forced to use anaerobic respiration even in the presence of oxygen (Stritzker et al., 2004; Stritzker et al., 2005). In addition, anaerobic growth of *L. monocytogenes* enhanced the secretion of LAP and promoted adherence to intestinal epithelial cells (Burkholder et al., 2009). Lastly, we showed that InlA enhanced intracellular persistence of *L. monocytogenes* in the lamina propria of the colon, but not the ileum (Bou Ghanem et al., 2012). This suggests that InlA mediates intestinal colonization by either the invasion or growth in colonic lamina propria cells.

IV. Mononuclear phagocytes

A. Hematopoiesis of myeloid cells

In the bone marrow, hematopoietic stem cells continually self-renew and give rise to a heterogeneous population of multipotent progenitor cells (MPP). Through a series of differentiation events, MPP cells give rise to the common lymphoid progenitor and common myeloid progenitor (CMP) (Seita and Weissman, 2010). The oligopotent CMP give rise to megakaryocyte/erythrocyte progenitors and myeloid granulocyte/macrophage progenitors, the latter of which develop into either granulocyte progenitors or monocyte-macrophage dendritic cell progenitors (MDP) (Cortez-Retamozo et al., 2012; Fogg et al., 2006). Myeloid cells are thought to best support the intracellular growth of *L. monocytogenes*, and therefore, the differentiation of CMP into mature effector cells *in vivo* and *in vitro* is outlined below. The heterogeneity of mononuclear phagocytes combined with the lack of a uniformed nomenclature using a limited number of surface markers makes it difficult to compare cell types described in different studies. Therefore, in lieu of giving a definitive label (*i.e*., DC or macrophage) to a specific cell population described in a particular study, the surface phenotype will be often listed instead.

1. Monocytes and macrophages

MDP can give rise to common monocyte progenitors (cMoP) resident in the bone marrow and spleen, which develop into monocytes and macrophages, as well as monocyte-derived dendritic cells (DC) (Hettinger et al., 2013). In mice and humans, there are two main types of monocytes that circulate in the blood. Murine $Ly6C^{hi}CCR2^{+}CX_3CR1^{lo}$ cells are known as classical monocytes and are derived from cMoP with a steady state half-life of 20 hours in the bloodstream (Geissmann et al., 2003; Yona et al., 2013). Classical monocytes can become $Ly6C^{lo}$ nonclassical monocytes in the bloodstream, cells that have a relatively longer half-life of 2.2 days (Yona et al., 2013). Nonclassical monocytes, also known as patrolling or resident monocytes, are thought to exhibit wound-healing or anti-inflammatory activity when patrolling vascular endothelial cells and atherosclerotic plaques (Thomas et al., 2015). $Ly6C^{hi}$ monocytes are considered inflammatory monocytes because they rapidly egress from the bone marrow during infection and become pro-inflammatory effector cells

resembling classically-activated macrophages in inflamed tissues (Sunderkotter et al., 2004; Zigmond et al., 2012). In the steady state, classic Ly6C^{hi} monocytes constantly replenish CX_3CR1^{hi} tissue-resident mononuclear phagocytes in a macrophage colony-stimulating factor (M-CSF)-dependent manner (Bogunovic et al., 2009). Furthermore, M-CSF is crucial for the development of macrophages and can be used to generate cultured bone marrow-derived macrophages *in vitro* (Cecchini et al., 1994).

2. Dendritic cells

DC can arise from either circulating monocytes or pre-DC, which arise from common dendritic progenitors in the bone marrow (Naik et al., 2007; Onai et al., 2007; Randolph et al., 1999). CD8α^+ and CD8α^- DC differentiate predominantly from myeloid progenitors, but a small fraction of CD8α^+ DC can also arise from common lymphoid progenitors (Manz et al., 2001; Traver et al., 2000). FMS-related tyrosine kinase 3 ligand (FLT3-L) is a key growth factor that promotes the differentiation of committed DC progenitors into conventional DC (cDC) and plasmacytoid DC (pDC) (McKenna et al., 2000; Naik et al., 2007; Onai et al., 2007). Granulocyte macrophage colony-stimulating factor (GM-CSF) also contributes to the development of monocyte-derived DC *in vivo* and *in vitro* (Inaba et al., 1992; Vremec et al., 1997); however, GM-CSF also drives the differentiation of macrophage-like cells and granulocytes.

B. Mononuclear phagocytes in the intestinal LP

1. CX_3CR1^{hi} macrophages

One of the most prominent mononuclear phagocytes is defined by the high expression of CX_3CR1 and is located throughout the subepithelial lamina propria (Bain et al., 2013; Cerovic et al., 2014). CX_3CR1^{hi} cells were described by their unique ability to extend processes into the lumen to sample luminal contents and thus were first labeled as DC (Niess et al., 2005). However, CX_3CR1^{hi} cells are now thought to be macrophages due to their ontogeny (M-CSF-dependent from Ly6C^{hi} monocytes), surface antigen profile (CD64$^+$F4/80$^+$), high phagocytic activity, and morphology (Cerovic et al., 2014). These cells are considered tissue-resident and do not migrate to the draining lymph nodes during the steady state (Schulz et al., 2009). In addition, a subset of CX_3CR1^{hi} macrophages express CD169 and are located near the basement membrane

of the intestinal lamina propria and in the marginal zone of the spleen and lymph nodes (Asano et al., 2015). $CD169^{+}CX_3CR1^{hi}$ macrophages are thought to serve as a barrier near the submucosa at the interface of blood and lymphatic vessels (Asano et al., 2015).

2. Dendritic cell subsets

Intestinal DC can be broadly distinguished from macrophages by the lack of CD64 and F4/80 surface antigens, expression of the DC-restricted zinc-finger transcription factor, Zbtb46, and dependence on FLT3-L for differentiation (Bogunovic et al., 2009; Cerovic et al., 2014). Conventional DC can be categorized into four sub-populations based on CD103 and CD11b expression levels (Cerovic et al., 2014). CD103 (integrin α_E chain) is expressed on the majority of DC in the LP and is thought to be involved in adherence and the generation of gut-tropic $CD8^{+}$ effector T cells by inducing the expression of CCR9 (Johansson-Lindbom et al., 2005). The only identified ligand of CD103 is E-cadherin (Cepek et al., 1994).

The majority of DC in the small intestine LP are $CD103^{+}CD11b^{+}$, but this subset is relatively less common in the colon compared to other DC subsets (Cerovic et al., 2014). $CD103^{+}CD11b^{-}$ DC appear to be more abundant in Peyer's patches and are thought to correspond to conventional $CD11b^{-}CD8\alpha^{+}$ DC (Bogunovic et al., 2009; Cerovic et al., 2014). $CD103^{-}CD11b^{+}$ can express intermediate levels of CX_3CR1 and are less numerous than $CD103^{+}$ DC in the small intestinal LP. The smallest subset of DC are $CD103^{-}CD11b^{-}$ and are typically omitted from analyses, or pooled with $CD103^{-}CD11b^{+}$ DC (Cerovic et al., 2013). It is believed that $CD103^{-}CD11b^{-}$ DC are mainly localized in isolated lymphoid follicles and Peyer's patches of the LP because they are the only DC subset with significantly lower numbers in the LP of $ROR\gamma t^{-/-}$ mice, which lack secondary lymphoid tissues except for the spleen (Cerovic et al., 2013; Sun et al., 2000).

C. Inflammatory cells

The profile of inflammatory immune cells that infiltrate the gut during *L. monocytogenes* infection remains severely understudied. It is even less clear how the tissue-resident mononuclear phagocyte subsets described above change during infection. Studies investigating the overall role of inflammatory monocytes and neutrophils during systemic *L. monocytogenes* infection will be discussed below.

1. Inflammatory monocytes

The observation that *L. monocytogenes* elicit a robust monocytosis became a hallmark of infection in rabbits, which contributed to the species name, “monocytogenes” (Murray et al., 1926). *L. monocytogenes* express a monocytosis producing activity (MPA), which is a relatively undefined anionic material associated with the plasma membrane that does not contain amino acids or carbohydrate (Galsworthy and Fewster, 1988). The injection of MPA induced a dramatic monocytosis in mice by elevating the number of macrophage colony forming units in the bone marrow (Galsworthy and Fewster, 1988). C-C chemokine receptor type 2 (CCR2) is required for the egress of $CCR2^{+}Ly6C^{hi}$ monocytes from the bone marrow towards CCL2, also known as monocyte chemoattractant protein-1 (MCP-1) (Serbina and Pamer, 2006). CCR2-deficient mice have significantly higher *L. monocytogenes* burdens in the spleen and liver after i.v. infection (Kurihara et al., 1997; Serbina and Pamer, 2006). Serbina and Pamer have led most of the work describing a subset of monocyte-derived DC known as “TipDC”, which produce high levels of iNOS and TNF-α and are found in the spleen of mice after i.v. infection with *L. monocytogenes* (Serbina et al., 2003b). It is debated whether “TipDC” should be labeled as DC and not inflammatory macrophages, but nonetheless, these cells are crucial for mediating the innate immune clearance of *L. monocytogenes* and do not migrate out of the bone marrow in *ccr2*$^{-/-}$ mice (Serbina et al., 2003b).

2. Neutrophils

Neutrophils are bactericidal against *L. monocytogenes* by efficiently inhibiting the escape of bacteria from the phagocytic vacuole (Arnett et al., 2014). Early studies indicated that neutrophil depletion prior to intravenous *L. monocytogenes* infection resulted in significantly higher *L. monocytogenes* burdens in the liver compared to control animals (Conlan and North, 1991; Conlan and North, 1994). However, these results are confounded by the use of neutralizing antibody clones 5C6 and RB6-8C5, also known as CD11b and Gr-1, respectively, which deplete both $Ly6C^{hi}$ monocytes and neutrophils. Later studies using neutrophil-specific antibodies suggested that neutrophils were relatively less important than inflammatory monocytes in regards to mediating bacterial clearance and reducing overall mortality after lethal intravenous infections (Carr et al., 2011; Shi et al., 2011). However, it is clear that both monocytes and neutrophils are important for protection against *L. monocytogenes* infection in regards to bacterial

clearance and overall survival. Interestingly, the recruitment of inflammatory monocytes to the inflamed gut is important for mediating intestinal homeostasis by limiting neutrophil-mediated pathology via prostaglandin E2 secretion (Grainger et al., 2013).

V. Dissemination beyond the gastrointestinal tract

There are two proposed routes *L. monocytogenes* may use to disseminate beyond the gut to cause systemic disease following the invasion of either blood or lymphatic vessels in the intestine. These routes could involve either the flow of extracellular bacteria or cell-associated bacteria with migratory phagocytes, which will be discussed below. These pathways are depicted in Figure 1.1 in the context of systemic listeriosis.

A. Bloodborne spread

The venous blood supply of the intestine is directed into the hepatic portal vein which is responsible for 80% of all the total blood received by the liver (Crispe, 2011). Thus, food antigens and bacterial products from the gut microbiota, such as LPS, are readily transported from the intestine to the liver (Crispe, 2011). Accordingly, Melton-Witt *et al.* found that signature-tagged *L. monocytogenes* clones rapidly seeded the liver, but were absent from the spleen after oral infection of guinea pigs, suggesting a direct route of spread from the gut to the liver (Melton-Witt et al., 2012). This implies that the direct invasion of venous capillaries in the intestine by *L. monocytogenes* could lead to infection of the liver, and the rate of spread by this route is likely dependent on the dose of ingested bacteria, or invasion efficiency of the capillaries.

B. Lymphatic spread

The intestinal mucosa contains lymphatic capillaries, which are blind-ended structures composed of lymphatic endothelial cells specialized to absorb interstitial fluid (Randolph et al., 2005). These terminal lymphatic vessels are highly endocytic and permeable to mediate the uptake of antigens and migratory immune cells including mainly $CD4^+$ T cells and DC (Randolph et al., 2005). Lymphatic capillaries branch into larger collecting vessels which are surrounded by smooth muscle cells that pump lymphatic contents to the draining lymph nodes (Randolph et al., 2005). Lymphatic fluid passages through multiple lymph nodes and eventually reaches the bloodstream via the

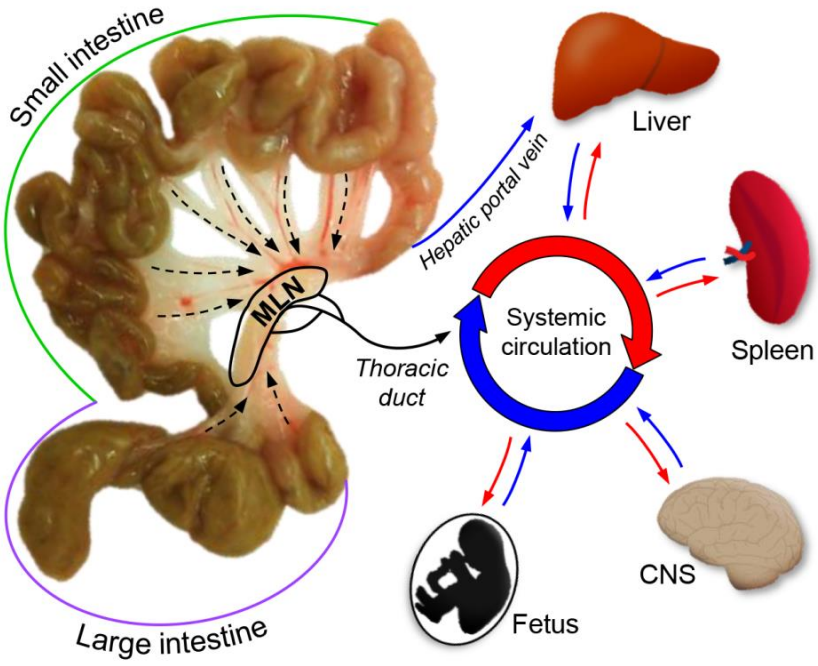

Figure 1.1: Proposed routes of systemic dissemination from the gut.

Blue arrow from the intestine to the liver represents hepatic portal vein that leads directly from the intestine to the liver. Black, dashed lines represent mesenteric lymphatic vessels that drain from the intestine to the mesenteric lymph nodes (MLN). Solid black lines represent efferent lymphatic vessels containing lymphatic fluid that drains into the bloodstream via the thoracic duct. Shorter red and blue parallel arrows from the bloodstream to systemic organs represent the arterial and venous blood supply, respectively. After entering the systemic circulation, *L. monocytogenes* can invade the liver, spleen, CNS, or fetus.

thoracic duct. Lymphatic collecting ducts shuttle gut-derived antigens and bacteria via lymphatic fluid to the mesenteric lymph nodes (MLN). Recent data suggests that acute intestinal infection enhances the permeability of mesenteric lymphatic vessels leading to prolonged inflammation of the mesentery and disruption of adaptive immunity in the MLN (Fonseca et al., 2015).

C. Mesenteric lymph nodes

1. Bottleneck for systemic spread

The MLN represent an indirect route of spread from the intestine to the spleen and liver. Oral infection of guinea pigs with signature-tagged *L. monocytogenes* clones indicated that after growth in the MLN, a secondary wave of dissemination occurred to the liver and spleen, which originated from the MLN (Melton-Witt et al., 2012). Moreover, the MLN were thought to serve as a reservoir for the continuous systemic spread of *L. monocytogenes*, as the same subset of *L. monocytogenes* clones repeatedly infected the spleen (Melton-Witt et al., 2012). It is unknown if this route of spread from the MLN to blood-borne organs involves the migration of free bacteria, “stealth” transport inside a migratory cell, or adherent *L. monocytogenes* associated with migratory cells.

2. Migration of intestinal dendritic cells to the MLN

It is possible that *L. monocytogenes* could traffic inside intestinal DC that migrate from the Peyer’s patches to the MLN (Pron et al., 2001). The expression of CC-chemokine receptor 7 (CCR7) on tissue-resident DC promotes migration to the draining lymph nodes (LN) by homing towards CC-chemokine ligands 19 (CCL19) and CCL21, which are expressed by high endothelial venules and stromal cells within the LN (Forster et al., 2008; Jang et al., 2006). All of the DC subsets described above expressed CCR7 and were found in the “pseudo-afferent” lymph after cannulation of the thoracic duct in mice that had undergone mesenteric lymphadenectomy (Cerovic et al., 2013). During oral infection with *Salmonella enterica* Typhimurium, $CD103^{+}CD11b^{+}$ DC were the first DC subset in the MLN to be infected with *Salmonella* after oral infection, and thus, DC have been suggested to transport *Salmonella* to the MLN (Bogunovic et al., 2009; Voedisch et al., 2009).

3. Other routes of spread to the MLN

The extracellular dissemination of facultative intracellular pathogens beyond the primary site of infection is considered a virulence strategy *in vivo*. Despite evidence that DC are thought to shuttle *Salmonella* Typhimurium to the MLN, CFU burdens in the MLN were reduced less than 10-fold in either *ccr7*$^{-/-}$ mice or mice with reduced numbers of DC (Bogunovic et al., 2009; Kaiser et al., 2013; Voedisch et al., 2009). This suggests that trafficking inside DC is not required for the spread of *Salmonella* from the intestine to the MLN. Likewise, after direct inoculation of the oral mucosa in sheep, 88% of *Salmonella abortusovis* were extracellular in pseudo-afferent lymphatic fluid, whereas, the minor fraction of cell-associated bacteria were found with monocytes and neutrophils, but not DC (Bonneau et al., 2006). The spread of *Yersinia pestis* to the popliteal lymph node was dependent on the migration of mononuclear phagocytes including DC and monocytes after attenuated *Y. pestis* were injected into the footpad of mice (St John et al., 2014). However, the intradermal inoculation of fully virulent *Y. pestis* in the ear to mimic a flea bite indicated that the vast majority of bacteria were extracellular inside afferent lymphatic vessels draining the ear (Gonzalez et al., 2015). The dissemination of *L. monocytogenes* either extracellular or adherent to migratory cells remains an unappreciated potential route of spread beyond the intestine.

VI. Overall Hypothesis

The underlying goal of my dissertation research is to better define the intestinal stage of *L. monocytogenes* infection prior to systemic spread. To do this, our lab previously developed an oral feeding model of listeriosis in mice to model human disease (Bou Ghanem et al., 2012). We previously showed that a high-affinity InlA interaction significantly enhanced intracellular persistence in the colon LP and dissemination to the MLN compared to a low-affinity InlA interaction (Bou Ghanem et al., 2012). Therefore, we hypothesized that myeloid cells such as migratory DC, which express E-cadherin (Siddiqui et al., 2010), serve as an intracellular growth niche for *L. monocytogenes* and promote spread to the MLN. To determine the roles of migratory phagocytes and the intracellular growth of *L. monocytogenes* during the intestinal stage of infection, I performed the following studies to:

Chapter 3: Characterize the proportion of intracellular *L. monocytogenes* in the MLN

Chapter 4: Define the myeloid cell types infected with *L. monocytogenes* in the MLN

Chapter 5: Determine if intestinal DC serve as an intracellular growth niche for *L. monocytogenes*

Chapter 6: Evaluate if extracellular *L. monocytogenes* can migrate extracellularly to the MLN

Chapter 2: Materials and Methods

A. Bacteria

L. monocytogenes EGDe and an isogenic *inlA* deletion mutant (*L. monocytogenes* Δ*inlA*) were provided by Cormac Gahan (University College Cork, Ireland). All *L. monocytogenes* used in this study were derivatives of this strain. All strains, plasmids, and oligonucleotide primers used are listed in Table 1. *L. monocytogenes* were routinely grown in BHI broth or agar (Difco). Intestinal homogenates were plated on BHI agar supplemented with 15 g/L LiCl and 10 g/L glycine (BHI/L+G) to inhibit the growth of most intestinal microbiota. Suspect colonies were confirmed to be *L. monocytogenes* by plating on CHROMagar *Listeria* plates. For selection of *L. monocytogenes*, antibiotics were used at the following concentrations: chloramphenicol, 5 µg/ml (pKSV7) or 7.5 µg/ml (pPL2 or pIMC3); erythromycin, 5 µg/ml; kanamycin, 50 µg/ml; and tetracycline, 10 µg/ml.

For selection of *E. coli*, the following antibiotic concentrations were used: carbenicillin, 100 µg/ml (pTM2, pAF1a, pAF1-1); chloramphenicol, 10 µg/ml (pGJ-cGFP) or 100 µg/ml (pTML1); erythromycin, 250 µg/ml; kanamycin, 50 µg/ml; and tetracycline, 10 µg/ml. For the growth of bacteria transformed with pIMC3 plasmids, IPTG (1 mM final concentration) was added to induce the expression of antibiotic resistance genes encoded on pIMC3 derivatives. Recombinant plasmids were transformed into *E. coli* DH5α or *E. coli* SURE. All DNA purifications were done using Qiagen kits. For each strain, aliquots were prepared and stored at -80ºC, and thawed prior to use in either *in vivo* or *in vitro* infections (Bou Ghanem et al., 2013a).

B. Construction of recombinant *L. monocytogenes* strains

PCR primers were purchased from Integrated DNA Technologies (Coralville, IA) or Sigma-Aldrich (St. Louis, MO). The temperature-sensitive shuttle vector pKSV7 was used to generate integrations and deletions on the *L. monocytogenes* chromosome as described previously (Smith and Youngman, 1992). Electrocompetent *L. monocytogenes* strains were generated as described by Monk *et al*. (Monk et al., 2008b) using either filter-sterilized BHI or Vegetable Peptone Broth (VGP) (OXOID) supplemented with 500 mM sucrose to improve bacterial growth rate and electroporation efficiency. After electroporation, bacteria were immediately recovered in 1 ml of room temperature BHI or

Table 2.1: Plasmids, strains, and oligonucleotide primers used in this study

	Description	Antibiotic Resistance[1]	Source or Reference
Plasmids			
pKSV7	temperature-sensitive shuttle vector	Cb,Cm	(Smith and Youngman, 1992)
pPL2	site-specific integration vector	Cm	(Lauer et al., 2002)
pIMC3*ery*	site-specific integration vector with IPTG-induced expression of Ery	Cm,Ery	(Monk et al., 2008a)
pIMC3*tet*	site-specific integration vector with IPTG-induced expression of Tet	Cm,Tet	(Monk et al., 2008a)
pIMC3*kan*	site-specific integration vector with IPTG-induced expression of Kan	Cm,Kan	(Monk et al., 2008a)
pAD_1-cGFP	P*hyper* driven expression of GFP (constitutive) in pPL2 derivative	Cm	(Balestrino et al., 2010)
pTM2	$InlA^m$ subcloned into PstI/BamHI-digested pKSV7	Cb,Cm	(Jones et al., 2015)
pGJ-cGFP	P*help* from pIMC3 subcloned into SacI/EagI-digested pAD_1-cGFP	Cm	(Jones et al., 2015)
pAF1a	0.98 kb fragment upstream of *lplA1* (-988 to -1) in pKSV7	Cb,Cm	(Jones et al., 2015)
pAF1-1	1.042 kb fragment from bp 954 of *lplA1* to +1001 bp downstream adjacent to 0.98 kb fragment upstream of *lplA1* in pAF1a	Cb,Cm	(Jones et al., 2015)
pTML1	*lplA1* plus 988 bp of upstream DNA from *Lm* $InlA^m$ in SalI/PstI-digested pIMC3*ery*	Cm,Ery	(Jones et al., 2015)
Bacterial strains			
E. coli DH5α	F^- *endA1 hsdR17* ($r_K^-m_K^-$) *supE44 thi-1* λ^- *recA1 gyrA96 relA1* ϕ80d*lacZ*Δ*M15*	none	M.N. Starnbach
E. coli SURE	*mcrA mcrCB mcrF mrr hsdR endA recB recJ* F' *lacIqZΔM15*	Kan,Tet,Cm_{40}	Agilent Technologies
Lm EGDe	wild type *Lm*	none	C.G. Gahan
Lm Δ*inlA*	*inlA* deletion mutant derived from *Lm* EGDe	none	C.G. Gahan
Lm $InlA^m$	mouse-adapted *Lm;* InlA S192N, Y369S	none	W-D. Schubert
Lm SD1902	*Lm* $InlA^m$::pIMC*ery*	Cm,Ery	(Jones et al., 2015)
Lm SD2000	*Lm* Δ*inlA*::pTM2 ($InlA^m$)	none	(Jones et al., 2015)
Lm SD2001	*Lm* SD2000::pIMC3*kan*	Cm,Kan	(Jones et al., 2015)
Lm SD2002	*Lm* SD2000::pIMC3*ery*	Cm,Ery	(Jones et al., 2015)
Lm SD2300	Δ*lplA1 Lm* SD2000	none	(Jones et al., 2015)
Lm SD2301	*Lm* SD2300::pIMC3*kan*	Cm,Kan	(Jones et al., 2015)
Lm SD2302	*Lm* SD2300::pTML1 (+ *lplA1*)	Cm,Ery	(Jones et al., 2015)
Lm SD2610	*Lm* EGDe::pGJ-cGFP	Cm	(Jones and D'Orazio, 2017)
Lm SD2710	*Lm* SD2000::pGJ-cGFP	Cm	(Jones et al., 2015)
Lm SD2800	*Lm* Δ*inlA*::pIMC3*tet*	Cm,Tet	(Jones et al., 2015)
Lm SD2900	*Lm* EGDe::pIMC*ery*	Cm,Ery	(Jones et al., 2015)
Lm SD2901	*Lm* EGDe::pIMC*kan*	Cm,Kan	(Jones and D'Orazio, 2017)

Primers	Sequence (5'-3')	Restriction enzyme site
$InlA^m$ -1053 bp FWD	GCCTTCCTGCAGCGCCCAAAAATCAGGTCATATCAT	PstI
$InlA^m$ +924 bp REV	TTTTTCGGATCCGCCATCATCACTTATTATTTCTGGAGT	BamHI
$InlA^m$ -500 bp FWD	AACAAAAATTCTCACACCCTTATGTG	none
Phelp FWD	ATAAGCGGCCGCCATGGGTTTCACTCTCC	NotI
Phelp REV	CCGCGAGCTCATCCCATTATGCTTTGGC	SacI
lplA1 -988 bp FWD	AGATGCAAGCTTAACGCTGATTACTTGTGA	HindIII
lplA1 -1 bp REV	ATTGTTATCTATAAATCTAGAACTCCTACCCCTTTTCTT	XbaI
lplA1 +954 bp FWD	GAGGCTTCTAGAGATATAGACGTAAAAGAATACTTT	XbaI
lplA1 +1001 bp REV	AACAGCGAATTCTGGCTTTATTTACTTAATTATAGT	EcoRI
lplA1 -988 bp FWD	AGATCGGTCGACAACGCTGATTACTTGTG	SalI
lplA1 +192 bp REV	AGGTGGCTGCAGAATAAAAGTATTCGCTATTAGCTATA	PstI

[1]Cb, Carbenicillin; Cm, chloramphenicol; Ery, erythromycin; Kan, kanamycin; Tet, tetracycline

VGP supplemented with 500 mM sucrose (filter-sterilized) and incubated statically for 2-3 hours at 37ºC (or 30ºC for pKSV7) prior to plating.

1. Isogenic InlA^m and Δ*inlA*

Tanya Myers-Morales performed the following methods to create isogenic strains of *L. monocytogenes* InlA^m and Δ*inlA.* A 4.4 kb DNA fragment comprising InlA^m with flanking regions (~1 kb upstream and downstream) was amplified from mouse-adapted *L. monocytogenes* EGDe (Wollert et al., 2007) using Platinum Taq DNA Polymerase High Fidelity (Invitrogen) using primers that had PstI and BamHI sites added. The PCR product was ligated into PstI- and BamHI-digested pKSV7 and transformed into *E. coli* SURE, resulting in pTM2. InlA^m was integrated into the chromosome of *L. monocytogenes* ∆*inlA* (provided by Cormac Gahan, University College Cork) to create *L. monocytogenes* SD2000 and confirmed by determining the DNA sequence of the region spanning 500 bp upstream and 924 bp downstream of InlA^m. Unless otherwise indicated, all work performed here was done using isogenic wild type *L. monocytogenes* EGDe (Gahan origin) or *L. monocytogenes* SD2000.

2. GFP-expressing *L. monocytogenes*

P_{hyper} was excised from pAD_1-cGFP by digestion with SacI and EagI. The P_{help} promoter was amplified from the pIMC backbone (bp 4379 to 4581; GenBank: AM940001.1) using primers containing SacI and NotI sites to create compatible ends and ligated to SacI- and EagI-digested pAD_1-cGFP. The resulting plasmid, pGJ-cGFP, was electroporated into *L. monocytogenes* SD2000 to create *L. monocytogenes* SD2710. *L. monocytogenes* EGDe was transformed with pGJ-cGFP to create *L. monocytogenes* SD2610 and pIMC3*kan* to create *L. monocytogenes* SD2901. The listeriophage PSA integrates the plasmid into the 3' end of an arginine tRNA gene (Lauer et al., 2002). GFP expression was verified using flow cytometry. The construction of pGJ-cGFP is depicted in a plasmid map shown in Fig. 1.2.

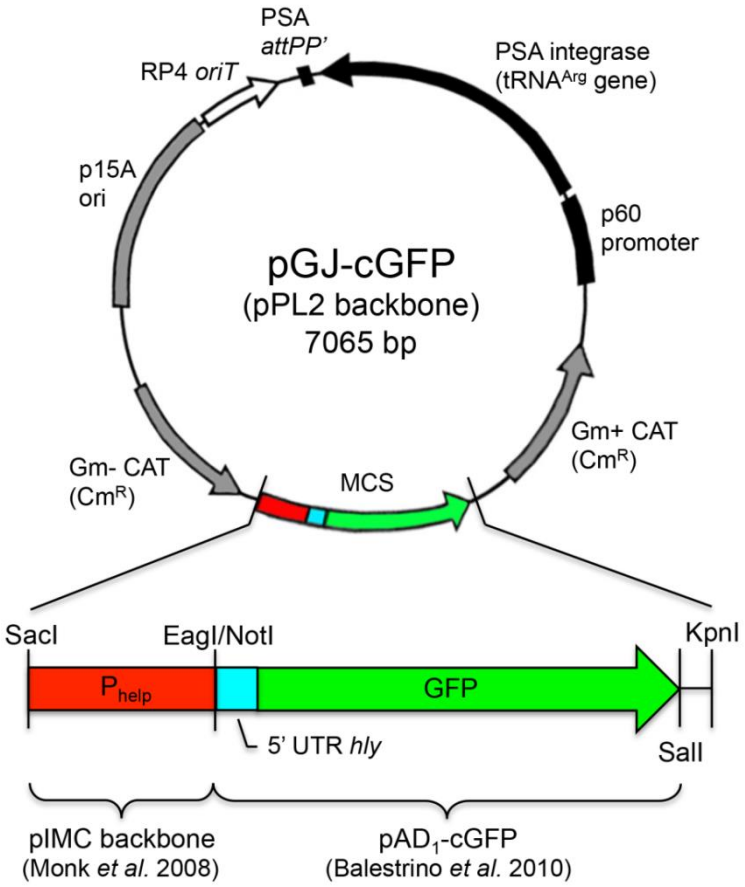

Figure 2.1: Plasmid map of pGJ-cGFP for constitutive GFP expression in *Lm.*

1. *lplA1*-deficient *L. monocytogenes*

Abigail M. Fieldhouse, with assistance by Tanya Myers-Morales, created *lplA1*-deficient *L. monocytogenes*. A DNA fragment spanning from -988 bp to -1 bp upstream of *lplA1* was amplified from *L. monocytogenes* $InlA^m$ and ligated into HindIII- and XbaI-digested pKSV7, resulting in pAF1a. Next, a 1.042 kb DNA fragment spanning from 954 bp of the *lplA1* coding sequence to 1001 bp downstream of *lplA1* was amplified from *L. monocytogenes* $InlA^m$ using primers that had EcoRI and XbaI sites added. The PCR product was ligated into EcoRI- and XbaI-digested pAF1a immediately downstream of the first *lplA1* insert, resulting in pAF1-1. *L. monocytogenes* SD2000 was electroporated with pAF1-1 to create *L. monocytogenes* SD2300. After the recovery of Cm^S mutants, the chromosomal deletion of *lplA1* was confirmed by determining the DNA sequence of the region spanning 988 bp upstream and 192 bp downstream of *lplA1*. To complement the *lplA1* mutation, *lplA1* plus 988 bp of upstream DNA was amplified from *L. monocytogenes* $InlA^m$ and ligated into PstI- and SalI-digested pIMC3*ery*, resulting in pTML1.

C. Lipoate starvation

For lipoate starvation, *L. monocytogenes* were grown in improved minimal medium (IMM), which was prepared fresh from concentrated stocks and used within two weeks (Phan-Thanh and Gormon, 1997). Freshly isolated colonies grown on BHI agar were used to inoculate 3 ml of BHI broth in 16 x 150 mm glass tubes with caps and incubated at 37ºC in a rotating rack for 8 hours. Growth was normalized by OD_{600} and bacteria were washed with PBS, inoculated in 20 ml of fresh IMM without lipoic acid and incubated for ~16 h at 37ºC shaking. For growth curves, lipoate-starved bacteria were diluted to an OD_{600} of 0.05 and growth was monitored over time. Aliquots of lipoate-starved *L. monocytogenes* were prepared as previously described for animal infections (Bou Ghanem et al., 2013a) with the exceptions that *L. monocytogenes* were suspended in IMM without lipoic acid before storage at -80ºC, and recovered in IMM before use in infections.

D. Mice

Female BALBc/By/J (BALB), C57BL/6/J (B6), or B6.129S4-*Ccr2*^{tm1Ifc}/J (*ccr2*$^{-/-}$) mice were purchased from The Jackson Laboratory (Bar Harbor, ME) at 4 weeks of age. Mice were housed in a specific-pathogen free facility with a 10 h dark cycle and a 14 h light cycle for at least two weeks before being used in experiments when they were 6 to 10 weeks old. All procedures were approved by the Institutional Animal Care and Use Committee (IACUC) at the University of Kentucky.

E. Foodborne infection

Mice were infected using a natural feeding model as previously described (Bou Ghanem et al., 2013a; Bou Ghanem et al., 2013b). Briefly, mice were transferred to cages with raised wire flooring to prevent coprophagy and fasted for 16-24 h. Aliquots of late-exponential phase *L. monocytogenes* were recovered in either BHI or improved minimal media (IMM) for 1.5 h at 30ºC. Bacteria suspended in a mixture of PBS and salted sweet cream butter (2:3 ratio) were used to saturate a 2-3 mm bread piece (Kroger). Mice were fed *L. monocytogenes*-contaminated bread pieces near the onset of their dark cycle. For co-infections, two *L. monocytogenes* strains with different antibiotic resistances were mixed in a 1:1 ratio and added to a single bread piece. Unless indicated otherwise, each mouse was fed 10^8 CFU of *L. monocytogenes.*

F. Ligated ileal loop infection

6 to 10-week old BALB/cBy/J mice were fasted for 12 hours on raised wire flooring to allow for gastric emptying before being anesthetized with isoflurane and surgically prepared on a recirculating warm water heating pad in a BSL-2 safety cabinet. A small midline laparotomy was made to exteriorize a distal portion of the small intestine. An approximate 4-cm section of the ileum was ligated by proximal and distal application of circumferential sutures that preserved circulatory and lymphatic circulation from the mesentery. The prepared ligated intestinal loop was injected through the suture at the proximal end with varying numbers (up to 10^9 CFU) of *L. monocytogenes* SD2710 in 100-150 ul of PBS. The loop was then replaced inside the peritoneum while the mouse remained under surgical anesthesia. 45 minutes later, mice were euthanized by cervical dislocation and the intestine was harvested. In pilot experiments, 400 µg Texas Red

dextran was injected intravenously two minutes before euthanasia to label blood, but not lymphatic, vessels.

G. Bacterial loads in tissue homogenates

Colons and ileums (approximated by cutting the terminal third of the small intestine) were harvested aseptically, flushed with 8 ml PBS, and squeezed with sterile forceps to remove intestinal contents (Bou Ghanem et al., 2013a). Flushed intestines were cut longitudinally with a sterile scalpel blade then cut laterally into several small pieces. Intestinal fragments were homogenized for 1 minute in 2 ml sterile water using a PowerGen 1000 homogenizer at 60% power. Serial dilutions were prepared in sterile water and plated on BHI/L+G agar. Spleen and liver were harvested aseptically and homogenized in 2.5 ml sterile water for 30 seconds. Gall bladders were placed in 1 ml sterile water in a microcentrifuge tube, ruptured with sterile scissors, and vortexed for 30 seconds. Femurs and tibias were flushed with 10 ml cold RPMI and 10% of the volume was added to sterile water and plated on BHI agar. Serial dilutions of tissue samples were plated on BHI agar. For co-infections, competitive index (CI) ratios were determined by dividing the number of CFU recovered for the mutant strain by the number of CFU recovered for the reference strain. If no CFU were recovered, the limit of detection was used for the calculation.

H. Dissociation of MLN

For total CFU determination, MLN (5-7 per mouse) were mashed through sterile steel screens (mesh # 80) into 1.5 ml sterile water. Serial dilutions were prepared in sterile water and plated on BHI. To generate a single-cell suspension using enzymatic digestion, MLN were cut into 4-5 pieces with a sterile scalpel and digested using collagenase type IV (300 U/ml) and DNase I (120 U/ml; Worthington) in 4 ml of RP5/HEPES (RPMI 1640 (Invitrogen # 21870) supplemented with 20 μM HEPES and 5% FBS). MLN pieces were incubated for 30 minutes at 37ºC with orbital shaking (250 rpm) in a 50 ml conical tube containing a sterile stir bar (2 cm). Trypan blue staining indicated that digestion with collagenase and DNase I resulted in 95% viability of dissociated MLN cells.

I. Isolation of intestinal LP cells

Large intestines (cecum and colon) were flushed with 8 ml cold CMF buffer (Ca^{2+}/Mg^{2+}-free HBSS/10 mM HEPES/25 mM sodium bicarbonate/2% FBS) and then everted using a sterile weaving needle with button thread (Resendiz-Albor et al., 2005). Mucus was removed by shaking in a 50 ml conical tube with 25 ml CMF for 1 minute. Epithelial cells were removed by three consecutive digestions in EDTA (5 mM) and dithiothreitol (1 mM) in 4 ml RP5/HEPES for a total of 40 minutes at 37°C. LP cells were digested with collagenase type IV (100 U/ml) and DNAse I (120 U U/ml) for one hour at 37°C before being isolated from the interface of a 44%/70% Percoll gradient as described previously (Bou Ghanem et al., 2013a).

An alternative protocol was performed (Koscso and Bogunovic, 2016) that increased overall cell yield for some experiments including the isolation of myeloid cells from the large intestine (Fig. 5.3 & 5.5). The large intestine was cut into three pieces, stool was removed using forceps, and small scissors were used to make a single longitudinal incision to expose the lumen. Mucus was removed by vigorously shaking the tissue in complete HBSS (Ca^{2+}/Mg^{2+}-free HBSS/2% FBS), and epithelial cells were removed by consecutive incubations in complete HBSS with dithiothreitol (20 minutes) followed by EDTA (40 minutes) at 37°C (Koscso and Bogunovic, 2016). The remaining tissue was cut into 1-2 mm pieces using small scissors and then digested statically in 8 ml RPMI/2% FBS with collagenase type IV (840 U/ml) and DNAse (120 U/ml) in a 6-well plate for one hour at 37°C/7% CO_2. Lastly, the partially digested tissue was homogenized by repeatedly passing it through a 18-G needle attached to a 5 ml syringe until completely dissociated (Koscso and Bogunovic, 2016).

J. Antibodies and flow cytometry

Antibodies specific for CD16/CD32 (93), CD45 (30-F11), F4/80 (BM8), CD11c (N418), CD11b (M1/70), Ly6G (1A8-Ly6g), B220 (RA3-6B2), cKit (2B8), MHC-II (M5/114.15.2), IgG2a (eBr2a), CD3 (145-2C11), CD49b (DX5), CD103 (2E7), α-mouse podoplanin (eBio8.1.1) from eBioscience; Ly6C (HK1.4), Ly6G (1A8), CD64 (X54-5/7.1), Gr-1 (RB6-8C5) from BioLegend; E-cadherin (36/E-Cadherin) from BD Biosciences were used.

For phagocyte enrichment (Chapter 3), MLN cells were pre-incubated with anti-CD16/32 (Fc block), then stained with either F4/80-PE or CD11c-APC. $CD11c^+$ or $F4/80^+$

cells were positively selected by incubating with either PE or APC specific magnetic particles-DM (BD Bioscience). Magnetic selection was performed using three consecutive 6 minute incubations and the cells were recovered in RP-10 media (described below) supplemented with 25 µg/ml gentamicin.

Data were acquired using an iCyt Synergy and analyzed with FlowJo (Tree Star); negative gating controls shown are FMOs (grey histograms); MFI refers to mean fluorescence intensity. Sorted monocytes used in Chapter 3 had an average purity of 96% and were recovered for at least 30 minutes at 37°C in media with 20% FBS. For intracellular cytokine staining, cells were incubated in Brefeldin A (3 µg/ml) for 4 h at 37°C in 7% CO_2, fixed and permeabilized (BD Cytofix/Cytoperm), and stained with either NOS2 (CXNFT; eBioscience) or IFN-γ (XMG1.2; BioLegend) antibodies. Debri and cell aggregates were excluded by using FSC vs. SSC and FSC-A vs. FSC-H parameters, respectively, resulting in "singlets". To identify *L. monocytogenes*-infected cells, the percentage of GFP^+ cells in each population was determined by using mice infected with *L. monocytogenes* SD2001 as a negative gating control in each experiment.

K. Determination of intracellular and extracellular *L. monocytogenes* in MLN

For determination of minimal bactericidal concentration (Chapter 3), exponential phase *L. monocytogenes* SD2000 were resuspended in PBS at 4 x 10^7/ml and seeded in triplicate (25 µl/well) in a 96-well plate. RP-10 media supplemented with various concentrations of gentamicin was added and the plate was incubated for 20 minutes at 37°C in 7% CO_2. Serial dilutions were prepared in sterile water and plated on BHI. For *in vivo* gentamicin experiments (Chapter 3), mice were given a single i.p. injection of 2 mg gentamicin in PBS and control mice received an injection of 500 µl PBS. To determine if residual gentamicin present in tissue homogenates could kill *L. monocytogenes* during *in vitro* processing, uninfected mice were treated with gentamicin or PBS for 12 hours and then tissue homogenates were prepared. *L. monocytogenes* SD2000 (1.5 x 10^3 CFU) was added to each homogenate and then incubated for one hour on ice (to mimic normal harvest conditions) before plating on BHI.

For phagocyte enrichment experiments (Chapter 3), the number of extracellular bacteria ("supernatant") was determined after MLN cells were centrifuged for 10 minutes at 300 x *g.* The supernatant was collected, serial dilutions were prepared in sterile water, and plated on BHI. The number of intracellular bacteria associated with enriched

phagocyte populations was determined after gentamicin-treated cells were lysed in sterile water.

Following enzymatic processing of MLN, intracellular *L. monocytogenes* were identified by centrifuging a sample of MLN cells (10% of total volume) for 6 minutes at 300 x *g*. The cell pellet was suspended in 1 ml of RP-10 media supplemented with gentamicin (Gibco # 15750-060). Cells were incubated statically for 20 minutes at 37°C in 7% CO_2, and then washed once with RP-10 media. The cells were centrifuged for 8 minutes (20,000 x *g*) and suspended in sterile water before being plated on BHI. To identify the total number of *L. monocytogenes*, a sample of untreated MLN cells (10% of total volume) was centrifuged for 8 minutes at 20,000 x *g*. Bacteria and cells were suspended in sterile water and serial dilutions were plated on BHI. The number of extracellular *L. monocytogenes* was calculated by subtracting the number of intracellular CFU from the total number of CFU recovered from the MLN of each mouse.

L. *In vitro* cell culture

J774 cells were maintained in RPMI 1640 (Invitrogen # 21870), L-glutamine, HEPES, 2-mercaptoethanol, and 10% FBS (RP-10 media) supplemented with penicillin and streptomycin. The day before infection, cells were washed once with warm RPMI and suspended in RP-10 without antibiotics.

Bone marrow-derived monocytes (BMMO) were generated as described previously (Francke et al., 2011). Macrophages used in Fig. 2 were derived from BMMO cultures by transferring lightly-adherent cells on day 5 of culture into 96-well-flat-bottom dishes; cells were allowed to adhere for 3 h before infection. Caco-2 cells (provided by Terrence Barrett, UK) were cultured in DMEM (Invitrogen, # 11960) with 10% FBS.

To generate bone marrow-derived DC using GM-CSF, bone marrow cells were cultured in RP-10 media supplemented with 3% J558 supernatant at a density of 2 x 10^6 cells in 10 ml volume in 100 mm non-TC-treated petri plates. An additional 10 ml media was added on day 3. GM-CSF-derived cells were harvested on day 6 and sorted into $CD11c^+MHC\text{-}II^{lo}$ and $CD11c^+MHC\text{-}II^{hi}$ populations. In other experiments, half of the media was replaced with fresh media on day 6 and the cells were cultured until days 8-9. CHO Flag Flk2 (Flt3) ligand cell line was provided by Thomas Mitchell (University of Louisville) with permission from the original owner, Nick Nicola (The Walter and Eliza Hall Institute of Medical Research, Australia). CHO FLT3-L-secreting cells were cultured to generate FLT3-L as described (Naik et al., 2010). Briefly, CHO cells were cultured in

RPMI 1640 with 5% FBS in T-175 flasks until confluent and fresh media was periodically added to reduce the serum concentration over time (Naik et al., 2010). The supernatant was collected on day 13 and the supernatants were harvested, filtered, and stored at -80°C. Batch activity was determined by testing bone marrow cells with various concentrations of FLT3-L to determine the optimum concentration that generated the highest proportion of $CDC11^+B220^-CD103^+$ cells. For day 6 FLT3-L-derived cells, 1.5 x 10^6 bone marrow cells/ml were cultured in 10 ml RP10 with 20% FLT3-L supernatant in 100 mm non-TC-treated petri plates. 10 ml of fresh media was added on day 3 and the cells were harvested on day 6 for experiments. To generate day 16 $CD103^+$ cells, 1.5 x 10^6 bone marrow cells/ml were grown in 10 ml RP10 media with 12.5% FLT-3L supernatant and 0.75% GM-CSF supernatant in 100 mm non-TC petri plates as described (Mayer et al., 2014). 5 ml of fresh media was added on day 5, non-adherent cells were removed on day 9, added to new plates in fresh media (3 x 10^5 cells/ml) and then the cells were used on day 15-16.

M. *In vitro* infection

Aliquots of *L. monocytogenes* were incubated statically in BHI for 1.5 h at 37°C and then suspended in sterile PBS. J774 or day 8 GM-CSF-derived DC (5 x 10^5 /ml) were seeded onto round glass coverslips (12 mm diameter) in wells of 24-well plate. Cultured monocyte populations and DC populations (10^5/well unless indicated otherwise) were seeded in 96-well round-bottom ultra-low attachment plates (Corning), infected for 30-60 minutes in suspension, and then washed 3 times with pre-warmed HBSS. For assays using adherent cells (J774, BMMΦ, or Caco-2), plates were centrifuged at 300 x *g* for 5 minutes after the addition of *L. monocytogenes* to synchronize infection. Total cell-associated CFU was determined by lysing cells in sterile water and plating serial dilutions on BHI agar. For intracellular *L. monocytogenes*, cells were incubated in RP-10 with 10 µg/ml gentamicin for 20 minutes at 37°C in 7% CO_2, then washed once, lysed and plated. For cells attached to glass coverslips (J774 or day 9 GM-CSF-derived DC), coverslips were removed, placed in 5 ml sterile water, vortexed for 30 seconds, and serial dilutions were plated on BHI agar. Adherent *L. monocytogenes* were calculated by subtracting the number of intracellular *L. monocytogenes* from the total cell-associated CFU. In some experiments, *L. monocytogenes* were opsonized prior to infection by incubating in Ca^{2+}/Mg^{2+}-free HBSS with 10% normal mouse serum for 30 minutes at

37°C. Serum was obtained by collecting whole blood from the hearts of naïve uninfected BALB mice into serum separator tubes (BD Microtainer®).

N. Phagocytosis assay

Cells were incubated with FluoSpheres® biotinylated 1 µm latex beads (ThermoFisher) at a 2:1 ratio in RP-10 for 1 h at 37°C in 7% CO_2. Cells were washed three times with cold buffer (Ca^{2+}/Mg^{2+}-free HBSS/1% FBS/1 mM EDTA) and then the surface-stained with specific antibodies and streptavidin-PE (eBioscience). Some cells were pretreated with either 20 µg/ml cytochalasin D (Sigma) or vehicle (DMSO) for 30 minutes prior to incubation with beads.

O. ELISA

Femurs and tibias were flushed with a total of 0.5 ml cold RPMI, and the bone marrow collected was centrifuged at 300 x *g* for 6 minutes. Serum was isolated from blood using serum separator tubes (BD Microtainer®). Bone marrow supernatants and serum were stored at -80°C. IFN-γ and IL-12 (p70) concentrations were determined using Ready-SET-Go!® ELISA kits (eBioscience). IL-18 concentrations were determined using capture antibody (clone 74) at 4 µg/ml, a biotin-labeled detection antibody (clone 93-10C) (1:2000), and rIL-18 standards ranging from 15-2000 pg/ml (MBL).

P. Epifluorescence microscopy

For Diff-Quik® (Dade-Behring) staining, cells were spun onto Superfrost slides (VWR) for 6 minutes at 600 rpm using a Cytospin and fixed in methanol 5 seconds, followed by staining in solution I for 10 seconds, and solution II for 5 seconds. Cells were dried and mounted with Permount®under glass coverslips.

For fluorescent differential “in/out” staining of *L. monocytogenes*, cells were washed 3 times with cold buffer (Ca^{2+}/Mg^{2+}-free HBSS/1% FBS/1 mM EDTA) and then incubated with Difco *Listeria* O Antiserum Poly (BD Biosciences) (1:10) in PBS with 3% BSA for 20 minutes on ice. The cells were washed and then incubated with goat anti-rabbit IgG-Texas Red® (ThermoFisher) for 20 minutes on ice. Cells were spun onto poly-L-lysine-coated Superfrost slides (VWR) for 6 minutes at 600 rpm using a Cytospin. Dried slides were formalin fixed at 4°C for 10 minutes, washed with PBS, and mounted

under coverslips with ProLong® Diamond antifade (Molecular Probes). For F-actin staining, cells were spun onto slides, air-dried, formalin-fixed for 10 minutes, washed 3 times with PBS, and then permeabilized in TBS-T (TBS/0.1% Triton X-100/1% BSA, pH=8.8) for 15 minutes at room temperature Texas Red®-X Phalloidin (ThermoFisher) was added for 20 minutes at room temperature followed by 8 washes in TBS-T, and 8 washes with TBS alone. Cells were visualized using a Zeiss Axio Imager.Z1 with a 100x/1.4NA PlanApo oil immersion objective and analyzed with AxioVision software. Each slide was analyzed independently by two different investigators.

Q. Whole-mount mesentery

Immediately after isolating the gastrointestinal tract, a suture was used to ligate mesenteric vessels immediately adjacent to the MLN. Then, the MLN were carefully removed using a scalpel for CFU analysis and sutures were used tie off lymphatic vessels adjacent to the intestine both for preservation of contents and for later identification of vessels that were located within the ligated ileal section. The proximal small intestine and colon were removed and the mesentery was oriented as flat as possible and pinned onto styrofoam using 27G needles. The tissue was fixed overnight submerged in 4% paraformaldehyde with slow rocking at 4°C in the dark. The next day, the mesentery was excised from the intestine using a scalpel and transferred to a 35 mm dish for staining. The tissue was washed three times with PBS and then permeabilized with 1% Triton-X100 in PBS for 4-6 hours on a rocker at room temperature. Next, 1 ml of 1% BSA in 0.2% Triton-X100 in PBS was used as a blocking agent for 1-2 hours on a rocker at room temperature. At the end of the day, CD45-eFluor450 and Podoplanin-eFluor660 (1 µg/ml) were added to the well in 1 ml blocking buffer (save as above) and incubated at 4°C overnight on a slow rocker. The next day, the tissue was washed four times with PBS for a total of 4 hours. Then, the mesentery was transferred to a µ-Slide 2 well glass-bottom dish (ibidi # 80287) in anti-fade liquid mounting medium (Vectashield) under a glass coverslip. This procedure is outlined in Fig. 6.3.

R. Confocal microscopy

A laser scanning inverted confocal microscope (Leica TCS SP5) was used to image the mesentery. Sequential scans at 400 Hz were performed using a 405 diode, Argon, HeNe 594, and HeNE 633 laser to excite CD45, GFP^+ *L. monocytogenes*, Texas

Red-dextran, and podoplanin, respectively, which were detected after assigning the appropriate emission spectrum. A 40X or 63X oil objective was used to visualize lymphatic vessels along the z-axis in which 30-60 μm z-stacks were acquired with a 2-4 μm step size. Individual steps and maximum projections were saved, orthogonal views were created in ImageJ, and minor adjustments to brightness and contrast were made in Photoshop.

S. Statistics

Unless indicated otherwise, mean values ± SD are shown in all panels and pooled data from at least two separate experiments are shown. Statistical analysis was performed using Prism for Macintosh (version 6; Graph Pad) and the specific tests used are indicated in each figure legend. *P* values of <0.05 were considered significant and are indicated as follows: *, *P* <0.05; **, *P* <0.01; ***, *P* <0.001; ****, *P* <0.0001.

Chapter 3: Intracellular *Listeria monocytogenes* comprise a minimal but vital fraction of the intestinal burden following foodborne infection

The following chapter is modified from: Jones, G.S., K.M. Bussell, T. Myers-Morales, A.M. Fieldhouse, E.N. Bou Ghanem, and S.E. D'Orazio. 2015. Intracellular *Listeria monocytogenes* comprises a minimal but vital fraction of the intestinal burden following foodborne infection. *Infection and immunity* 83:3146-3156.

I. Summary

L. monocytogenes are highly adaptive bacteria that replicate as free-living saprophytes in the environment, as well as facultative intracellular pathogens that cause invasive foodborne infections. The intracellular life cycle of *L. monocytogenes* is considered to be its primary virulence determinant during mammalian infection; however, the proportion of *L. monocytogenes* that are intracellular *in vivo* has not been studied extensively. In this report, we demonstrate that the majority of wild type (EGDe) and mouse-adapted ($InlA^m$-expressing) *L. monocytogenes* recovered from the MLN were extracellular within the first few days after foodborne infection. In addition, significantly lower burdens of *L. monocytogenes* were recovered from the colon, spleen, and liver of gentamicin-treated mice compared to control mice. This led us to investigate whether intracellular replication of *L. monocytogenes* was essential during the intestinal phase of infection. We found that lipoate protein ligase-deficient *L. monocytogenes (Δ*lplA1)*, which display impaired intracellular growth, were able to colonize the colon, but did not persist efficiently and had a significant defect in spreading to the MLN, spleen, and liver. Together, these data indicate that the majority of the *L. monocytogenes* burden in the gastrointestinal tract is extracellular, but the small proportion of intracellular *L. monocytogenes* is essential for dissemination to the MLN and systemic organs.

II. Introduction

L. monocytogenes is a highly adaptable bacterial pathogen that can grow in diverse environments, including the cytosol of mammalian cells (Chaturongakul et al., 2008; Xayarath and Freitag, 2012). Much research effort has focused on defining the factors that allow cell-to-cell spread of *L. monocytogenes* without encountering the extracellular environment, since this is thought to be the primary virulence strategy of *L.*

monocytogenes in vivo. However, as a facultative intracellular pathogen, *L. monocytogenes* can readily survive and multiply in extracellular spaces, and there may be multiple environments that harbor extracellular bacteria during infection. For example, we previously showed that extracellular *L. monocytogenes* were present in the lamina propria of both the ileum and the colon after foodborne infection (Bou Ghanem et al., 2012). The liver, spleen, and placenta were each shown to contain gentamicin-sensitive *L. monocytogenes* during systemic infection of mice or guinea pigs (Bakardjiev et al., 2006; Glomski et al., 2003). There is also evidence that *L. monocytogenes* replicate extracellularly in the lumen of the murine gall bladder, and it was suggested that the presence of these organisms may prolong intestinal infection if infected bile is released into the small intestine (Hardy et al., 2004). These previous studies indicate that extracellular *L. monocytogenes* can be present in a variety of tissues during mammalian infection, however, the relative proportion of extracellular *L. monocytogenes* and their role in virulence have not been clearly established.

Studies using signature-tagged bacteria have been fundamental in modeling the systemic spread of enteric pathogens by highlighting two routes of spread from the gut (Barnes et al., 2006; Lim et al., 2014; Melton-Witt et al., 2012). One route presumably involves direct invasion of the bloodstream and dissemination via the portal vein since it results in colonization primarily in the liver. The mechanisms used by bacteria to promote this invasion are unclear, and it is possible that the use of excessively large inocula or physically traumatic transmission methods can facilitate rapid spread by this route. Bacteria can also reach the spleen and liver after colonizing the draining MLN (Barnes et al., 2006; Lim et al., 2014; Melton-Witt et al., 2012). Melton-Witt *et al.* showed that this indirect route of spread led to continual seeding of the spleen, presumably due to the flow of efferent lymphatic fluid into the bloodstream via the thoracic duct (Melton-Witt et al., 2012). They found that MLN contained the highest percentage of bacterial clones compared to all other organs tested and proposed that the MLN represented a bottleneck for a secondary wave of *L. monocytogenes* dissemination to the spleen and liver (Melton-Witt et al., 2012). To spread via this indirect route, *L. monocytogenes* could be transported inside a migratory phagocyte, or it is possible that extracellular *L. monocytogenes* could traffic within afferent lymphatic vessels to the MLN. Lymph nodes also represent an important bottleneck for systemic spread during bacterial infections that occur via other routes of transmission. For example, Gonzalez *et al*. recently showed that extracellular *Yersinia pestis* disseminated from the dermis of the skin to

draining lymph nodes, and that only a subset of the clones that reached the lymph nodes could spread to the spleen (Gonzalez et al., 2015).

Based on retrospective analysis of foodborne listeriosis outbreaks, the infectious dose for humans is thought to be approximately 1 x 10^6 CFU (FAO/WHO, 2004). Mice appear to be more resistant to oral infection than humans, and this has led investigators to use much higher inocula (10^9-10^{11} CFU) to establish intestinal infection with *L. monocytogenes*. The relative resistance of mice has been attributed mainly to the species specificity of the interaction between E-cadherin expressed on intestinal epithelial cells and the bacterial surface protein internalin A (InlA) (Gaillard et al., 1991; Lecuit et al., 1999a). Two approaches have been developed to circumvent this species barrier. The Lecuit group generated "humanized" mice with a single amino acid substitution (E16P) in murine E-cadherin (Disson et al., 2008). Wollert *et al.* constructed a mouse-adapted *L. monocytogenes* strain expressing a modified InlA protein ($InlA^m$) that binds murine E-cadherin with a similar affinity as native InlA binds human E-cadherin (Wollert et al., 2007). Using this mouse-adapted strain, intestinal infection can be established with doses as low as 10^6-10^7 CFU in susceptible animals (Bou Ghanem et al., 2012; Wollert et al., 2007). Tsai *et al.* recently reported that the mouse-adapted *L. monocytogenes* strain has an altered cell tropism for intestinal invasion compared to infection in the E16P humanized mice, but it is not entirely clear how that may affect dissemination to the MLN during foodborne infection (Tsai et al., 2013).

In this study, we used a foodborne model of listeriosis to test how both the mouse-adapted and wild type *L. monocytogenes* strains spread to the MLN. Surprisingly, we found that there were very few intracellular *L. monocytogenes* within the MLN during the first few days after infection. This led us to investigate whether intracellular growth was essential for the dissemination of *L. monocytogenes* to the MLN or other peripheral tissues. The results presented here using lipoate protein ligase A1 (*lplA1*)-deficient bacteria that are unable to replicate in cells demonstrate that the minimal fraction of intracellular *L. monocytogenes* present during the intestinal phase of the infection is crucial for efficient spread to the MLN, spleen, and liver after foodborne infection.

III. Results

A. Wild type *L. monocytogenes* EGDe spread beyond the intestine similarly to a murinized strain after foodborne infection in mice

The mouse-adapted strain of *L. monocytogenes* is ideal for studying oral transmission of listeriosis in mice because it can be used at doses that are 10 to 100-fold lower than the 10^9 CFU typically required to establish intestinal infection with wild type *L. monocytogenes* EGDe (Bou Ghanem et al., 2012; Wollert et al., 2007). However, Tsai *et al.* recently showed that the InlA^m protein expressed by the mouse-adapted strain altered the tropism for *L. monocytogenes* in the intestinal epithelium by promoting binding to N-cadherin as well as E-cadherin (Tsai et al., 2013). It is unclear how this may affect subsequent dissemination to peripheral tissues and the remainder of the infection in mice. To find out if wild type *L. monocytogenes* EGDe had a similar course of infection to that previously published using the murinized strain (Bou Ghanem et al., 2012; Wollert et al., 2007), we fed both susceptible BALB/cBy/J (BALB) and resistant C57BL/6J (B6) mice 3 x 10^9 CFU and determined the bacterial loads in various tissues over the course of eight days. As expected, a small percentage of the initial inoculum was recovered from the ileum and colon 24 hours post-infection (Fig. 3.1A). Three days post-infection, the colon harbored more *L. monocytogenes* than the ileum in both mouse strains. These findings were similar to what was previously observed in the gut after mice were fed a ten-fold lower dose (10^8 CFU) of the mouse-adapted *L. monocytogenes* strain (Bou Ghanem et al., 2012). However, *L. monocytogenes* EGDe did not continue to multiply exponentially in the intestines of susceptible BALB mice (Fig. 3.1A).

Once *L. monocytogenes* EGDe disseminated beyond the intestines, the growth curves in the spleen and liver (Fig. 3.1A) closely mimicked previously published time course experiments that were performed using *L. monocytogenes* InlA^m (Bou Ghanem et al., 2012). Exponential growth of *L. monocytogenes* was observed in the gall bladders of susceptible BALB, but not resistant B6 mice (Fig. 3.1A). The peak bacterial burden occurred five days post-infection in all three of these tissues. Small numbers of *L. monocytogenes* EGDe were detected in the brain starting at five days post-infection in both BALB and B6 mice (Fig. 3.1A). Together, these results suggested that oral infection with wild type *L. monocytogenes* resulted in a similar pattern of dissemination from the gut as the mouse-adapted strain shown in a previous study, but wild type *L.*

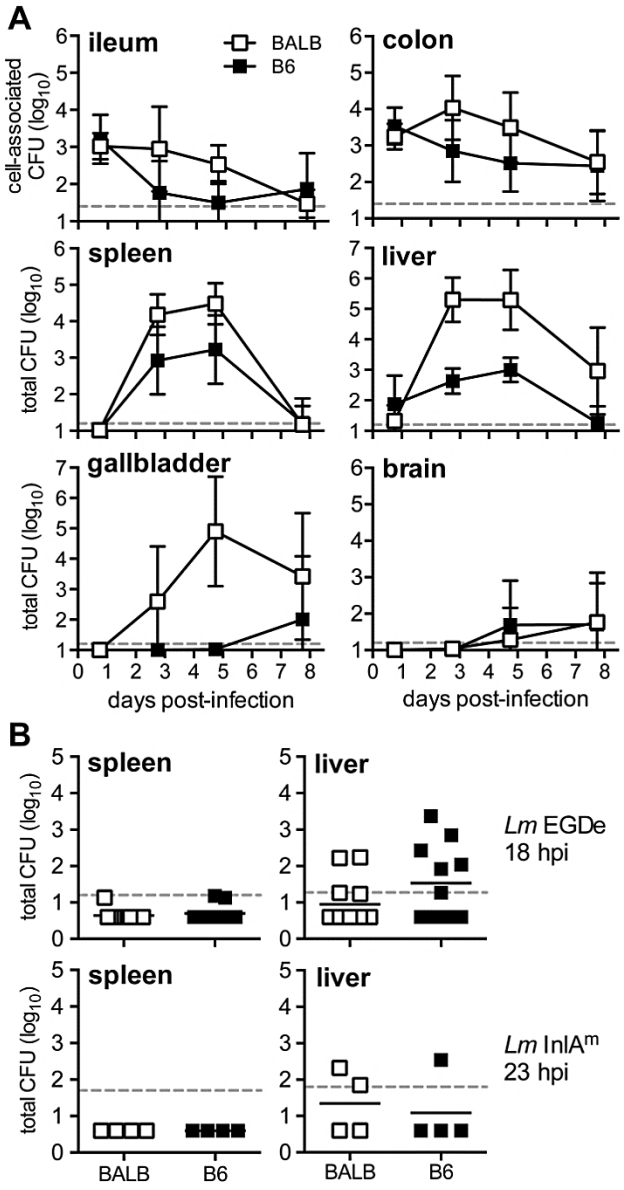

Figure 3.1: *L. monocytogenes* EGDe invaded the intestine and spread to systemic organs after foodborne infection of mice.

(A) BALB/c/By/J (BALB) or C57BL/6J (B6) mice were fed 3 x 10^9 CFU of *Lm* SD2900 (Ery^R EGDe). Tissue-associated CFU (in ileum and colon) or total CFU was determined at indicated time points. Data from two separate experiments was pooled (n=9-10 per group); mean values ± SD are shown. **(B)** Total CFU recovered from the spleen or liver of individual mice fed 3 x 10^9 CFU of *Lm* SD2900 shown in panel A, or 3 x 10^9 *Lm* $InlA^m$. Horizontal lines indicate mean values for each group. Dashed horizontal lines indicate the limit of detection for each tissue.

monocytogenes required a 10-fold higher inoculum to achieve comparable bacterial loads to InlA^m.

Although the course of infection in mice fed 10^9 *L. monocytogenes* EGDe was similar to previous results using *L. monocytogenes* InlA^m, there was one noticeable difference. During foodborne infection with 10^8 CFU of the mouse-adapted strain, there was a reproducible delay of at least 36-48 hours until *L. monocytogenes* reached the spleen or liver (Bou Ghanem et al., 2012). In contrast, when mice were fed 3 x 10^9 *L. monocytogenes* EGDe, spread to the liver occurred within 18 hours in about half of the mice (Fig. 3.1B). To determine if this was related to the bacterial strain difference or the higher inoculum size BALB and B6 mice were fed 3 x 10^9 CFU of the mouse-adapted strain and total CFU in the spleen and liver was determined one day later. As shown in Fig. 3.1B, *L. monocytogenes* InlA^m spread to the liver in 3 out of 8 mice tested. Thus, an inoculum of 10^9 CFU promoted rapid spread to the liver, regardless of which bacterial strain was used, suggesting that inocula greater than or equal to 10^9 CFU may overwhelm innate immune defenses and promote direct spread from the gut to the liver via the portal vein. Therefore, a key advantage of using the *L. monocytogenes* InlA^m strain is that it can be fed to mice at low enough doses to study the bottleneck that occurs in the gut as bacteria spread via the MLN to the spleen.

B. The majority of *L. monocytogenes* in the mesenteric lymph nodes were extracellular

We previously showed that when BALB mice were co-infected with wild type *L. monocytogenes* EGDe and the mouse-adapted strain, the wild type *L. monocytogenes* had a bimodal distribution in the MLN, with some mice having low or undetectable numbers while others had high bacterial loads comparable to mice infected with *L. monocytogenes* InlA^m (Bou Ghanem et al.). The bimodal distribution suggested that there was a bottleneck in the intestinal lamina propria and that expression of InlA^m enhanced dissemination of *L. monocytogenes* to the MLN. One mechanism to explain this could be that InlA^m promoted invasion of a migratory cell type in the lamina propria that could transport intracellular *L. monocytogenes* from the intestinal lamina propria to the MLN.

To test this, we assessed the amount of *L. monocytogenes* associated with either CD11c$^+$ cells, which represent primarily migratory subsets of dendritic cells, or F4/80$^+$ cells, which represent mainly tissue-resident macrophages. BALB mice were co-infected

with an equal ratio of *L. monocytogenes* InlA^m and an InlA deletion mutant strain (Δ*inlA*) that had been tagged with two different antibiotic resistance genes. Three days post-infection, CD11c$^+$ or F4/80$^+$ cells were enriched from the MLN by positive selection and the total number of either *L. monocytogenes* InlA^m or *L. monocytogenes* Δ*inlA* associated with these cells was determined. As shown in Fig. 3.2A, CD11c-enriched MLN cells harbored approximately 10-fold more *L. monocytogenes* InlA^m compared to *L. monocytogenes* Δ*inlA*. In contrast, similar numbers of *L. monocytogenes* InlA^m and *L. monocytogenes* Δ*inlA* were recovered from F4/80-enriched MLN cells (Fig. 3.2B).

These results suggested that expression of InlA^m may enhance invasion of dendritic cells, but not macrophages. However, the combined number of *L. monocytogenes* associated with either CD11c$^+$ or F480$^+$ cells was surprisingly small, ranging from ~400 to 2300 CFU per mouse. Typically, the total number of *L. monocytogenes* found in the MLN three days post-infection for either the wild type (Fig. 3.2C) or mouse-adapted strain (Bou Ghanem et al.) is approximately 10^5 CFU. To find out if the remaining CFU were associated with other cell types, or were simply present in the extracellular environment, supernatant fractions from the processing of the CD11c$^+$ and F480$^+$ enriched cells were collected and plated. As shown in Fig. 3.2A and 3.2B, the majority of the total CFU was found in the supernatant. Since the number of CFU recovered from the intracellular and supernatant fractions was approximately equal to the total MLN burdens shown in Fig. 3.2C, this suggests that adherent CFU were likely to be only a minor proportion of *L. monocytogenes* in the MLN.

It was possible that the large proportion of extracellular *L. monocytogenes* in the MLN was an artifact of the *ex vivo* processing techniques used to enrich for either CD11c$^+$ or F4/80$^+$ cells. Mechanical dissociation, in particular, could have lysed heavily infected, fragile cells. To avoid mechanical forces, MLN from infected mice were digested into single cell suspensions using only collagenase. A portion of the cell suspension was lysed with water and plated to determine the number of total *L. monocytogenes* in the MLN. Another portion of MLN cells was treated with gentamicin (25 μg/ml) for 20 minutes, and then lysed and plated to determine the number of intracellular *L. monocytogenes.* Extracellular *L. monocytogenes* were calculated by subtracting the number of intracellular *L. monocytogenes* from the total CFU. Using this approach, intracellular *L. monocytogenes* InlA^m comprised only 1% of the total bacterial load in the MLN at both two and three days post-infection (Fig. 3.3A). Gentamicin

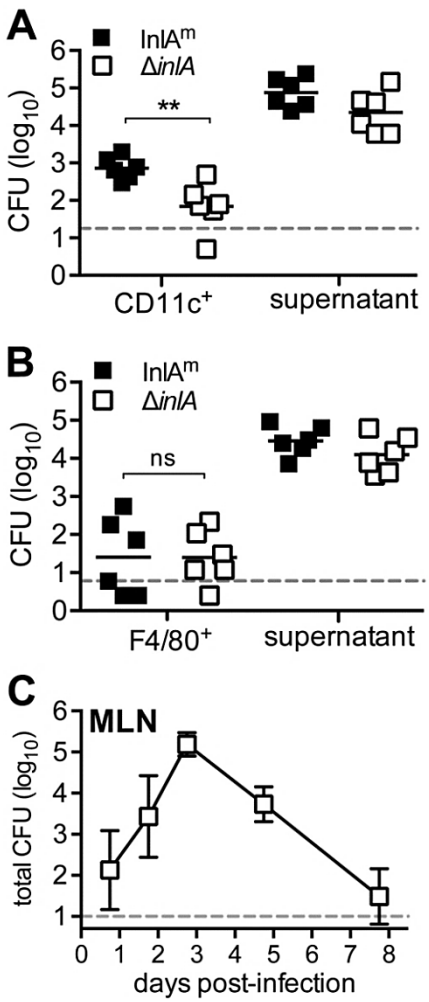

Figure 3.2: Intracellular *L. monocytogenes* were a minor proportion of total CFU in the MLN.

BALB mice were co-infected with equal proportions of *Lm* SD1902 ($InlA^m$) and *Lm* SD2800 (Δ*inlA*) for a total inoculum of 5 x 10^8 CFU and MLN were harvested three days post-infection. The number of extracellular CFU (supernatant) and the total number of intracellular ($Gent_{25}^R$) CFU associated with either $CD11c^+$ **(A)** or $F4/80^+$ **(B)** MLN cells are shown. CFU for individual mice are shown; horizontal lines indicate mean values. Statistical significance was determined by two-tailed Mann-Whitney analysis. **(C)** BALB mice were infected with 2-3 x 10^9 CFU of *Lm* SD2900 (Ery^R EGDe) and the total number of CFU in the MLN was determined. Mean values (± SD) for pooled data from n=9 (1 & 8 dpi), n=4 (2 dpi), n=10 (3 & 5 dpi) mice are shown. Dashed lines indicate limits of detection.

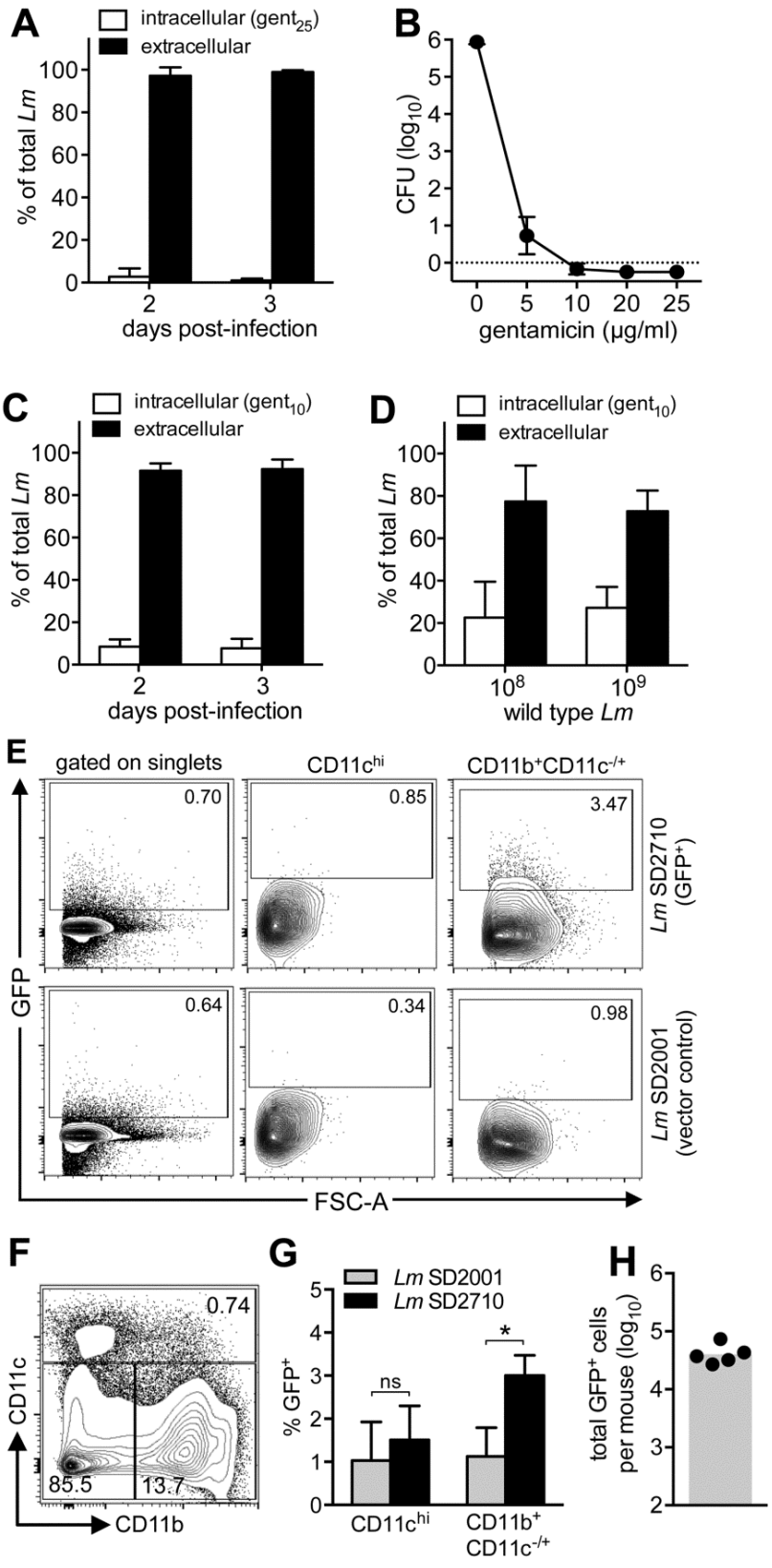
A
intracellular (gent25)
extracellular
% of total Lm
days post-infection
B
CFU (log10)
gentamicin (μg/ml)
C
intracellular (gent10)
extracellular
% of total Lm
days post-infection
D
intracellular (gent10)
extracellular
% of total Lm
wild type Lm
E
gated on singlets
CD11chi
CD11b+CD11c-/+
0.70
0.85
3.47
0.64
0.34
0.98
GFP
FSC-A
Lm SD2710 (GFP+)
Lm SD2001 (vector control)
F
0.74
85.5
13.7
CD11c
CD11b
G
Lm SD2001
Lm SD2710
% GFP+
ns
*
CD11chi
CD11b+ CD11c-/+
H
total GFP+ cells per mouse (log10)

Figure 3.3: The majority of *L. monocytogenes* in the MLN were not resistant to gentamicin.

(A) BALB mice were fed 3-8 x 10^8 CFU *Lm* InlA^m. MLN cut into 3 or 4 pieces with a sterile scalpel and digested with collagenase type IV in 4 ml of RP5/HEPES for 20 minutes at 37ºC in 7% CO_2. The partially digested MLN were then mashed through sterile steel screen (mesh # 80) or cell strainers (BD Falcon; 40 µm pore size) using the end of a 3 ml syringe plunger. Mean percentages (± SD) of intracellular ($Gent_{25}^R$) and extracellular CFU in collagenase-treated MLN of mice harvested two (n=6) and three (n=11) days post-infection are shown. **(B)** Mean number of *Lm* SD2000 (± SD) surviving after 20 minute incubation at 37˚C with CO_2 at the indicated concentration of gentamicin. **(C)** BALB mice were fed 2-7 x 10^8 CFU *Lm* InlA^m and MLN were dissociated using only enzymatic digestion (n=7-11 per group). Mean percentages (± SD) of intracellular ($Gent_{10}^R$) and extracellular CFU in the MLN are shown. **(D)** BALB mice were fed 3 x 10^8 or 3 x 10^9 *Lm* EGDe (n=4 per group) and MLN were dissociated using enzymatic digestion three days post-infection. Mean percentages (± SD) of intracellular ($Gent_{10}^R$) and extracellular CFU in the MLN are shown. **(E, F)** BALB mice were fed 2-5 x 10^8 CFU of *Lm* SD2710 (GFP^+) or *Lm* SD2001. MLN were collected two days post-infection and analyzed by flow cytometry. Representative dot plots showing the percentage of GFP^+ cells in either total MLN (singlets), or the $CD11c^{hi}CD11b^{-/+}$ and $CD11b^+CD11c^{-/+}$ populations are shown in panel E; the gating strategy is shown in panel F. **(G)** Mean percentages (± SD) of GFP^+ cells in each myeloid-derived MLN population (n=5 mice) are shown. Statistical significance was determined by two-tailed Mann-Whitney analysis. **(H)** Symbols indicate the total number of GFP^+ cells identified in the MLN of each mouse; the shaded bar represents the mean value for the group.

treatment is commonly used to selectively kill extracellular bacteria; however, gentamicin can penetrate mammalian cells when used at high enough concentrations. To determine the minimal bactericidal concentration for our experimental conditions, we exposed $1x10^6$ *L. monocytogenes* $InlA^m$ to increasing concentrations of gentamicin. The lowest concentration that killed 100% of the inoculum was 10 µg/ml (Fig. 3.3B). We repeated the analysis of intracellular and extracellular *L. monocytogenes* in the MLN two and three days post-infection using 10 µg/ml gentamicin and recovered approximately 10-fold higher percentages of intracellular *L. monocytogenes* (Fig. 3.3C vs. Fig. 3.3A). Thus, 10% of the bacterial burden in the MLN was intracellular and approximately 90% was extracellular (gentamicin resistant). To ensure that these results applied to both the wild type and murinized strains, we fed groups of mice two different doses of *L. monocytogenes* EGDe. Slightly higher proportions of intracellular *L. monocytogenes* EGDe were found relative to *L. monocytogenes* $InlA^m$, but the majority of the bacteria in the MLN were still extracellular (Fig. 3.3D).

To confirm these findings, flow cytometry was used to quantify cell-associated *L. monocytogenes* in the MLN. Mice were fed 10^8 CFU of either a *L. monocytogenes* $InlA^m$ derivative that constitutively expressed GFP (*L. monocytogenes* SD2710), or a vector control strain (*L. monocytogenes* SD2001). As expected, only a small fraction of MLN cells were infected. It was difficult to detect the small number of GFP^+ cells when bulk populations were analyzed, due to some auto-fluorescence of MLN cells using a 525/50 nm filter (Fig. 3.3E). Therefore, myeloid-derived cell subsets were analyzed by gating on either $CD11c^{hi}$ cells (dendritic cells), or $CD11b^+CD11c^{-/+}$ cells, which included monocytes, macrophages, and neutrophils (Fig. 3.3F). As shown in representative dot plots (Fig. 3.3E) and in collected data from groups of mice (Fig. 3.3G), clear shifts in GFP expression were visible when analyzing these myeloid-derived subsets. However, even when these two subsets were combined, an average of only 4.3×10^4 GFP^+ MLN cells were detected in each mouse (Fig. 3.3H) even though the total number of *L. monocytogenes* recovered from the MLN in these experiments ranged from $1.5\text{-}7 \times 10^5$ CFU. This suggested that either each infected cell contained at least four, and up to sixteen *L. monocytogenes*, or that some portion of the total CFU burden was extracellular.

C. *In vivo* treatment with gentamicin significantly reduced *L. monocytogenes* burdens following foodborne challenge

Since all *in vitro* approaches involve some degree of processing and handling, we next used an *in vivo* approach to assess the degree to which extracellular *L. monocytogenes* were present in the gut and the draining lymph nodes. To do this, mice were fed *L. monocytogenes* InlA^{m} and three days later, half the animals received an intraperitoneal injection of 2 mg of gentamicin and the other half were injected with PBS. The number of viable bacteria present in each tissue was determined 12 hours later. As shown in Fig. 3.4A, significantly lower numbers of *L. monocytogenes* were recovered from mice treated with gentamicin compared to control mice. The average number of *L. monocytogenes* recovered from the colons of gentamicin-treated mice represented only 14% of the bacterial load in the colons of PBS-treated mice. Likewise, a significantly reduced number of CFU were observed in the MLN, spleens, and livers of mice treated with gentamicin (Fig. 3.4A). In each tissue, gentamicin-sensitive *L. monocytogenes* represented approximately 60-80% of the bacterial load recovered. It was possible that the lower number of CFU recovered from gentamicin-treated mice occurred because of residual gentamicin present in the tissue homogenates, which may have killed intracellular *L. monocytogenes* that were released during cell lysis and plating. To test this, uninfected mice were treated with gentamicin or PBS. Tissue homogenates were prepared 12 hours later and inoculated *in vitro* with *L. monocytogenes*. As shown in Fig. 3.4B, there was no inhibition of *L. monocytogenes* growth in the gentamicin-treated homogenates compared to the PBS-treated homogenates. Therefore, the results of both the *in vitro* and *in vivo* approaches strongly suggest that intracellular *L. monocytogenes* represent only a minimal fraction of total *L. monocytogenes* during the first few days following oral challenge.

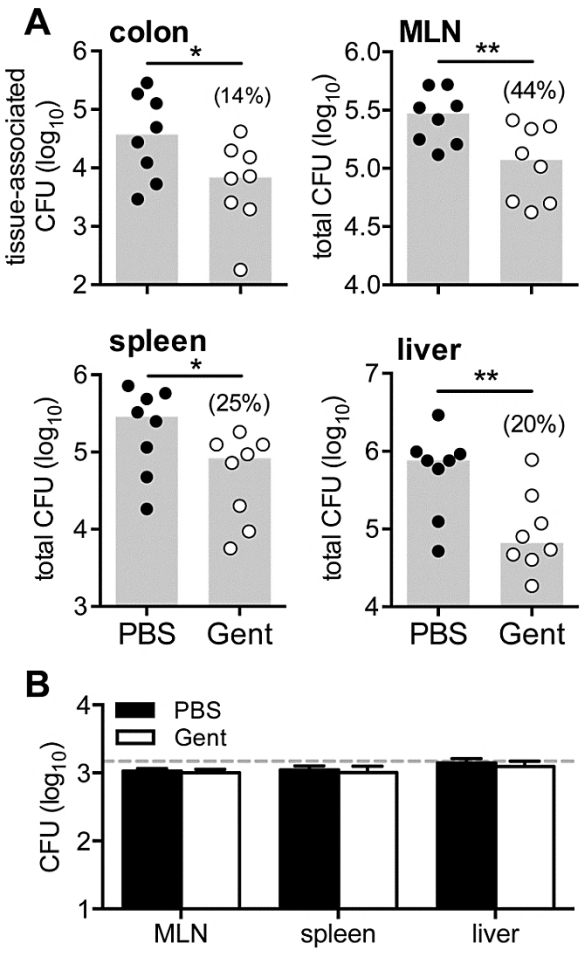

Figure 3.4: Gentamicin treatment reduced bacterial burdens in mice fed *L. monocytogenes*.

(A) BALB mice were orally infected with 2-5 x 10^8 *Lm* SD2000 (InlA^m). Three days post-infection, mice were injected (i.p.) with either 2 mg of gentamicin or PBS and the colons, MLN, spleens, and livers were harvested 12 h later. Symbols indicate CFU values for individual mice; gray bars indicate the median for each group. The mean percentage of CFU recovered from gentamicin-treated mice relative to PBS-treated mice is shown in parentheses. Data from two separate experiments was pooled and statistical significance was determined by one-tailed Mann-Whitney analysis. **(B)** Uninfected BALB mice were treated with 2 mg gentamicin or PBS, and tissues were harvested 12 hours later. Homogenates were inoculated with 1.5 x 10^3 *Lm* SD2000 and incubated on ice for one hour before plating on BHI agar. The horizontal dashed line indicates the inoculum and the bars indicate the mean CFU (± SD) recovered from each homogenate; (n=3 mice per group).

D. Intracellular replication was not required for *L. monocytogenes* to establish intestinal infection

The relatively small proportion of intracellular *L. monocytogenes* in the intestines and MLN led us to question if intracellular replication was necessary during the intestinal phase of foodborne infection. Therefore, we constructed a mutant strain of mouse-adapted *L. monocytogenes* that had a defect only in intracellular replication, with normal growth in extracellular environments. O'Riordan *et al*. previously showed that lipoate protein ligase A1 (LplA1)-deficient *L. monocytogenes* were unable to scavenge lipoate from host cell-derived lipoyl peptides, and thus, had a significant defect in intracellular growth in J774 macrophages (O'Riordan et al., 2003). Therefore, we generated an $InlA^m$-expressing Δ*lplA1* mutant to study when intracellular replication was important during foodborne infection.

L. monocytogenes store large quantities of lipoic acid, and the intracellular growth phenotype of the Δ*lplA1* mutant can only be observed when these reserves have been depleted (Keeney et al., 2007). To do this, *L. monocytogenes* were grown overnight in improved minimal media (IMM) in the absence of lipoic acid. *L. monocytogenes* Δ*lplA1* grew as well as either the parental strain $InlA^m$ (*L. monocytogenes* SD2000) or the complemented strain (+ *lplA1*) when lipoate-starved bacteria were transferred to rich media (BHI) (Fig. 3.5A). During further growth in minimal media with limiting quantities of nutrients, all strains had an extended lag phase of 12 to 15 hours (Fig. 3.5B, 3.5C). Lipoate-starved *L. monocytogenes* $InlA^m$ required supplementation with at least 0.25 nM lipoic acid to reach late exponential phase (Fig. 3.5B). As expected, none of the lipoate-starved bacteria grew in minimal media lacking lipoate, and all three strains reached similar optical densities after the addition of 25 nM lipoic acid (Fig. 3.5C). To verify that lipoate-starved *L. monocytogenes* Δ*lplA1* did not replicate inside mammalian cells, we conducted intracellular growth assays with J774 macrophages. Lipoate-starved *L. monocytogenes* Δ*lplA1* were able to survive, but not grow in these cells (Fig. 3.5D). In contrast, the complemented mutant grew exponentially in J774 cells after an extended lag phase.

Since lipoate-starved *L. monocytogenes* had an extended lag phase in both liquid medium and in J774 cells, we were concerned that this might reduce the ability of the bacteria to establish infection in mice. To test this, BALB mice were fed an equal

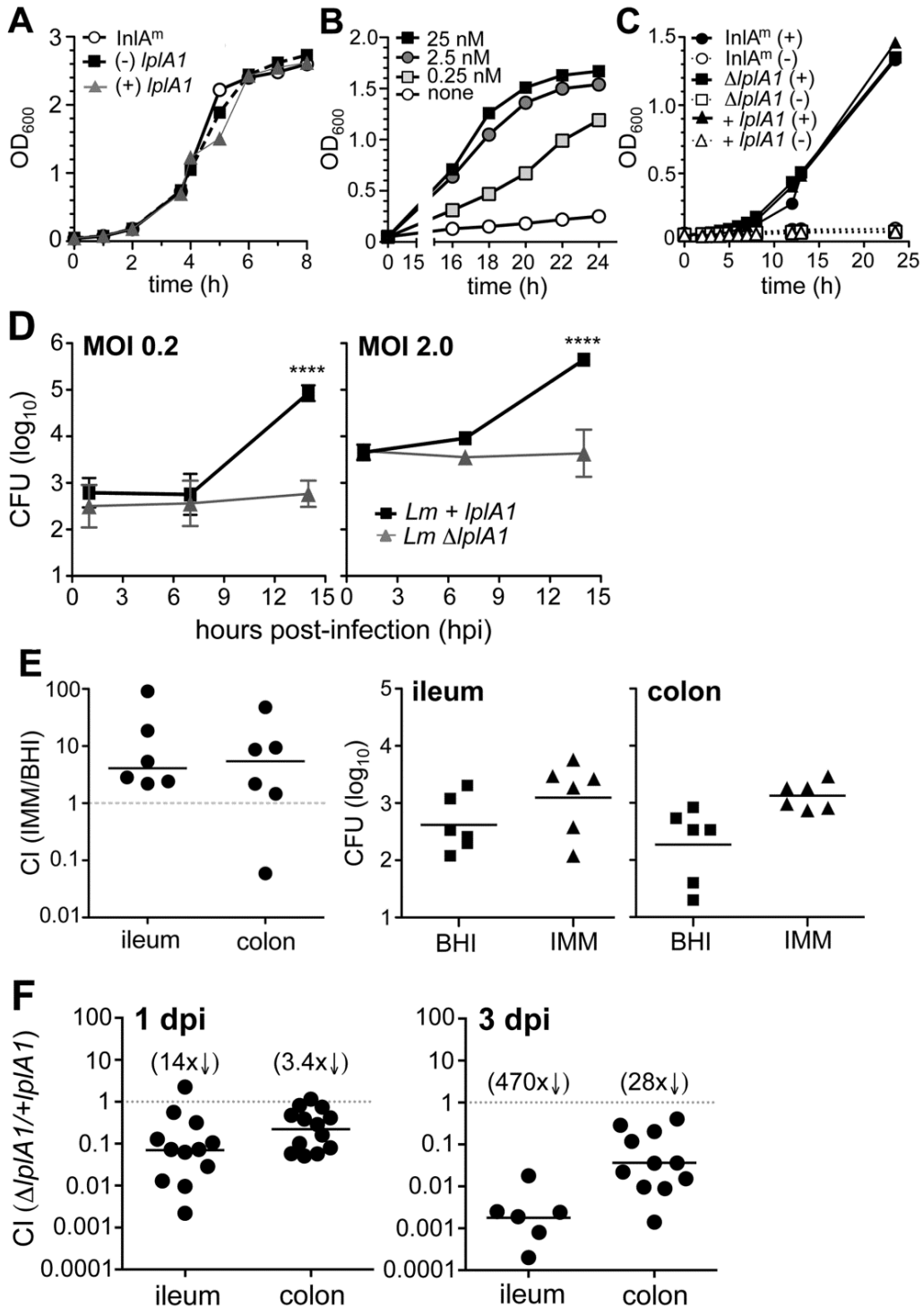
A
InlA^m
(-) lplA1
(+) lplA1
OD600
time (h)
B
25 nM
2.5 nM
0.25 nM
none
OD600
time (h)
C
InlA^m (+)
InlA^m (-)
ΔlplA1 (+)
ΔlplA1 (-)
+ lplA1 (+)
+ lplA1 (-)
OD600
time (h)
D
MOI 0.2
MOI 2.0
****
****
CFU (log10)
Lm + lplA1
Lm ΔlplA1
hours post-infection (hpi)
E
CI (IMM/BHI)
ileum
colon
ileum
CFU (log10)
BHI
IMM
colon
BHI
IMM
F
1 dpi
3 dpi
CI (ΔlplA1/+lplA1)
(14x↓)
(3.4x↓)
(470x↓)
(28x↓)
ileum
colon
ileum
colon

Figure 3.5: Lipoate-starved *L. monocytogenes* grew slowly in minimal media, but were able to establish intestinal infection in mice.

Freshly streaked colonies of *Lm* were incubated in IMM(-) media overnight to deplete lipoate reserves, and then diluted into fresh media with or without lipoic acid **(A-C)** or frozen at -80˚C prior to infection of cells **(D)** or mice **(E)**. **(A)** The rate of growth shaking at 37˚C in a rich medium (BHI) was similar for *Lm* SD2301 (Δ*lplA1*), the complemented mutant *Lm* SD2302 (+ *lplA1*), and the parental strain (*Lm* SD2000). **(B)** Lipoate-starved *Lm* SD2000 had a long lag phase in IMM medium, but achieved exponential growth in at least 0.25 nM lipoic acid. **(C)** The *lplA1* deletion strain (Δ*lplA1*) and the complemented mutant (+ *lplA1*) did not grow in the absence of exogenous lipoate, but reached similar growth densities as the parental strain in IMM media supplemented with 25 nM lipoic acid. **(D)** J774 cells were infected in triplicate and the mean number (± SD) of gentamicin-resistant (10 µg/ml) CFU per well was determined over time. Statistical significance was determined by Mann Whitney analysis. For panels A-D, data from one of at least two separate experiments is shown. **(E)** Mice were co-infected with a 1:1 ratio of *Lm* SD2001 (Kan^R $InlA^m$ prepared in IMM) and *Lm* SD2002 (Ery^R $InlA^m$ prepared in BHI) for a total inoculum of 2 x 10^8 CFU. Tissue-associated *Lm* in the ileum or colon was determined 24 hours later and is shown as both a competitive index (CI) and as the absolute number of cell-associated CFU recovered from each mouse. **(F)** BALB mice were co-infected with a 1:1 mixture of *Lm* SD2301 (Δ*lplA1*) and the complemented mutant *Lm* SD2302 (+ *lplA1*) for an average total inoculum of 8 x 10^8 CFU. Tissue-associated *Lm* was determined and is shown as a CI; the fold difference from the hypothetical value of 1.0 is shown in the parentheses above. Pooled data from at least two separate experiments are shown. Kate M. Bussell, second author on the published manuscript, generated the data presented in this figure.

ratio of antibiotic-tagged parental strain *L. monocytogenes* InlA^m that were grown in either rich medium (BHI), or under lipoate starvation conditions (IMM without lipoic acid). These bacteria were fully capable of scavenging lipoate from host cells, but were transmitted to the gastrointestinal tract in a lipoate-starved state that might require a considerable lag time before bacterial replication could occur. The ileum and colon from each mouse was harvested 20 hours later, flushed extensively, and the total number of each bacterial strain present in the flushed tissue was determined by plating on BHI supplemented with either erythromycin or kanamycin. As shown in Fig. 3.5E, the lipoate-starved *L. monocytogenes* InlA^m did not have a defect in establishing intestinal invasion, and in fact, had a slight advantage compared to *L. monocytogenes* InlA^m grown in BHI. Therefore, although lipoate starvation did cause *L. monocytogenes* to have an extended lag phase during growth in lipoate-limiting conditions, it did not reduce bacterial fitness to colonize the intestinal tract in mice.

Next, to establish the importance of intracellular growth during the gastrointestinal phase of foodborne listeriosis, BALB mice were fed lipoate-starved *L. monocytogenes* Δ*lplA1* mutant and the complemented strain mixed in a 1:1 ratio. The total number of each strain present in either the ileum or the colon was determined, and is presented as a competitive index (CI) ratio in Fig. 3.5F. The Δ*lplA1* strain had very little defect in establishing infection in the colon, but on average, 14-fold fewer *lplA1* mutant bacteria were recovered from the ileum one day post-infection. By three days after infection, however, the complemented strain outcompeted the mutant by an average of ~500-fold in the ileum and ~30-fold in the colon (Fig. 3.5). Together, these results suggested that intracellular replication was not necessary for *L. monocytogenes* to establish intestinal infection in mice, but that the ability to grow inside of a host cell strongly promoted persistence, particularly in the small intestine.

E. Intracellular replication of *L. monocytogenes* was vital for spread beyond the intestine

To find out if intracellular replication was essential for *L. monocytogenes* to disseminate beyond the intestine, CFU counts in the MLN, spleen, and liver were determined three days after co-infection with a 1:1 mixture of lipoate-starved *L. monocytogenes* Δ*lplA1* and the complemented strain. As shown in Fig. 3.6A, *L. monocytogenes* Δ*lplA1* had a dramatic defect (2500-fold) in reaching the MLN compared to the complemented (+ *lplA1*) strain. The MLN is thought to be a bottleneck for further

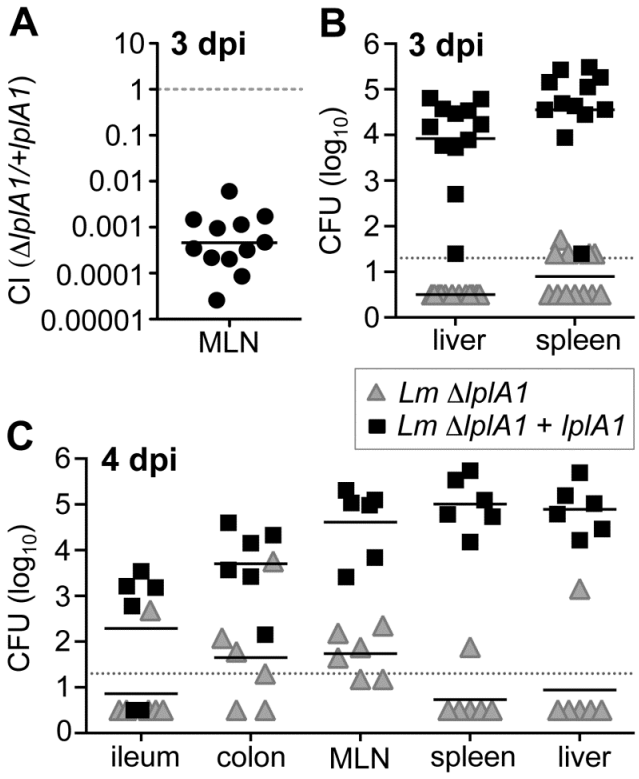

Figure 3.6: LplA1-deficient *L. monocytogenes* had a severe dissemination defect in mice.

BALB mice were co-infected with a 1:1 mixture of *Lm* SD2301 (Δ*lplA1*) and the complemented mutant *Lm* SD2302 (+ *lplA1*) for a total inoculum of 3-7 x 10^8 CFU. Pooled data from at least two separate experiments are shown. **(A)** The percentage of each strain recovered from the MLN three days post-infection is expressed as a competitive index (CI); solid horizontal line indicates geometric mean. **(B)** The absolute number of CFU of each strain recovered three or **(C)** four days post-infection. Solid horizontal lines indicate mean values and dashed lines indicate limits of detection. Kate M. Bussell, second author on the published manuscript, generated the data presented in this figure.

dissemination to the spleen and liver via the blood stream, and accordingly, no *L. monocytogenes* Δ*lplA1* were recovered from the liver three days post-infection, while an average of 10^4 CFU of the + *lplA1* complemented strain was detected in the spleen (Fig. 3.6B). Likewise, only a few mice had any *L. monocytogenes* Δ*lplA1* in the spleen, whereas, on average, 10^4 to 10^5 CFU of the complemented strain were recovered three days post-infection (Fig. 3.6B).

Although dissemination to the MLN was greatly reduced for *L. monocytogenes* unable to replicate intracellularly, approximately 60 CFU of *L. monocytogenes* Δ*lplA1* were recovered from the MLN three days post-infection (data not shown). Therefore, it was possible that dissemination of these bacteria was simply delayed, rather than inhibited. To test this, we also evaluated bacterial burdens in both the gut and in peripheral tissues four days after co-infection. As shown in Fig. 3.6C, very few *L. monocytogenes* Δ*lplA* were detected in either the ileum, colon, MLN, spleen, or liver four days post-infection. In contrast, the complemented strain had increased numbers in all tissues relative to the day three counts. Thus, dissemination beyond the intestinal lamina propria was severely limited for *L. monocytogenes* Δ*lplA.* Together, these results indicate that the minor proportion of *L. monocytogenes* that invade cells in the gut and replicate is crucial for *L. monocytogenes* to disseminate via the MLN during foodborne infection.

IV. Discussion

Invasion of mammalian cells is considered to be the main virulence strategy of *L. monocytogenes,* but a significant portion of the bacterial burden in *L. monocytogenes*-infected animals appears to be extracellular. Although the focus of this study was primarily the MLN, the predominance of extracellular *L. monocytogenes* was noted in all tissues examined, and is consistent with previous reports using other small animal models of listeriosis (Bakardjiev et al., 2006; Glomski et al., 2003). We conclude from these studies that intracellular *L. monocytogenes* are actually a minimal component of the bacterial load during the early stages of infection. Silva and Pestana recently suggested that the extracellular phase of many facultative intracellular pathogens could be important for virulence and that the presence of extracellular bacteria was greatly underappreciated in most infection models (Silva and Pestana, 2013). The data presented here suggest that virulence strategies used by extracellular *L. monocytogenes* may be particularly important for initial colonization and survival in the gastrointestinal

tract. In that regard, Travier *et al*. recently reported that ActA, the sole *L. monocytogenes* protein required to mediate actin-based motility in the host cell cytosol (Smith et al., 1995b), was also required for extracellular aggregation and biofilm formation *in vitro* (Travier et al., 2013). The authors further showed that ActA-dependent aggregation promoted both colonization and persistence of extracellular *L. monocytogenes* in the intestinal lumen of mice infected by the intragastric route.

In this study, intracellular *L. monocytogenes* were not crucial for bacterial survival in the gastrointestinal tract until relatively late in the infection (3 days after foodborne challenge). During this time frame, *L. monocytogenes* will have invaded the intestinal epithelium, penetrated the underlying lamina propria, and potentially replicated exponentially either in the interstitial fluid or within a phagocyte. Most available data suggest that *L. monocytogenes* do not replicate extensively within intestinal epithelial cells. For example, Nikitas *et al.* demonstrated that InlA-mediated uptake could occur rapidly with *L. monocytogenes* transcytosing across goblet cells in the murine small intestine and being deposited into the lamina propria without ever leaving the endocytic vacuole (Nikitas et al., 2011). Accordingly, we previously showed that the number of intracellular *L. monocytogenes* in the colonic epithelium peaked three days post-infection, but *L. monocytogenes* in the colonic lamina propria continued to increase exponentially until five days post-infection (Bou Ghanem et al., 2012). The fate of *L. monocytogenes* once the bacteria cross the mucosal barrier is not well understood, and may depend on the route used for invasion. For example, uptake via M cells in the small intestine would result in deposition within a lymphoid follicle or Peyer's patch, where rapid phagocytosis is likely to occur by a unique subset of dendritic cells localized near M cells in the subepithelial dome (Lelouard et al., 2012; Lelouard et al., 2010). In contrast, InlA-mediated transcytosis across the goblet cells prominent in the colon may increase the chance that extracellular *L. monocytogenes* could avoid phagocytosis in the underlying lamina propria and traffic in the lymphatic fluid to the draining lymph node. In support of this idea, we showed here that intracellular replication of *L. monocytogenes* was more important for colonization and persistence in the ileum than in the colon.

The primary strategy used here for determining the proportion of intracellular *L. monocytogenes* was treatment with gentamicin, an aminoglycoside that does not penetrate mammalian cells at low concentrations. Although this is a widely used technique in the field of bacterial pathogenesis, one must be cautious in interpreting data from gentamicin protection assays, since excessively high concentrations of gentamicin

can kill or stress intracellular bacteria, possibly due to the pinocytosis of extracellular fluid containing antibiotics (Drevets et al., 1994; Menashe et al., 2008; Qazi et al., 2004). As we showed here, even treatment with 25 µg/ml gentamicin *in vitro* slightly underestimated the proportion of intracellular organisms in the MLN compared to using only 10 µg/ml in tissue culture media. Glomski *et al.* reported serum gentamicin levels of 5.6 µg/ml 12 h after the subcutaneous injection of 1 mg gentamicin (Glomski et al., 2003). Thus, we treated mice with 2 mg gentamicin to approximate the minimal bactericidal concentration determined *in vitro* (10 µg/ml; Fig. 3.4B). Using this approach, it is difficult to confirm that the antibiotic penetrated all tissues efficiently; however, we did recover significantly lower CFU from the colon, MLN, spleen and liver of gentamicin-treated mice compared to control mice. Notably, we found that the liver harbored a larger fraction of extracellular *L. monocytogenes* than the spleen, a result that is consistent with previous studies that utilized different animal models of listeriosis (Bakardjiev et al., 2006; Drevets et al., 2001; Glomski et al., 2003). All of the approaches we used to quantify extracellular *L. monocytogenes* in the MLN have the caveat that some processing of the tissue was required, and we cannot rule out the possibility that some of the extracellular bacteria we identified were present in fragile, heavily infected cells that lysed *in vitro*. However, the combined results from both the *in vitro* and *in vivo* gentamicin treatments strongly suggest that a large proportion of the *L. monocytogenes* burden in the gut is extracellular during the first few days following foodborne challenge.

To address the role of intracellular *L. monocytogenes* during the early stages of infection in the gut, we used lipoate-starved Δ*lplA1 L. monocytogenes*. These bacteria were able to invade cells, escape from the vacuole, and mediate actin-based motility to avoid autophagy (Mitchell et al., 2015; Tattoli et al., 2013; Yoshikawa et al.), but could not replicate efficiently due to an inability to scavenge lipoate from the host cell cytosol. A more common approach to study *L. monocytogenes* that cannot survive intracellularly has been to use listeriolysin O (LLO) mutants that are killed following invasion of murine cells because they cannot mediate escape from the vacuole (Cossart et al., 1989; Gaillard et al., 1986). But our primary objective was to determine if intracellular localization of *L. monocytogenes* was needed for dissemination to the MLN, and use of an LLO mutant could abort infection prior to colonization of the lamina propria (Krawczyk-Balska and Bielecki, 2005; Vadia et al., 2011), making it difficult to distinguish invasion defects from dissemination defects. When grown in minimal defined media, lipoate-starved Δ*lplA1 L. monocytogenes* required a minimum of 0.25 nM lipoate to

replicate (Fig. 6B). Although the concentration of lipoic acid present in the tissues of mice is unknown, it was previously reported that plasma concentrations of lipoic acid in healthy humans ranged from 3.1 to 50 ng/ml (~15 to 242 nM) and the concentration in in normal human liver tissue was 198 ng/mg protein (Baker et al., 1998; Carlson, 2008). Therefore, it is likely that during *in vivo* growth in mice, extracellular Δ*lplA1 L. monocytogenes* can readily obtain free lipoate from the host, and the persistence and dissemination defects we observed were due to a lack of intracellular replication.

It is possible that invasion of a particular cell type in the intestinal lamina propria is critical for *L. monocytogenes* to be transported to MLN. For example, InlA may enhance invasion into a subset of dendritic cells that express E-cadherin. E-cadherin-positive dendritic cells are known to be recruited to the intestine and MLN using a T cell-mediated model of colitis (Siddiqui et al., 2010), but their role in inflammation induced by infection has not yet been explored. However, the Δ*lplA1* data reported here suggest that it is replication, and not just intracellular localization of *L. monocytogenes*, that is important for persistence and spread beyond the gut. Exponential replication in the cytosol of a more permissive cell type in the gut, such as a tissue-resident macrophage, may serve as an amplification step to increase *L. monocytogenes* burdens above a particular threshold that is needed for efficient dissemination. These results further highlight the importance of studying dissemination in the context of natural foodborne transmission, using relatively low doses, because innate immune defenses that limit bacterial spread can be overwhelmed by excessively large intragastric inocula. In support of this idea, Gonzalez *et al.* showed that the dermis represented a significant bottleneck for the spread of *Y. pestis* to the skin-draining lymph nodes, but this bottleneck was partially ablated when higher doses of bacteria were used (Gonzalez et al., 2015).

Extracellular *L. monocytogenes* predominated in the gut whether we infected mice with wild type *L. monocytogenes* EGDe or with a mouse-adapted derivative of this strain. Tsai *et al*. recently raised the concern that InlA^{m}-expressing strains of *L. monocytogenes* may cause more inflammation than wild type *L. monocytogenes* during intestinal infection, and that this could lead to prolonged colonization in the gut (Tsai et al., 2013). In this regard, we showed here that foodborne transmission of wild type *L. monocytogenes* resulted in a more transient infection of the intestines than was previously observed with *L. monocytogenes* InlA^{m}-expressing strains. Likewise, we did find that approximately twice as many InlA^{m} *L. monocytogenes* were extracellular

compared to wild type *L. monocytogenes* EGDe, and it is possible that this was due to increased cellular damage in the inflamed gut. However, during infection with the wild type strain, we still found that the vast majority of *L. monocytogenes* in the MLN (70-80%) were extracellular, and the kinetics of systemic spread and clearance in peripheral tissues was similar to that previously published for the mouse-adapted strain (Bou Ghanem et al., 2012). We propose that extracellular localization of *L. monocytogenes* during the early stages of intestinal infection is a feature that is likely to be shared by all *L. monocytogenes* strains, and that the large proportion of extracellular bacteria in the gut may be involved in promoting dissemination.

Chapter 4: Monocytes are the predominant cell type associated with *Listeria monocytogenes* in the gut but they do not serve as an intracellular growth niche

The following chapter is modified from: Jones, G.S., and S.E. D'Orazio. 2017. Monocytes Are the Predominant Cell Type Associated with *Listeria monocytogenes* in the Gut, but They Do Not Serve as an Intracellular Growth Niche. *Journal of Immunology* 198:2796-2804.

I. Summary

After foodborne transmission of the facultative intracellular bacterial pathogen *L. monocytogenes*, most of the bacterial burden in the gut is extracellular. However, we previously demonstrated that intracellular replication in an as yet unidentified cell type was essential for dissemination and systemic spread of *L. monocytogenes*. Here, we show that the vast majority of cell-associated *L. monocytogenes* in the gut were adhered to Ly6C^{hi} monocytes, a cell type that inefficiently internalized *L. monocytogenes*. With bone marrow-derived *in vitro* cultures, high multiplicity of infection (MOI) or the use of opsonized bacteria enhanced uptake of *L. monocytogenes* in CD64-negative monocytes, but very few bacteria reached the cell cytosol. Surprisingly, monocytes that had up-regulated CD64 expression in transition towards becoming macrophages fully supported intracellular growth of *L. monocytogenes*. In contrast, "inflammatory" monocytes that increased CD64 expression in the bone marrow of BALB/c/By/J mice prior to *L. monocytogenes* exposure in the gut did not support *L. monocytogenes* growth. Thus, contrary to the perception that *L. monocytogenes* can infect virtually all cell types, neither naïve nor inflammatory Ly6C^{hi} monocytes served as a productive intracellular growth niche *L. monocytogenes.* These results have broad implications for innate immune recognition of *L. monocytogenes* in the gut and highlight the need for additional studies on the interaction of extracellular, adherent *L. monocytogenes* with the unique subsets of myeloid-derived inflammatory cells that infiltrate sites of infection.

II. Introduction

L. monocytogenes is a facultative intracellular bacterial pathogen that causes foodborne disease in humans. The primary virulence strategy of *L. monocytogenes* is thought to be the ability to invade mammalian cells. *L. monocytogenes* survive and

replicate inside a wide variety of cell types including epithelial cells (Gaillard et al., 1987), endothelial cells (Drevets et al., 1995), hepatocytes (Dramsi et al., 1995), lymphocytes (McElroy et al., 2009), cardiomyocytes (Alonzo et al., 2011), and neurons (Dramsi et al., 1998). *L. monocytogenes* induce uptake into non-phagocytic epithelial and endothelial cells using internalin A (InlA) and internalin B to interact with the mammalian receptors, E-cadherin and c-Met, respectively (Cossart et al., 2003). The pore-forming toxin listeriolysin O can promote uptake of *L. monocytogenes* during membrane repair of certain epithelial cells (Vadia et al., 2011), and other surface proteins and adhesins have also been implicated in the invasion of mammalian cells (Burkholder and Bhunia, 2010; Cabanes et al., 2005; Reis et al., 2010).

For myeloid-derived phagocytic cells, both ontogeny and activation status dictate whether a cell type can support intracellular replication of *L. monocytogenes.* For example*, L. monocytogenes* can grow in the cytosol of macrophages*,* but pre-treatment with inflammatory cytokines such as IFN-γ or TNF-α renders the cells bactericidal by efficiently retaining *L. monocytogenes* in the phagocytic vacuole (Biroum, 1977; Shaughnessy and Swanson, 2007). In contrast, neutrophils readily kill *L. monocytogenes* regardless of activation status (Arnett et al., 2014; Rogers and Unanue, 1993)*. L. monocytogenes* are less efficient at escaping from the vacuoles of bone marrow-derived, GM-CSF cultured dendritic cells (Westcott et al., 2010; Westcott et al., 2007). However, those cells do not closely resemble the conventional dendritic cell subsets observed *in vivo* (Helft et al., 2015) so it is not yet clear whether *L. monocytogenes* replicate in true dendritic cells.

Despite the species name “monocytogenes”, which refers to a robust monocytosis first observed in rabbits (Murray et al., 1926), there is little published data describing the direct interaction of *L. monocytogenes* with monocytes. An early study suggested that mononuclear cells isolated from human peripheral blood could slowly take up adherent *L. monocytogenes* and kill the bacteria, but the cells were only divided into two subsets: neutrophils and non-neutrophils (Peterson et al., 1977). More recently, Drevets et al. showed that most of the *L. monocytogenes*-associated cells in the blood after i.v. infection of mice were Ly6C^{hi} monocytes (Drevets et al., 2004), and that only cells with an altered phenotype that appeared late (72 h) after lethal injection could efficiently internalize the bacteria (Drevets et al., 2010). Monocytes are produced in the bone marrow, and rapid egress into the bloodstream during inflammation is dependent on expression of the chemokine receptor CCR2 (Serbina and Pamer, 2006).

Subsequent extravasation of Ly6C^{hi} monocytes into peripheral tissues is mediated by adhesion molecules such as CD11b, CD62L, and ICAM-1 (Lauvau et al., 2014). It was long thought that all bloodborne monocytes differentiated into tissue macrophages, however, recent studies indicate that subsets of monocytes can migrate through tissues and transport antigen to draining lymph nodes *without* differentiating into macrophages (Jakubzick et al., 2013; Rodero et al., 2015).

In the process of identifying infected cell types in the gut during foodborne listeriosis in susceptible BALB/c/By/J mice, we unexpectedly found that monocytes were by far the major cell type associated with *L. monocytogenes* during the early stages of infection. This prompted us to better characterize the phenotype of monocytes that infiltrated gut tissues and to determine the exact nature of their interaction with *L. monocytogenes.* We show here that neither naïve monocytes cultured *in vitro*, nor inflammatory monocytes isolated from *L. monocytogenes*-infected MLN serve as a productive replicative niche for *L. monocytogenes* despite the prevailing dogma that *L. monocytogenes* can invade and replicate in nearly all cell types.

III. Results

A. Ly6C^{hi} monocytes are the primary *L. monocytogenes*-infected cell type in the MLN

To identify infected phagocytes in the gut, mice were fed mouse-adapted *L. monocytogenes* that constitutively expressed GFP and MLN cells were analyzed 48 h post-infection (hpi). Previous work showed that 48 hpi was the earliest time point at which *L. monocytogenes* was consistently detected in the lymph nodes of all infected mice (Bou Ghanem et al., 2012). Myeloid cells were broadly subset into the following populations: Ly6C^{hi} (P1), Ly6G^{hi} (P2), Ly6C^{lo}CD11c^{hi} (P3), and Ly6C^{lo}CD11b^{+} (P4) (Fig. 4.1A). The remainder of the cells, which were mainly lymphocytes, were analyzed as P5. As shown in Fig. 4.1B, the number of Ly6C^{hi} P1 cells and Ly6G^{hi} P2 cells in the MLN increased 100-fold within 48 h of infection, indicating that these cells were part of the early inflammatory infiltrate. In contrast, the total number of P3 and P4 cells (mostly macrophages and dendritic cells) did not change considerably during the course of the infection (Fig. 4.1B).

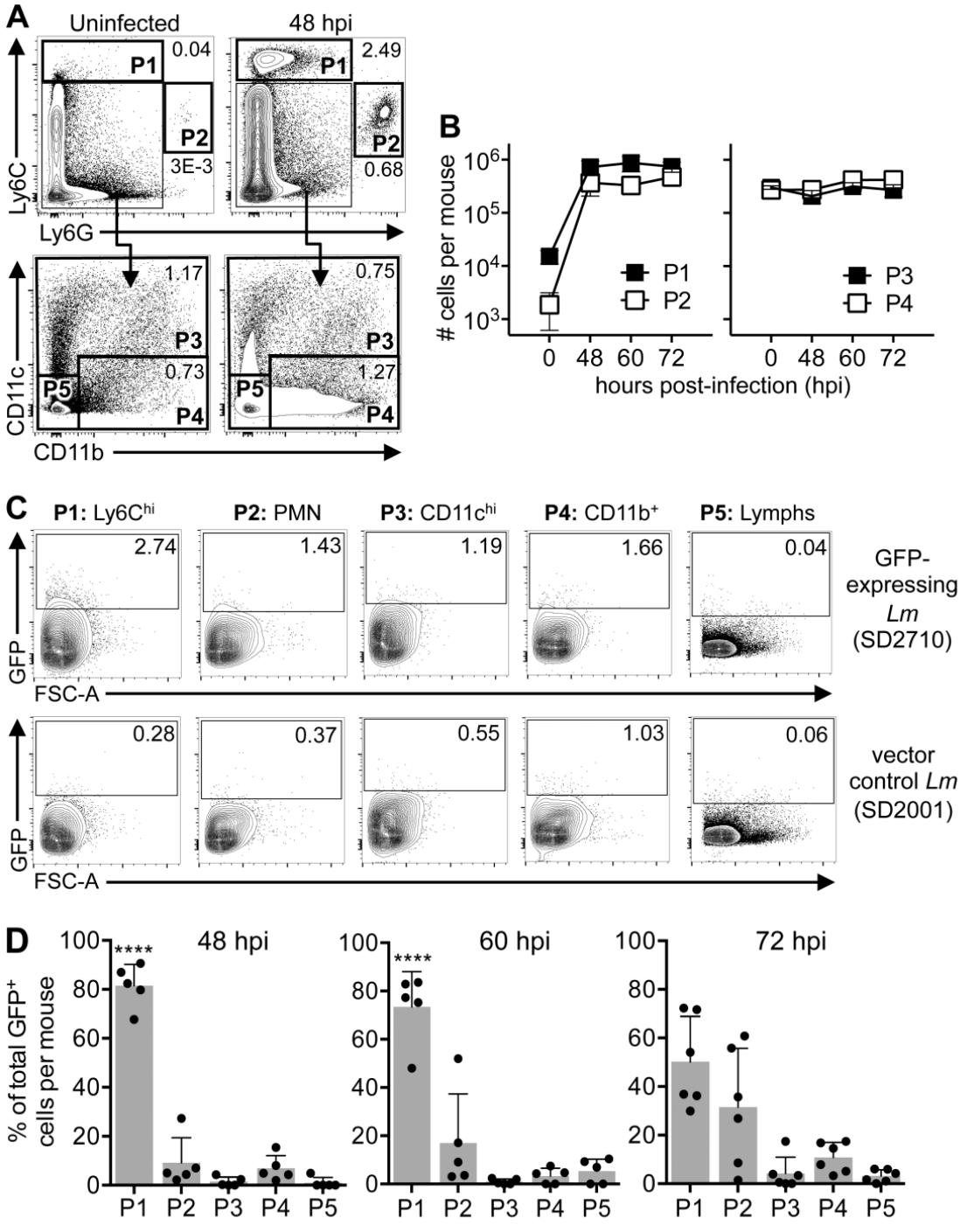
A
Uninfected
48 hpi
P1
P2
0.04
3E-3
2.49
0.68
Ly6C
Ly6G
1.17
0.73
0.75
1.27
P3
P4
P5
CD11c
CD11b
B
cells per mouse
10^6
10^5
10^4
10^3
P1
P2
P3
P4
0 48 60 72
hours post-infection (hpi)
C
P1: Ly6C^{hi}
P2: PMN
P3: CD11c^{hi}
P4: CD11b$^+$
P5: Lymphs
2.74
1.43
1.19
1.66
0.04
GFP-expressing *Lm* (SD2710)
GFP
FSC-A
0.28
0.37
0.55
1.03
0.06
vector control *Lm* (SD2001)
D
48 hpi
60 hpi
72 hpi
****
% of total GFP$^+$ cells per mouse
100
80
60
40
20
0
P1 P2 P3 P4 P5

Figure 4.1: Identification of *L. monocytogenes*-infected cells in the MLN using a flow cytometric approach.

(A) Gating scheme used to subset MLN populations (P1, P2, P3, P4, P5) in mice fed 10^8 CFU of mouse-adapted *Lm*. **(B)** Total number (±SEM) of cells in the MLN of uninfected (0 hpi) or infected mice (n=5). **(C)** Representative dot plots show how thresholds for GFP were set by comparison to cells from mice infected with *Lm* that lacked GFP (vector control strain). **(D)** Average proportion (±SD) of total GFP^+ cells in each population. Pooled data from 5 mice infected in two separate experiments was analyzed by one-way ANOVA with Tukey's multiple comparisons test.

GFP fluorescence was analyzed by comparison with cells isolated from mice fed an isogenic *L. monocytogenes* strain that lacked GFP (Fig. 4.1C). The vast majority (~80%) of all GFP^+ cells identified in the MLN 48 hpi were the $Ly6C^{hi}$ cells in the P1 gate (Fig. 4.1D). As the infection progressed, association with other cell types increased, but P1 remained the largest population of GFP^+ cells. Most of the P1 cells were $Ly6C^{hi}$ monocytes based on high expression of CD11b, intermediate F4/80 and CD64, and low CD11c (Fig. 4.2A). A minor proportion (~5-8%) of the P1 cells lacked CD11b, F4/80, and CD64 and expressed intermediate levels of CD11c and B220 (data not shown), a phenotype consistent with plasmacytoid dendritic cells. However, as shown in Fig. 4.2B, only the $Ly6C^{hi}CD11b^+$ monocytes, and not the plasmacytoid dendritic cells, were GFP^+. $Ly6C^{hi}$ cells also infiltrated the lamina propria (LP) of the large intestine 2 dpi (Fig. 4.2C) and approximately 1% of these cells were associated with GFP^+ *L. monocytogenes* (Fig. 4.2D). To confirm that the composition of the inflammatory infiltrate was not altered due to the use of murinized *L. monocytogenes* (Tsai et al., 2013), we performed similar analyses using mice fed wild type *L. monocytogenes* EGDe. As shown in Fig. 4.2E, similar numbers of P1, P2, P3, and P4 cells were found in the MLN. Furthermore, the predominant fraction of *L. monocytogenes*-infected (GFP^+) cells was $Ly6C^{hi}$ monocytes (Fig. 4.2F), and not the plasmacytoid DC (Fig. 4.2G). Therefore, at 48 hpi, the earliest time point *L. monocytogenes* can be detected in the MLN, the vast majority of the *L. monocytogenes*-associated cells were infiltrating $Ly6C^{hi}$ monocytes.

B. *L. monocytogenes* do not efficiently invade the cytosol of cultured monocytes

The flow cytometric approach shown in Fig. 4.1 demonstrated that *L. monocytogenes* associated with monocytes, but did not prove that the bacteria could survive and replicate in the cells. To test this, we cultured bone marrow cells with M-CSF (Fig. 4.3A), generating a mixture of cells that displayed the characteristic “waterfall of differentiation” (Tamoutounour et al., 2012) from $Ly6C^+CD64^{neg}$ monocytes (blue), $Ly6C^+CD64^+$ transitioning cells (orange), and $Ly6C^{neg}CD64^{hi}$ macrophages (black). Diff-Quik staining of sorted cells (Fig. 4.3B) revealed a classic kidney-shaped nucleus in the

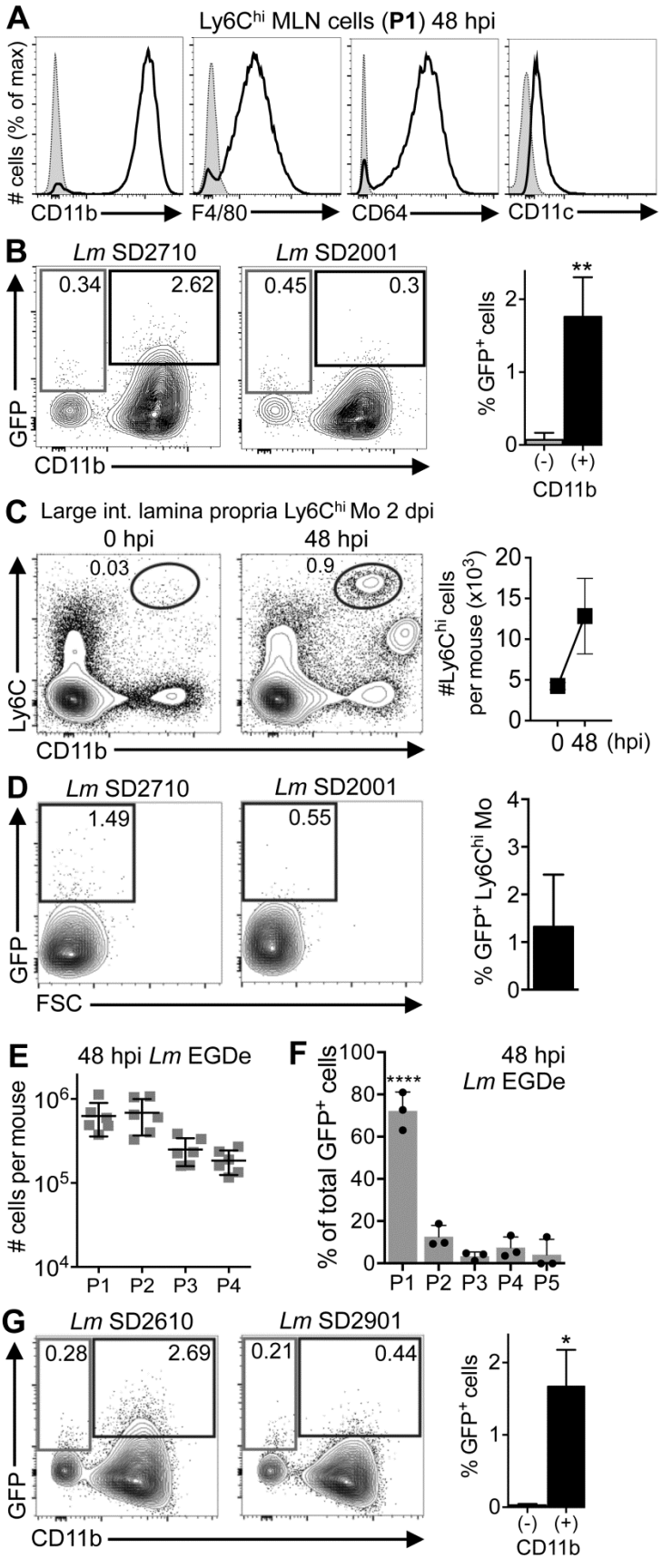
A
Ly6C^hi MLN cells (P1) 48 hpi
cells (% of max)
CD11b
F4/80
CD64
CD11c
B
Lm SD2710
Lm SD2001
0.34
2.62
0.45
0.3
GFP
CD11b
% GFP+ cells
**
(-) (+)
CD11b
C
Large int. lamina propria Ly6C^hi Mo 2 dpi
0 hpi
48 hpi
0.03
0.9
Ly6C
CD11b
#Ly6C^hi cells per mouse (x10^3)
0 48 (hpi)
D
Lm SD2710
Lm SD2001
1.49
0.55
GFP
FSC
% GFP+ Ly6C^hi Mo
E
48 hpi Lm EGDe
cells per mouse
P1 P2 P3 P4
F
48 hpi Lm EGDe
% of total GFP+ cells
****
P1 P2 P3 P4 P5
G
Lm SD2610
Lm SD2901
0.28
2.69
0.21
0.44
GFP
CD11b
% GFP+ cells
*
(-) (+)
CD11b

Figure 4.2: Ly6C^{hi}CD11b^{+} monocytes are the primary *L. monocytogenes*-infected cell type in the gut 48 hpi.

(A) Surface marker expression on P1 cells harvested from the MLN of infected mice; gray histograms are FMO controls. **(B)** Mean values (±SD) for GFP expression by CD11b^{+} vs CD11b^{neg} P1 cells (n=4). **(C)** Representative dot plots show the percentage of CD45^{+} cells in the large intestine LP that were Ly6C^{hi}CD11b^{+}; graph shows total (±SEM) number of Ly6C^{hi} monocytes in the LP of uninfected (0 hpi; n=4) or infected (48 hpi; n=8) mice. **(D)** Approximately 1% of the Ly6C^{hi}CD11b^{+} monocytes in the large intestine LP were GFP+ (n=8 mice). **(E-G)** Mice were fed 10^{9} CFU of wild type *Lm* EGDe and MLN populations were subset 48 hpi as shown in Fig. 4.1A. The total number of each population in the MLN **(E)**, the proportion of total GFP^{+} cells in each population **(F)**, and the CD11b phenotyping of the P1 cells **(G)** are shown. Data shown in panel F were analyzed by one-way ANOVA with Tukey's multiple comparisons test. Data in panels B & G were analyzed by unpaired two-tailed student's t-test.

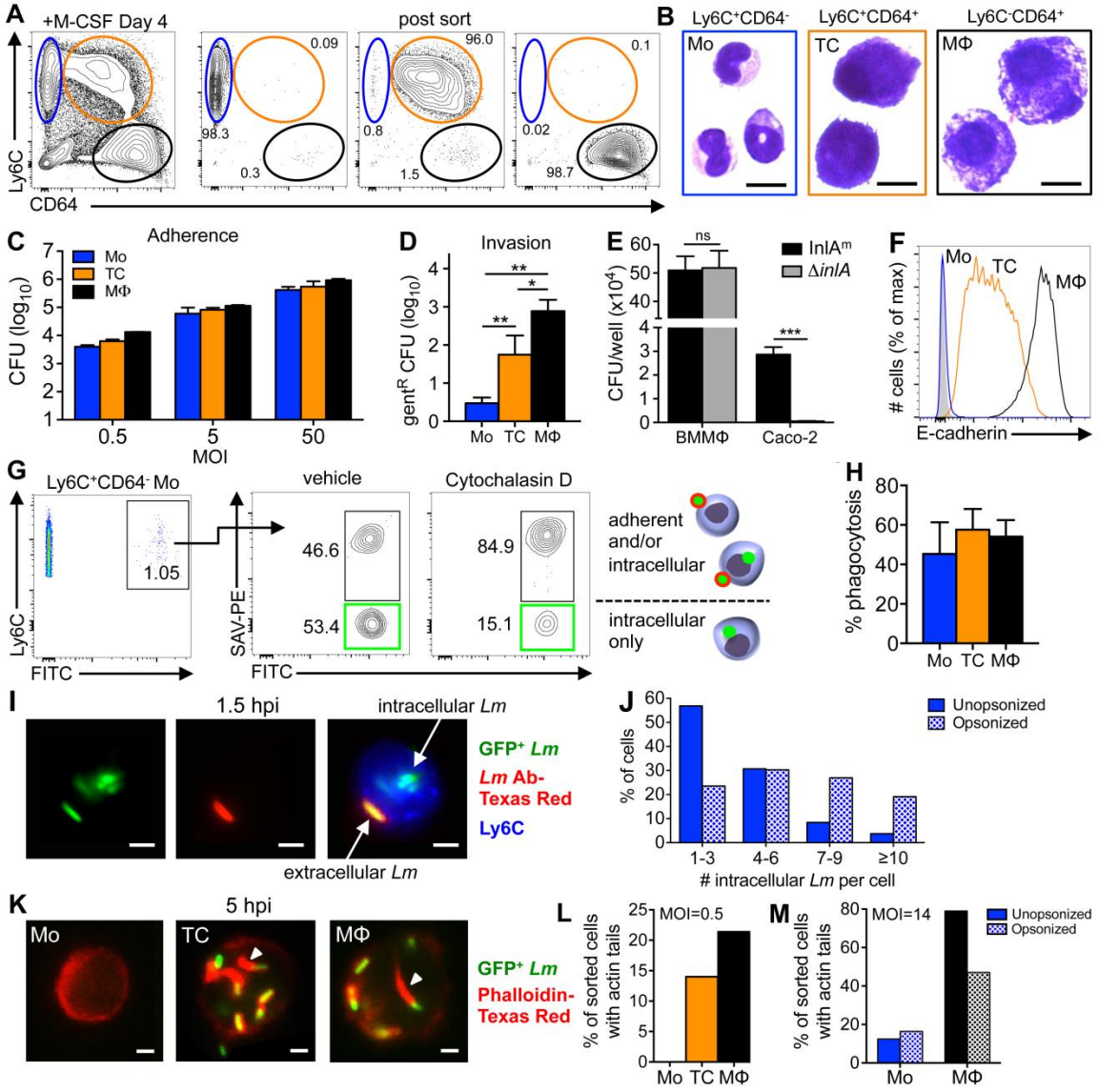
A
+M-CSF Day 4
post sort
Ly6C
CD64
0.09
98.3
0.3
96.0
0.8
1.5
0.1
0.02
98.7
B
Ly6C+CD64-
Ly6C+CD64+
Ly6C-CD64+
Mo
TC
MΦ
C
Adherence
CFU (log10)
Mo
TC
MΦ
0.5
5
50
MOI
D
Invasion
gentR CFU (log10)
Mo TC MΦ
E
ns
InlAm
ΔinlA
CFU/well (x10^4)
BMMΦ
Caco-2
F
Mo
TC
MΦ
cells (% of max)
E-cadherin
G
Ly6C+CD64- Mo
vehicle
Cytochalasin D
1.05
46.6
53.4
84.9
15.1
Ly6C
FITC
SAV-PE
adherent and/or intracellular
intracellular only
H
% phagocytosis
Mo TC MΦ
I
1.5 hpi
intracellular Lm
extracellular Lm
GFP+ Lm
Lm Ab-Texas Red
Ly6C
J
Unopsonized
Opsonized
% of cells
1-3
4-6
7-9
≥10
intracellular Lm per cell
K
5 hpi
Mo
TC
MΦ
GFP+ Lm
Phalloidin-Texas Red
L
MOI=0.5
% of sorted cells with actin tails
Mo TC MΦ
M
MOI=14
Unopsonized
Opsonized
% of sorted cells with actin tails
Mo
MΦ

Figure 4.3: *L. monocytogenes* inefficiently invade cultured CD64^{neg} monocytes.
(A) Bone marrow cultured with M-CSF for 4 days generated three CD117^{-} populations: monocytes (blue), transitioning cells (orange), and macrophages (black). Representative dot plots indicate the average purity of each population after sorting. **(B)** Diff-Quik staining of sorted cells. **(C)** Sorted monocytes, transitioning cells, and macrophages were infected with *Lm* SD2710 and the average number (±SD) of adherent CFU after washing was determined 1 hpi. **(D)** Total number (±SD) of intracellular (gentamicin$_{10}$-resistant) *Lm* SD2710 1 h after infection of sorted cells at a MOI of 0.5 (data from one of two separate experiments is shown). **(E)** Total number of intracellular (gent-resistant) *Lm* associated with triplicate wells of either macrophages (BMMΦ) or Caco-2 cells 1 hpi. **(F)** E-cadherin expression on BM-derived cells 4 days after *in vitro* culture. **(G)** Control plots for phagocytosis assay. Green boxes indicate cells that internalized all associated beads. **(H)** Percent complete phagocytosis (FITC^{+}PE^{-}) for each cell type 1 h after incubation with beads. **(I-J)** Sorted monocytes were infected with *Lm* SD2710 at a MOI of 14 for 90 min., washed 3 times, and then stained with *Lm*-specific antibodies. **(I)** Representative images of an infected monocyte show both green intracellular bacteria and yellow extracellular bacteria after merging green and red channels. **(J)** Number of intracellular *Lm* per monocyte with or without opsonization. **(K)** Representative images of sorted cells infected with *Lm* SD2710, fixed 5 hpi, and stained with phalloidin (red). Arrowheads indicate actin “tails”. **(L)** Sorted cells were infected for 5 h at low MOI (L) or high MOI with or without opsonization **(M)** Data from one of two separate experiments is shown; panels D & E were analyzed by two-tailed unpaired student’s t-test. Scale bars, 10 μm (B) or 2 μm (I & K).

monocytes, cytoplasmic vesicles in the larger macrophages, and an intermediate morphology for the transitioning cells.

First, we tested the ability of *L. monocytogenes* to adhere to each of these three cell types. Sorted cells were infected at various MOI for one hour, washed extensively and then plated for CFU. As shown in Fig. 4.3C, all three cell types displayed a dose-dependent association with *L. monocytogenes*. To assess invasion, the sorted cells were infected at a MOI of 0.5 for 1 h, washed, and then treated with gentamicin for 20 minutes prior to plating. As expected, a large proportion of the inoculum invaded the $Ly6C^{neg}CD64^{hi}$ macrophages (Fig. 4.3D). However, few gentamicin-resistant CFU were recovered from the monocytes, suggesting that either *L. monocytogenes* inefficiently invaded or were unable to survive inside the cells. Interestingly, there was a significantly higher number of gentamicin-resistant *L. monocytogenes* in the transitioning cells (Fig. 4.3D), indicating that monocytes can become a replicative niche for *L. monocytogenes* prior to becoming *bona fide* macrophages.

The *L. monocytogenes* surface protein InlA promotes invasion of non-phagocytic cells after interacting with its mammalian receptor, E-cadherin (Gaillard et al., 1991; Lecuit et al., 1999a) and it was previously suggested that InlA could also enhance the invasion of macrophage cell lines (Sawyer et al., 1996). We examined the ability of InlA-deletion mutant (Δ*inlA*) *L. monocytogenes* to invade $CD64^+$ macrophages, but found that InlA was not required for invasion (Fig. 4.3E). However, macrophages express multiple receptors that can promote uptake of bacteria, so it is possible that the loss of one ligand would not greatly alter invasion rates. Cultured $CD64^+$ macrophages expressed high levels of E-cadherin, and the transitioning cells expressed intermediate levels of E-cadherin (Fig. 4.3F). In contrast, cultured monocytes did not express any detectable E-cadherin on the cell surface. Thus, the level of E-cadherin on the cultured cells correlated directly with invasion efficiency.

To evaluate phagocytic capacity, we incubated the cultured cells with biotin-conjugated, green fluorescent beads for one hour and then counterstained with PE-conjugated streptavidin. To promote complete phagocytosis, a low bead-to-cell ratio of 0.5 was used, resulting in ~1% $FITC^+$ monocytes (Fig. 4.3G), which were then analyzed for PE expression. As expected, pre-treatment with cytochalasin D, an inhibitor of actin dynamics, reduced the proportion of cells with only internalized beads (green gate; $FITC^+PE^-$) and increased the percentage of cells that had adherent beads ($FITC^+PE^+$). As shown in Fig. 4.3H, there was no significant difference in the percentage of beads

internalized by cultured monocytes, transitioning cells, or macrophages. This suggested that monocytes should be capable of internalizing *L. monocytogenes*, even if they lack receptors to enhance phagocytosis. To find out if *L. monocytogenes* could invade monocytes, cultured $Ly6C^{+}CD64^{neg}$ cells were exposed to GFP-expressing bacteria at a higher MOI for a longer period of time (90 min.). The cells were then washed extensively and stained with TexasRed® conjugated *L. monocytogenes*-specific antibodies. Because the cells were not permeabilized, only extracellular bacteria bound the antibody, allowing us to use microscopy to differentiate between intracellular *L. monocytogenes* (green) and adherent, extracellular organisms (yellow) (Fig. 4.3I). Approximately half of the 258 monocytes we examined contained at least one intracellular bacterium at this time point (data not shown). Pre-treatment of the bacteria with normal mouse serum did not change the percentage of cells that contained intracellular *L. monocytogenes* (not shown); however, opsonization did cause an increase in the number of bacteria found inside each monocyte (Fig. 4.3J).

To track the fate of internalized *L. monocytogenes* in each cell type, sorted cells were infected *in vitro* for 1 hour, washed and then incubated for an additional 4 hours in media containing gentamicin. The cells were then stained with phalloidin and microscopy was used to co-localize GFP^{+} bacteria with cytosolic actin "tails" (Fig. 4.3K). Five hours after infection at low MOI, very few monocytes were associated with *L. monocytogenes*; however, cytosolic *L. monocytogenes* with actin tails were observed in both the transitioning cells and the macrophages (Fig. 4.3L). Increasing the MOI to promote enhanced invasion of the monocytes resulted in cytosolic localization of *L. monocytogenes* in 12% of the monocytes, compared to 79% for macrophages (Fig. 4.3M). Opsonization of the bacteria did not change the intracellular fate in monocytes, but did result in decreased numbers of actin tails in the cytosol of macrophages. Together, these data suggested that monocytes can take up *L. monocytogenes*, albeit less efficiently than transitioning cells or macrophages, but that escape to the cytosol was an infrequent occurrence.

C. Monocytes that infiltrate the MLN have a partially differentiated and partially activated phenotype.

Expression of CD64 (FcγR1) and down-regulation of Ly6C are commonly used surface phenotypes that signify progression of monocytes through the differentiation pathway towards becoming macrophages (Gautier et al., 2012). In a naïve animal, the largest number of monocytes are found in the bone marrow, but the few $Ly6C^{hi}CD11b^{+}$ cells present in the MLN were negative for CD64 or expressed only low levels when analyzed directly *ex vivo* (Fig. 4.4A), similar to the phenotype of cultured monocytes. However, "inflammatory" monocytes recruited to the MLN 2 dpi uniformly expressed increased levels of CD64 (Fig. 4.4A). The small size and the shape of the nuclei of these cells was suggestive of a monocyte morphology (Fig. 4.4B), but the increased expression of E-cadherin was suggestive of a transitioning cell (Fig. 4.4C). Many of the monocytes displayed increased expression of MHC-II on the cell surface (Fig. 4.4D) and a subset of the cells were producing iNOS (Fig. 4.4E). However, the phagocytic capacity of inflammatory monocytes sorted from the MLN was only half that of naïve $Ly6C^{hi}$ monocytes that had yet to leave the bone marrow of uninfected mice (Fig. 4.4F). Thus, $Ly6C^{hi}$ inflammatory monocytes that infiltrated the MLN during infection had a unique, partially differentiated and partially activated phenotype that did not precisely resemble either monocytes or macrophages cultured *in vitro* or naïve monocytes analyzed directly *ex vivo*.

D. Inflammatory monocytes are activated prior to egress from the bone marrow

Askenase *et al.* recently showed that systemic circulation of IL-12, produced in response to intestinal infection with the intracellular parasite *Toxoplasma gondii*, resulted in changes to $Ly6C^{hi}$ monocytes while the cells were still in the bone marrow, before they infiltrated the intestinal lamina propria (Askenase et al., 2015). Likewise, we noticed during the course of these studies that $Ly6C^{hi}$ monocytes in the bone marrow had an altered phenotype during *L. monocytogenes* infection. Two days after foodborne transmission, nearly all of the $Ly6C^{hi}$ monocytes in the bone marrow expressed moderate levels of CD64 and 50-60% of the $cKit^{+}Ly6C^{hi}CD11b^{neg}$ monocyte progenitors in the bone marrow had also up-regulated CD64 (Fig. 4.5A). Likewise, about 10% of the mature monocytes still present in the bone marrow of infected mice had increased levels

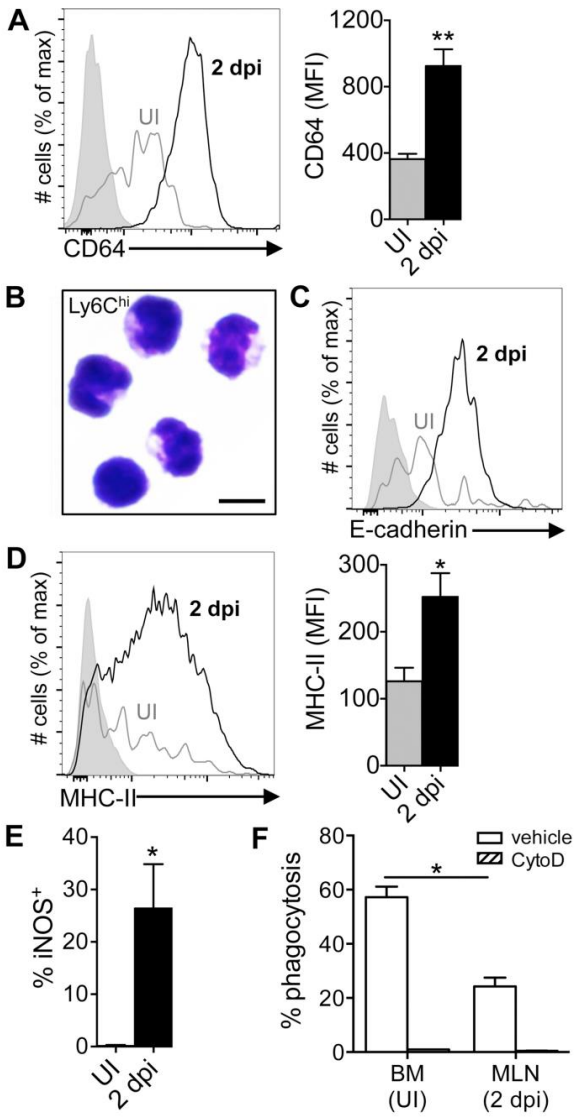

Figure 4.4: Inflammatory monocytes analyzed directly *ex vivo* have a partially differentiated and partially activated phenotype.

Mice were fed 10^8 CFU of *Lm* SD2710 (n=6) or left uninfected (UI; n=3) and MLN were analyzed 48 h later. **(A)** Representative histogram and MFI (±SD) of CD64 expression on $Ly6G^-Ly6C^{hi}CD11b^+$ monocytes. **(B)** Diff-Quik staining (100x) of inflammatory monocytes sorted from MLN 2 dpi; scale bar, 10 µm. **(C)** Representative E-cadherin expression on monocytes. **(D)** Representative histogram and MFI (±SD) of MHC-II expression. **(E)** Percentage of iNOS-producing $Ly6C^{hi}$ monocytes in the MLN. **(F)** Uptake of fluorescent beads by $Ly6C^{hi}$ monocytes from the bone marrow of uninfected mice or MLN of infected mice (n=6).

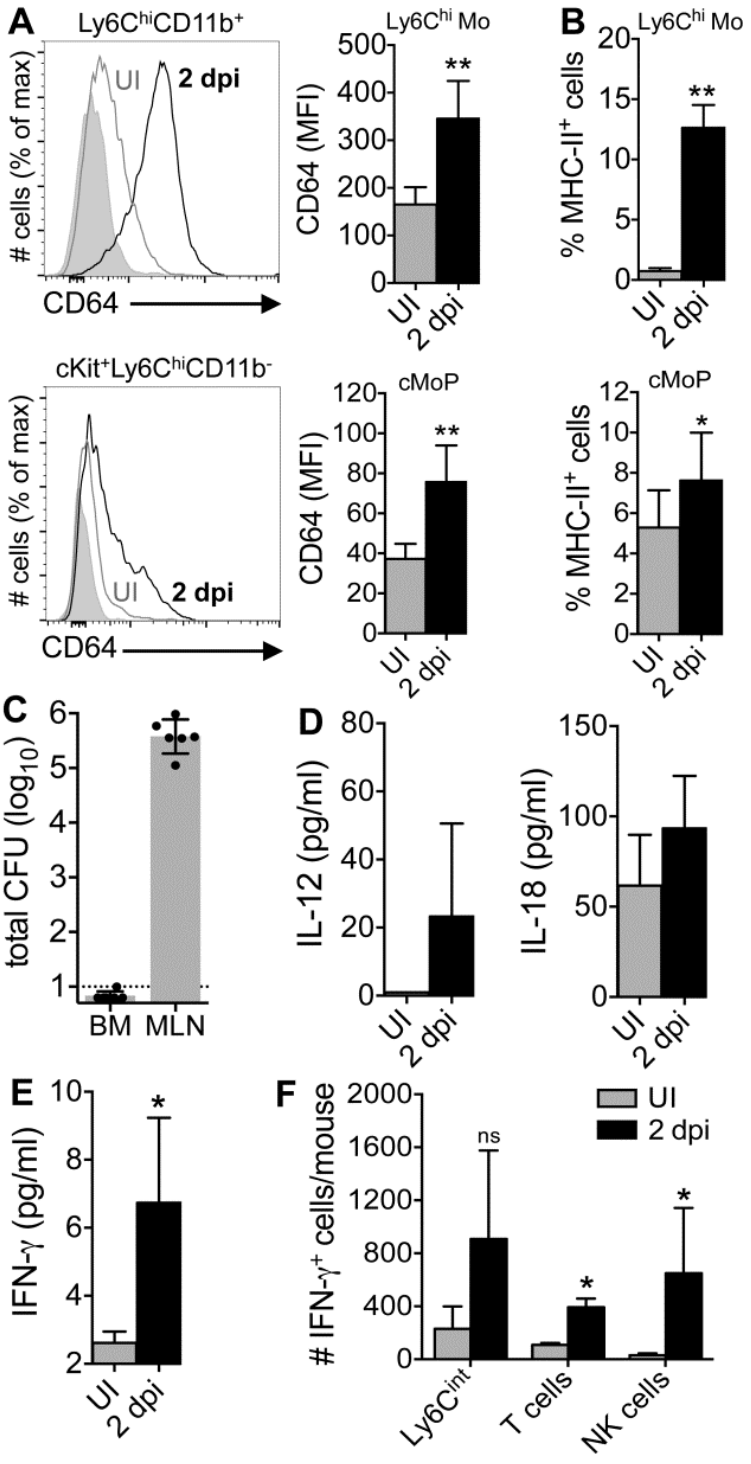
A
Ly6C^hiCD11b^+
UI
2 dpi
cells (% of max)
CD64
Ly6C^hi Mo
CD64 (MFI)
**
UI
2 dpi
B
Ly6C^hi Mo
% MHC-II^+ cells
**
cKit^+Ly6C^hiCD11b^-
cMoP
*
C
total CFU (log10)
BM
MLN
D
IL-12 (pg/ml)
IL-18 (pg/ml)
E
IFN-γ (pg/ml)
F
IFN-γ^+ cells/mouse
ns
Ly6C^int
T cells
NK cells

Figure 4.5: Inflammatory monocytes are activated prior to egress from the bone marrow.

Bone marrow (BM) from uninfected mice (UI) or mice fed 10^8 CFU of *Lm* SD2710 was analyzed 2 dpi (n=6). **(A)** CD64 expression on Ly6C^{hi} monocytes (Mo) and common monocyte progenitors (cMoP) (Hettinger et al., 2013). **(B)** Mean percentage (±SD) of MHC-II$^+$ Ly6C^{hi} Mo and cMoP. **(C)** BM harvested from both femurs and tibias was plated and *Lm* CFU were determined 2 dpi (n=6). **(D)** Mean concentration (±SD) of IL-12 and IL-18 in mouse sera (n=4). **(E)** Mean concentration of IFN-γ (±SD) in the bone marrow *without in vitro* stimulation (n=4). **(F)** Representative contour plots of cell populations isolated from the bone marrow of either uninfected or 2 dpi mice showing the percentage of IFN-γ$^+$ cells. Bar graphs to the right indicate mean number (±SD) of IFN-γ$^+$ Ly6C^{int}, T cells, or NK cells in the BM (n=4). Two-tailed Mann-Whitney tests were used for statistical analysis.

of MHC-II compared to uninfected mice (Fig. 4.5B). These data suggested that a stimulus present in the bone marrow was altering the differentiation of monocytes during infection compared to the steady state.

High dose i.v. infection leads to the presence of *L. monocytogenes* in the bone marrow (de Bruijn et al., 1998; Join-Lambert et al., 2005) so it was feasible that the bacteria could directly activate monocytes. To test this, mice were fed *L. monocytogenes* and 2 days later, the marrow from both femurs and tibias was collected and plated for CFU. As shown in Fig. 4.5C, only one out of six mice had detectable *L. monocytogenes*, and that mouse had only a single CFU present in the total marrow collected. In contrast, more than 100,000 total CFU were recovered from the MLN of those same mice at that time point. Although we did not detect live *L. monocytogenes* in the bone marrow, it was possible that *L. monocytogenes* replicating in the gut could cause systemic circulation of infection-induced cytokines IL-12 and/or IL-18 that could then stimulate IFN-γ production in the bone marrow. We found small increases in both serum IL-12 and serum IL-18 during foodborne infection, but neither of these changes were statistically significant (Fig. 4.5D). Nonetheless, the concentration of IFN-γ detected in the bone marrow increased about 3-fold during infection (Fig. 4.5E). Multiple cell types present in the bone marrow were actively secreting IFN-γ during *L. monocytogenes* infection (Fig. 4.5F), suggesting that the IFN-γ was produced locally. Together, these observations suggested that intestinal infection generated systemic mediators that caused both developing and mature Ly6C^{hi} monocytes in the bone marrow to have an inflammatory phenotype, prior to recruitment to *L. monocytogenes*-infected tissues.

E. *L. monocytogenes* adhere to, but do not efficiently invade inflammatory monocytes.

To find out if *L. monocytogenes* invaded inflammatory monocytes *in vivo*, Ly6C^{hi} cells were sorted from the MLN two days after mice were fed GFP^{+} *L. monocytogenes* and the cells were examined microscopically (Fig. 4.6A). Approximately 7% of the 4,024 sorted monocytes examined (pooled data from 6 different mice) were associated with GFP^{+} *L. monocytogenes* (Fig. 4.6B). The flow cytometric approach used previously identified only ~2% of the Ly6C^{hi} cells as GFP^{+} (Fig. 4.2C). The 3.5-fold difference in these results is likely due to issues with autofluorescence that led us to apply a rigorous threshold to the bulk population in order to definitively label a cell as GFP^{+} by flow

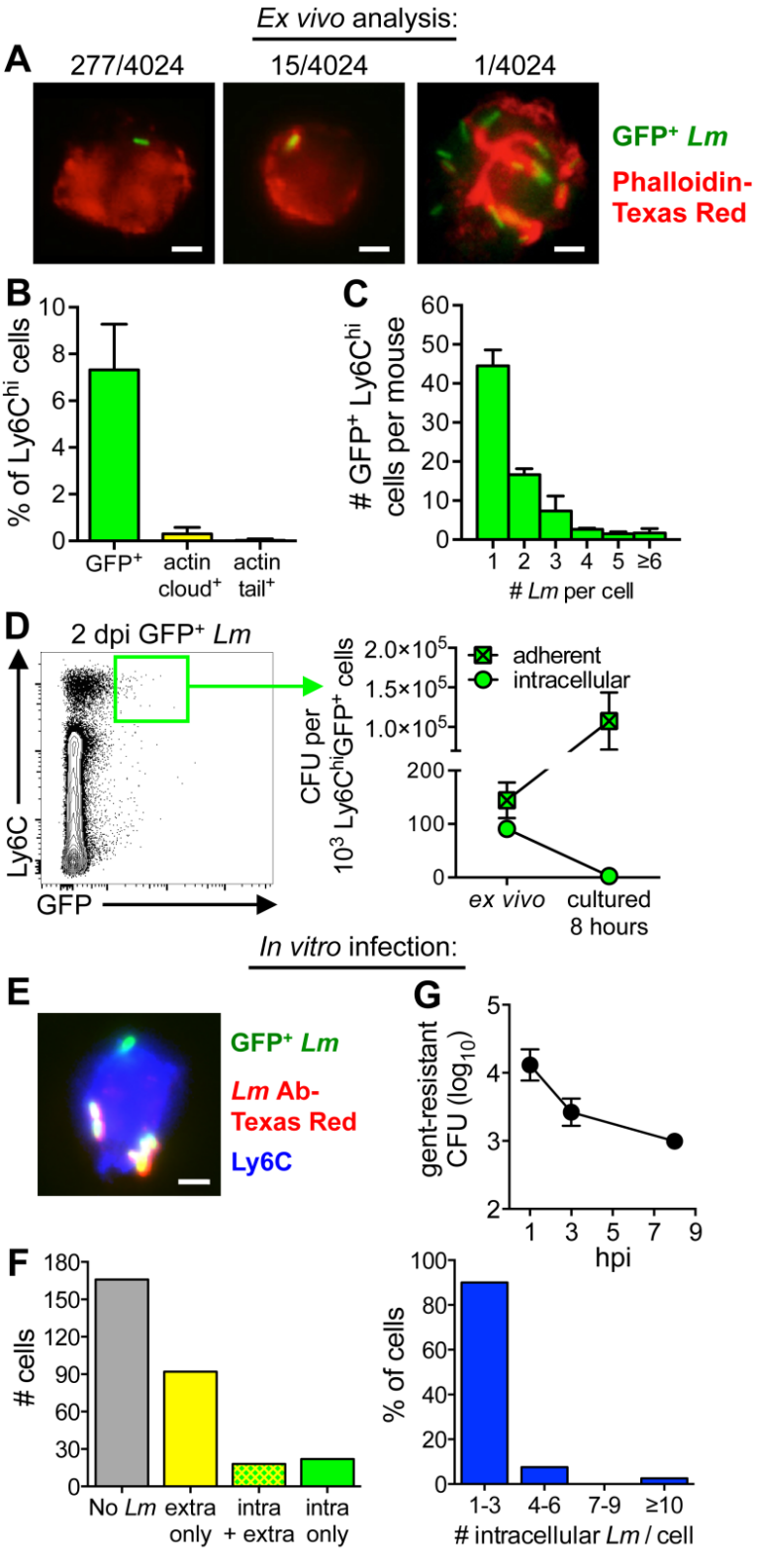
Ex vivo analysis:
A
277/4024
15/4024
1/4024
GFP+ Lm
Phalloidin-Texas Red
B
% of Ly6Chi cells
GFP+
actin cloud+
actin tail+
C
GFP+ Ly6Chi cells per mouse
Lm per cell
D
2 dpi GFP+ Lm
Ly6C
GFP
CFU per 10^3 Ly6ChiGFP+ cells
adherent
intracellular
ex vivo
cultured 8 hours
In vitro infection:
E
GFP+ Lm
Lm Ab-Texas Red
Ly6C
G
gent-resistant CFU (log10)
hpi
F
cells
No Lm extra only
intra + extra
intra only
% of cells
# intracellular Lm / cell

Figure 4.6: Inflammatory monocytes do not productively support intracellular growth of *L. monocytogenes.*

(A-C) Ly6C^{hi} cells were sorted from the MLN 2 d after infection with *Lm* SD2710 and visualized directly ex vivo. **(A)** A total of 4,024 cells from 6 different mice (200-800 cells /mouse) were visualized. Representative images and the total number of *Lm*-associated (GFP+), actin cloud+ cells or actin tail+ cells observed are shown. **(B)** Mean percentage (±SD) of *Lm*-associated monocytes per mouse (n=6). **(C)** Average number (±SD) of *Lm* per GFP^{+} cell. **(D)** GFP^{+} Ly6C^{hi} cells were sorted from the MLN 2 dpi (green gate) and the mean number of adherent or intracellular (gent$_{10}$-resistant) CFU (±SD) was determined directly ex vivo or after being cultured for 8 h in media with or without gentamicin. **(E-F)** Ly6C^{hi} cells (1 x 10^5/well) were sorted from the MLN 2 dpi with *Lm* SD2001 and infected in vitro for 90 min with *Lm* SD2710 at a MOI of 2. **(E)** Representative image for "in/out" differential staining shows a cell with both intracellular and extracellular *Lm*; scale bar, 2 μm. **(F)** A total of 300 cells were visualized; left graph indicates the number of uninfected cells (gray bar), cells with only extracellular *Lm* (yellow bar), cells with both intracellular and extracellular *Lm* (green/yellow bar), or cells with only intracellular bacteria (green bar). Graph on the right indicates the number of intracellular *Lm* observed per cell. **(G)** Intracellular growth assay performed on sorted GFP^{neg} Ly6C^{hi} cells (5 x 10^4/well) infected in vitro for 1 h at MOI of 2.

cytometry. The majority of monocytes associated with GFP$^+$ *L. monocytogenes* had only one or two bacteria per cell (Fig. 4.6C). Fifteen of the monocytes (0.4%) contained *L. monocytogenes* surrounded by an actin "cloud" (Tilney and Portnoy, 1989) and only one cell (0.02%) had actin tails. However, since the sort purity of the Ly6C^{hi} cells recovered from each mouse was only ~97-99%, it possible that the cell containing *L. monocytogenes* co-localized with actin was a contaminating macrophage-like cell.

To verify that *L. monocytogenes* could inefficiently invade, but not survive within inflammatory monocytes, GFP$^+$ Ly6C^{hi} cells were sorted from the MLN 2 dpi (Fig. 4.6D) and the number of intracellular and extracellular *L. monocytogenes* associated with those cells was determined by incubating the sorted cells with or without gentamicin for 20 minutes and then lysing and plating. Due to the small number of cells recovered in this experiment, the sort purity was not determined. As shown in Fig. 4.6D, ~38% of the total cell-associated CFU was intracellular (gentamicin-resistant) directly ex vivo. A portion of the sorted cells were further incubated for 8 hours with or without gentamicin to find out if intracellular (gentamicin-resistant) *L. monocytogenes* would replicate, or if only the adherent CFU increased over time. As shown in Fig. 4.6D, the total number of adherent CFU in each well increased ~500-fold. However, no intracellular (gentamicin-resistant) CFU were detected 8 hours after plating the sorted cells.

To further assess the ability of inflammatory monocytes to support intracellular growth, we sorted cells from the MLN of mice infected with *L. monocytogenes* lacking GFP and then exposed the cells *in vitro* to GFP-expressing bacteria for 90 min. and performed differential staining to identify intracellular and extracellular *L. monocytogenes* (Fig. 4.6E). As shown in Fig. 4.6F, 40 of the 300 cells visualized (13%) contained at least one intracellular bacterium, with most harboring 1-3 intracellular bacteria per cell. Thus, invasion of the inflammatory monocytes was less efficient than observed for naïve cultured monocytes (Fig. 4.3), consistent with the reduced phagocytic capacity of these cells (Fig. 4.6F). The number of gentamicin-resistant intracellular *L. monocytogenes* in the inflammatory monocytes steadily decreased over time (Fig. 4.6G). Thus, the majority of the Ly6C^{hi} inflammatory monocytes recruited to the MLN and analyzed directly *ex vivo* had only adherent *L. monocytogenes*, and the few bacteria that invaded these cells did not survive.

IV. Discussion

The results presented here highlight two important findings. First, within 48 hours of foodborne infection, the majority of myeloid-derived cells in the MLN are “inflammatory monocytes” that have been pre-activated in the bone marrow prior to *L. monocytogenes* exposure. These cells did not precisely resemble any cell type that can be cultured directly from bone marrow using only growth factors such as CSF-1 or GM-CSF, or the cells that are present in the steady state in an uninfected animal. Second, although *L. monocytogenes* is equipped for intracellular growth, the majority of cell-associated *L. monocytogenes* in the gut following foodborne infection were extracellular (Jones et al., 2015), presumably adhered to monocytes, a cell type that inefficiently internalized *L. monocytogenes*. Very few *L. monocytogenes* were associated with cells expressing markers typical of classical macrophages and DC. This observation has implications for innate immune recognition of *L. monocytogenes,* because there are a large number of genes that differ in expression level in monocytes compared to macrophages (Hume et al., 2016).

It was previously reported that InlA/E-cadherin interaction was important for invasion of macrophage-like cell lines (Sawyer et al., 1996); however, we found that Δ*inlA L. monocytogenes* were internalized efficiently in both bone marrow-derived macrophages (Fig. 4.3E) and THP-1 cells (data not shown). Interaction with E-cadherin could enhance uptake of *L. monocytogenes* in macrophages, but may not be required because the cells express a variety of other receptors that can trigger phagocytosis, including Gp96 and scavenger receptors class A (Cabanes et al., 2005; Ishiguro et al., 2001). In contrast, monocytes lack all three of these receptors based on data presented here and previous studies (Geng et al., 1994; Wolfram et al., 2013). Intriguingly, CD64 was shown to mediate the uptake of *L. monocytogenes* in an IgG-independent manner (Perelman et al., 2016), which could explain why CD64 expression was correlated with *L. monocytogenes* infection in our study. However, it is important to mention this CD64-mediated uptake of *L. monocytogenes* only occurred with human, and not mouse monocytes, therefore negating this possible mechanism (Perelman et al., 2016). We propose that *L. monocytogenes* can readily adhere to monocytes and that this attachment is mediated primarily by non-specific bacterial adhesins or pili. However, because they lack sufficient expression of surface receptors that can trigger cytoskeletal rearrangements to promote particle uptake, few adhered *L. monocytogenes* are

internalized by monocytes unless they are opsonized by specific antibodies or complement.

The microscopy studies presented here suggest that the few *L. monocytogenes* that do invade monocytes cannot escape into the cytosol. This is in agreement with Raybourne et al. who suggested that human blood monocytes could not support the growth of *L. monocytogenes* over time (Raybourne et al., 2001). It is possible that activity of the pore-forming toxin LLO is impaired in monocytes. The kinetics of phagosome acidification in murine monocytes has not been tested. However, the phagosomes of freshly-isolated human monocytes acidified to a pH of only 5.7 to 5.9 after phagocytosis of live *E. coli* (Horwitz and Maxfield, 1984) and LLO has a pH optimum of ~5.5 (Geoffroy et al., 1987). Westcott et al. further showed that vacuoles in murine monocyte-derived GM-CSF-cultured DC acidified at a slower rate than macrophage phagosomes (Westcott et al., 2010). Thus, it is possible that delayed or reduced acidification of the phagosome could reduce the efficiency of *L. monocytogenes* escape in monocytes.

It is likely that at least some of the $Ly6C^{hi}$ monocytes we analyzed ex vivo were in the process of differentiating into "Tip-DCs" as approximately 20-25% of the inflammatory monocytes were already producing iNOS. The nomenclature of "Tip-DCs" has been debated (Guilliams et al., 2014); it may be inaccurate to define "Tip-DCs" as a subset of dendritic cells, but it is clear that the production of TNF-α and iNOS by these cells is critical for clearance of *L. monocytogenes* (Serbina et al., 2003b). In agreement with our study, Shi et al. showed that $CCR2^{+}Ly6C^{hi}$ cells surrounded foci of infection in the liver following i.v. infection, and very few of those monocyte-derived cells harbored viable *L. monocytogenes* (Shi et al., 2010).

Despite the predominant monocyte infiltrate in the gut, the total number of $Ly6C^{lo}CD64^{+}$ macrophages did not change significantly during the first three days following foodborne *L. monocytogenes* infection. This suggests that monocytes recruited to the MLN were not differentiating into classical macrophages during this timeframe. This finding is in agreement with Bain et al., who used a DSS-induced model of colitis to show that maturation of $Ly6C^{hi}$ monocytes recruited to the intestinal LP was disrupted during inflammation (Bain et al., 2013). In addition, Rydström and Wick showed that the differentiation of $Ly6C^{hi}$ monocytes was inhibited following exposure to *Salmonella,* a process that was dependent on MyD88 signaling (Rydstrom and Wick, 2010).

The terms monocyte, macrophage, inflammatory monocyte and inflammatory macrophage have been used variously over the past few decades to describe myeloid-derived cell populations. Although the nomenclature is evolving, more definitive labels for cell subsets will probably require the use of better markers that correlate with cell function, rather than just surface marker expression (Hume et al., 2016). However, what is clear now is that bone marrow-derived macrophages and DC do not closely resemble the majority of cells that *L. monocytogenes* encounter *in vivo* in the gut and that very few *L. monocytogenes* replicate within phagocytes during the intestinal phase of the infection. Future studies should focus on the interactions of these unique subsets of inflammatory cells with extracellular bacteria, rather than cytosolic bacteria in macrophages, in order to define the earliest innate immune activation events that occur following foodborne *L. monocytogenes* infection in mice.

Chapter 5: Intracellular growth of *Listeria monocytogenes* inside dendritic cells is ontogeny-dependent

I. Summary

Intracellular replication of *L. monocytogenes* is thought to be most efficient in macrophage-like cells, and thus, it is commonly believed that all types of mononuclear phagocyte can support *L. monocytogenes* growth to some degree. However, remarkably little is known about the growth of *Listeria* in the distinct subsets of mononuclear phagocytes found *in vivo*. This led us to investigate which myeloid cells were associated with *L. monocytogenes* during the gastrointestinal stage of infection. The majority of cell-associated *Listeria* in the gut two days after foodborne infection were associated with neutrophils, whereas, only a minor fraction of myeloid cells with a tissue-resident phenotype were *L. monocytogenes*$^{+}$. *In vitro* infection of myeloid cells isolated from either the intestinal LP or MLN indicated that myeloid cells harvested from the MLN better supported the intracellular growth of *L. monocytogenes*. We previously showed that intracellular replication was crucial for spread to the MLN, and thus, we hypothesized than migratory DC served as an intracellular niche for *L. monocytogenes* in the MLN. However, *Listeria* inefficiently invaded and did not replicate inside DC isolated from the gut. Therefore, we focused on the growth of *L. monocytogenes* inside cultured DC that phenotypically resemble DC found in the gut. Unlike the gut-derived DC, the conventional method of generating "DC" using GM-CSF resulted in CD11c^{+} cells that fully supported the intracellular replication of *L. monocytogenes.* Interesting, we found that prolonged growth in GM-CSF-cultured CD11c^{+} cells was associated with enhanced growth of *L. monocytogenes.* We observed a similar result using FLT3-L to generate CD103^{+}CD11c^{+} cells, but overall, these cells were less efficient at supporting the growth of *L. monocytogenes* compared to GM-CSF-cultured cells. Together, our data indicate that DC vary in their ability to support the intracellular life cycle of *L. monocytogenes,* which was somewhat dependent on ontogeny and culture duration. These results highlight the need for additional studies on the interaction of *L. monocytogenes* with the unique subsets of mononuclear phagocytes that exist *in vivo*.

II. Introduction

The interaction of *L. monocytogenes* with DC found *in vivo* remains largely undefined, and practically nothing is known about the direct infection of DC after oral infection. Most of what is known about the growth of *L. monocytogenes* inside DC is derived from either bone marrow-derived cells cultured in the presence of GM-CSF, or inferred from systemic infection of mice in which DC have been ablated. Here, we describe the interaction of *L. monocytogenes* with DC in the gut during foodborne infection compared to bone marrow-derived DC generated using various culture methods.

Early studies indicated that GM-CSF was an important media component for generating human and mouse DC *in vitro* (Inaba et al., 1992; Reid et al., 1992; Sallusto and Lanzavecchia, 1994; Scheicher et al., 1992), which were originally thought to be derived from monocytes (see Fig. 5.1) (Chapuis et al., 1997; Schreurs et al., 1999). The resulting cell populations predominantly expressed intermediate to high levels of the integrin CD11c and MHC-II. Bone marrow cells cultured in the presence of GM-CSF have been commonly used as tool by immunologists due to their ability to efficiently internalize and present antigen to CD4 T cells, cross-present antigen to CD8 T cells, as well as efficiently driving T cell proliferation. As a result, the nomenclature of $CD11c^+$ GM-CSF-derived cells is often synonymous with a prototypic DC. However, it is now appreciated that DC can arise from either circulating monocytes or common dendritic progenitors in the bone marrow (Naik et al., 2007; Onai et al., 2007; Randolph et al., 1999). Activation of Flt3 receptor by FLT3-L promotes the differentiation of committed DC progenitors into conventional DC and plasmacytoid DC (see Fig. 5.1) (McKenna et al., 2000; Naik et al., 2007; Onai et al., 2007). The use of FLT3-L to generate DC from bone marrow progenitors is relatively recent (compared to the gold standard of GM-CSF) and is used to generate $CD8\alpha^+$ conventional DC (Brasel et al., 2000; Naik et al., 2005). Furthermore, *in vivo* treatment with FLT3-L induces the expansion of cDC in both non-lymphoid and lymphoid organs including the gut lamina propria (Cerovic et al., 2013; Maraskovsky et al., 1996).

It is thought that $CD8\alpha^+$ DC found in lymphoid organs are equivalent to $CD103^+$ DC found in nonlymphoid organs by transcriptional network analysis, sharing of key transcription factors required for development, migratory phenotype, and ability to

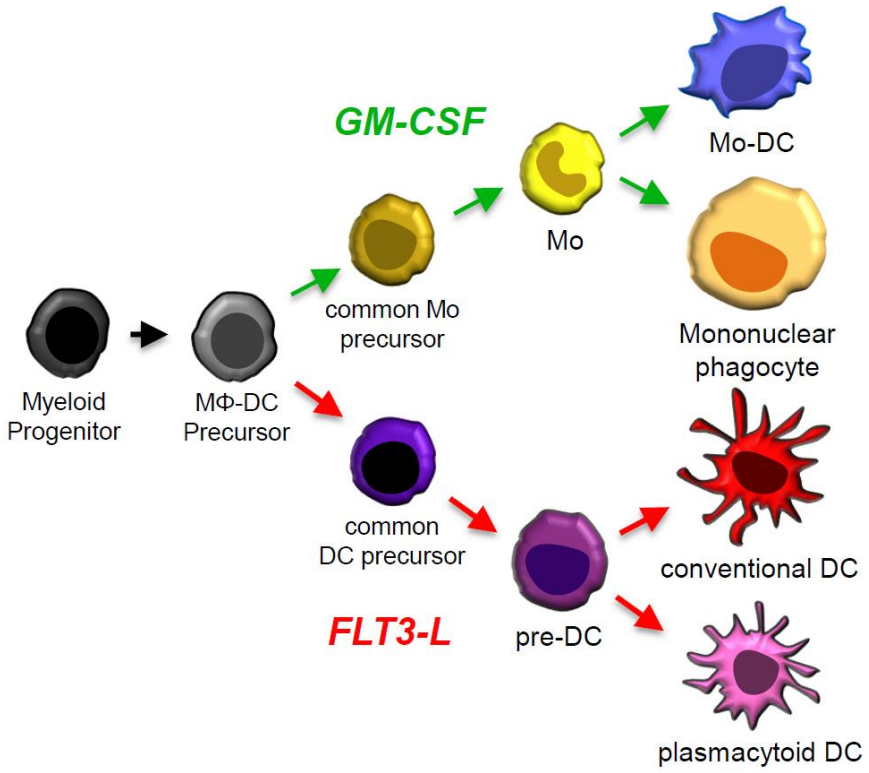

Figure 5.1: DC ontogeny

Cartoon depicting the ontogeny of dendritic cells differentiated *in vitro* using either GM-CSF (green lines) or FLT3-L (red lines) as growth factors.

efficiently cross present antigen to CD8 T cells (del Rio et al., 2010; Miller et al., 2012). In addition to mucosal DC, CD103 is also expressed by a subset of T cells, which is thought to be primarily important for adherence of both T cells and DC in epithelial compartments, as it is a receptor for E-cadherin (del Rio et al., 2010). $CD103^+$ DC are found in the intestinal LP, and have been shown to be seeded continually from committed DC progenitors, and not monocytes, as they are selectively depleted in *flt3*$^{-/-}$ mice (Bogunovic et al., 2009; Jaensson et al., 2008). In contrast, mice lacking the GM-CSF receptor had reduced numbers of $CD103^-CD11b^+$ DC in the gut lamina propria, which differentiate predominantly from $Ly6C^{hi}$ monocytes, and not from pre-DC or CDP (Bogunovic et al., 2009).

In order for a host cell to fully support the intracellular growth of *L. monocytogenes*, the bacterium has to invade by either phagocytosis or receptor-mediated uptake, escape the phagocytic vacuole, and then acquire nutrients to replicate in the host cell cytosol. The intracellular growth of *L. monocytogenes* is thought to be most efficient in the cytosol of macrophage-like cells, which are typically generated *in vitro* from bone marrow cells using M-CSF. The direct comparison of cells differentiated using either M-CSF or GM-CSF indicated that *L. monocytogenes* replicated more efficiently in cells grown using M-CSF (Westcott et al., 2007). This is thought to be due to the phagocytic vacuole of GM-CSF-derived cells, which was able to more efficiently restrict the escape of *L. monocytogenes* compared to M-CSF-derived cells (Westcott et al., 2010). However, it was clear from those studies that *L. monocytogenes* were still able to grow in GM-CSF-cultured cells in which a ~10-fold increase in CFU was observed over six hours compared to ~100-fold increase in CFU in the M-CSF-cultured cells (Westcott et al., 2007). Guzman *et al.* first showed that *L. monocytogenes* could survive inside a splenic DC cell line; however, it was not possible to evaluate growth rate in these cells since an extremely high MOI was used (1:100) and the number of intracellular *L. monocytogenes* did not increase following the initial infection period (Guzman et al., 1995). The rate at which *L. monocytogenes* replicate in the cytosol of conventional DC generated using FLT3-L also remains unknown.

The vast majority of studies investigating the interaction of *L. monocytogenes* with DC found *in vivo* was focused on the interaction of *L. monocytogenes* with splenic DC after intravenous infection. Multiple studies have suggested that *L. monocytogenes* preferentially interacted with $CD8\alpha^+$ DC 3 hours to one day after i.v. infection compared to $CD8\alpha^-$ DC and other myeloid cells after sorting and plating for live CFU (Mitchell et al.,

2011; Neuenhahn et al., 2006). However, another study found no evidence of $CD8a^+$ DC directly associated with *L. monocytogenes* in the spleen using flow cytometry, but rather, $CD8\alpha^-$ DC were associated with *L. monocytogenes* (Edelson et al., 2011). Despite the association of live *L. monocytogenes* with splenic DC, it is unclear if *L. monocytogenes* actively replicate inside these cells over time.

We previously reported that intracellular growth of *L. monocytogenes* was important for persistence in the gut and spread to the mesenteric lymph nodes (MLN) (Jones et al., 2015). The primary cell type associated with *L. monocytogenes* in the MLN were inflammatory monocytes, but these cells did not support *L. monocytogenes* growth, whereas, $CD11c^+$ cells were a minor proportion of *L. monocytogenes*-infected cells (Jones and D'Orazio, 2017). Thus, it is possible that a migratory DC in the intestine supports the growth of *L. monocytogenes* and traffics *L. monocytogenes* to the MLN. In addition, there is evidence that a subset of $CD103^+$ DC that infiltrate the gut during colitis express E-cadherin (Siddiqui et al., 2010), which *L. monocytogenes* could use to invade these cells via InlA in addition to being taken up by phagocytosis. Therefore, in this study, we investigated which cells in the gut might serve as an intracellular growth niche for *L. monocytogenes* with a focus on DC as a candidate cell type.

III. Results

A. *L. monocytogenes* replicate more efficiently inside myeloid cells isolated from the MLN compared to the intestinal LP.

Although most *L. monocytogenes* in the gut are extracellular, an as yet unidentified subset of cells serves as an intracellular growth niche for *L. monocytogenes* and is crucial for spread beyond the intestine (Jones et al., 2015). However, in the MLN, the majority of cell-associated *L. monocytogenes* was found with inflammatory monocytes 2-3 dpi, and these cells did not support *L. monocytogenes* growth (Jones and D'Orazio, 2017). Therefore, we investigated which cell types in the intestinal LP were infected with *L. monocytogenes* as done previously to identify *L. monocytogenes*-infected MLN cells (Fig. 5.2). Intracellular *L. monocytogenes* begin to be consistently recovered from the colonic lamina propria between 36 and 60 hours post-infection (Bou Ghanem et al., 2012). Therefore, the large intestine LP was isolated 2 dpi and myeloid cell populations were subset using the gating scheme in Fig. 5.2A. As observed in the MLN, $Ly6C^{hi}$ (P1) and $Ly6G^{hi}$ (P2) cells were recruited to the intestinal LP during infection

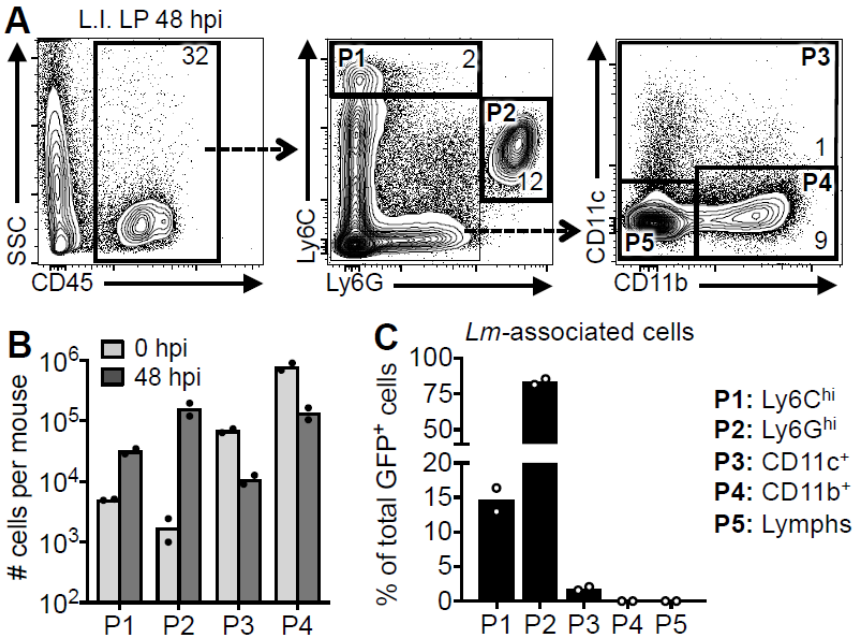

Figure 5.2: A minor proportion of *Listeria*-associated cells in the intestinal lamina propria are tissue-resident phagocytes.

BALB mice were fed 5x10^8 CFU of either *Lm* SD2710 (GFP$^+$ InlA^m) or *Lm* SD2001 (InlA^m + empty vector). **(A)** Gating scheme used to identify cell populations from the large intestine LP 48 hours after infection including Ly6C^{hi} (P1), Ly6G^{hi} neutrophils (P2), CD11c$^+$ (P3), CD11b$^+$CD11c$^{-/+}$ (P4), and remaining cells (P5) consisting of mainly lymphocytes. **(B)** Total number of cells in each population isolated from the large intestine LP of each mouse 48 hpi; symbols represent each mouse, n=2. **(C)** Proportion of total GFP$^+$ (*Lm*-associated) cells from mice infected with GFP$^+$ *Lm* (n=2) by using mice infected with the vector control strain (n=2) as a negative gating threshold for GFP, as performed in the previous chapter using MLN cells.

(Fig. 5.2B). Interestingly, the number of cells in P3 and P4 were reduced 2 dpi, suggesting either cell death or migration to the MLN had occurred (Fig. 5.2 B). Next, we compared the fluorescence of cells in each population isolated from mice fed mouse-adapted, GFP-expressing *L. monocytogenes* to cells from mice fed an isogenic *L. monocytogenes* strain that lacked GFP. As shown in Fig. 5.2C, the vast majority (80%) of *L. monocytogenes*-associated cells were P2 cells, whereas, ~15% of all GFP^+ cells were P1 cells. This indicates that nearly all of the cell-associated *L. monocytogenes* in the large intestinal LP were found with $Ly6G^{hi}$ neutrophils and $Ly6C^{hi}$ monocytes, which infiltrated the gut during *L. monocytogenes* infection (Fig. 5.2C). Neutrophils are known to be bactericidal against *L. monocytogenes* (Arnett et al., 2014), and we previously demonstrated that $Ly6C^{hi}$ monocytes exhibit bactericidal activity as they are activated prior to egress from the bone marrow during *L. monocytogenes* infection (Jones and D'Orazio, 2017). This suggests that the vital intracellular growth niche for *L. monocytogenes* is found among the minimal fraction of GFP^+ myeloid cells in P3 and P4, which phenotypes are consistent with tissue-resident dendritic cells and macrophages, respectively.

In addition to the intestinal LP, a small proportion of P3 and P4 cells were GFP^+ in the MLN 48 to 72 hpi (Fig. 4.1D). Therefore, we tested whether *L. monocytogenes* could replicate inside $Ly6C^{-/+}Ly6G^{-/+}$ myeloid cells isolated from either the intestinal LP or MLN of uninfected mice (Fig. 5.3A). The gating scheme used to sort myeloid cells from either the large intestine LP (Fig. 5.3B) or MLN (Fig. 5.3D) excluded T cells ($CD3^+$), B cells, ($CD19^+$), $Ly6C^{hi}$ and $Ly6G^{hi}$ cells ($Gr\text{-}1^{hi}$), and natural killer cells ($CD49b^+$). The negatively selected myeloid cells were subsequently infected with *L. monocytogenes* and the number of intracellular *L. monocytogenes* was determined one and four hours after infection. As shown in Fig. 5.3C, intracellular (gentamicin-resistant) *L. monocytogenes* was recovered from intestinal LP cells isolated from five out of six mice. However, three hours later, the number of intracellular *L. monocytogenes* had increased in only one out of six mice, whereas, cells isolated from other mice had either undetectable or decreased intracellular *L. monocytogenes* 4 hpi (Fig. 5.3C). *In vitro* infection of myeloid cells suggested that it was more common for *L. monocytogenes* to grow inside inside cells isolated from the MLN compared to the intestinal LP. As shown in Fig. 5.3E, three out of six mice had detectable numbers of intracellular *L. monocytogenes* within one hour, and at 4 hpi, these same mice had ~100-fold higher

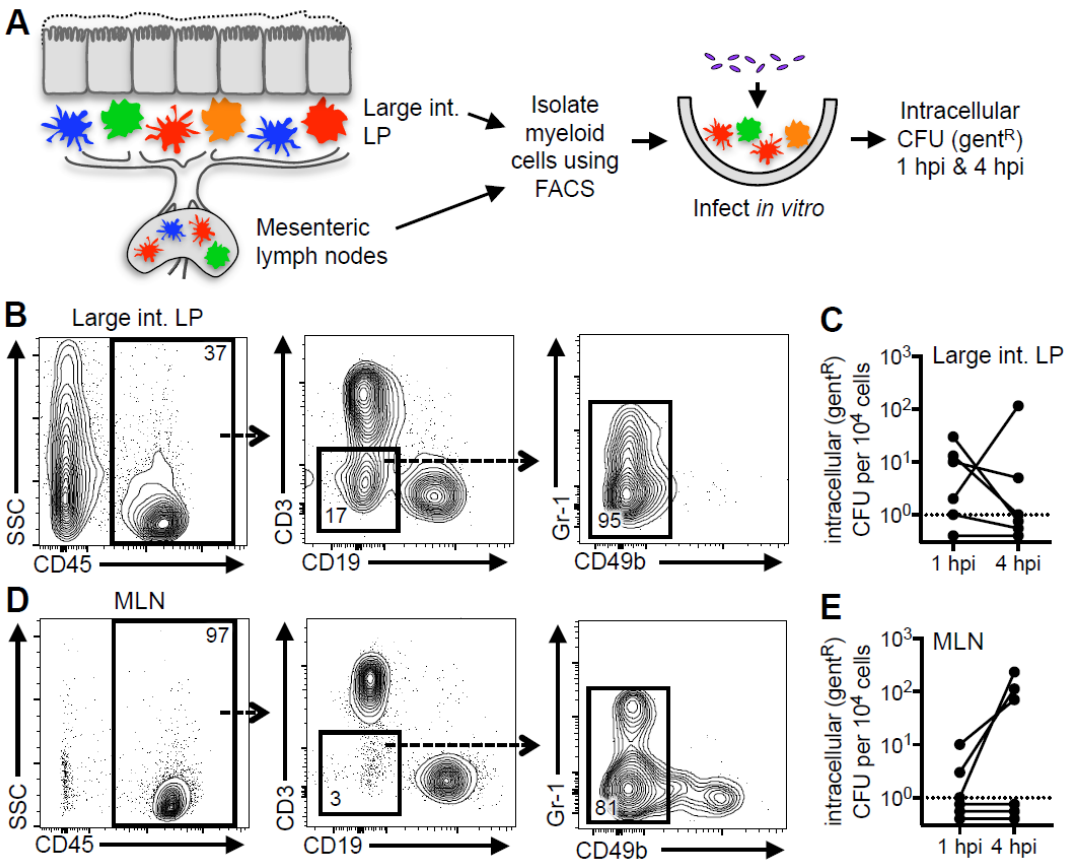

Figure 5.3: A minor subset of myeloid cells isolated from the MLN support the intracellular growth of *L. monocytogenes.*

(A) Schematic of experimental design after large intestine LP and MLN cells were isolated from uninfected mice. Myeloid cells were sorted from each tissue and 2-2.5 x 10^4 cells were infected for one hour at a MOI of 10-15 in wells of round-bottom 96-well plate. Intracellular (gentamicin-resistant) CFU was determined one and four hours post-infection. **(B & D)** Gating scheme used to sort myeloid-derived cells ($CD45^+CD3^-CD19^-DX5^-Gr\text{-}1^-$) from either large intestine lamina propria **(B)** or MLN **(D)** of uninfected mice. **(C & E)** Number of intracellular *Lm* per 10^4 myeloid cells from either the large intestine LP **(C)** or the MLN **(E)** one and four hours after infection. Connecting lines represent cells isolated from the same mouse at each time point (n=6). Data pooled from two separate experiments.

numbers of intracellular CFU. These data suggest that although intracellular CFU was recovered from the MLN cells of only half the mice analyzed, if *L. monocytogenes* invaded within an hour, they were able to replicate intracellularly over time. This suggests that a rare myeloid cell type in the MLN supports the growth of *L. monocytogenes,* which is relatively rarer in the intestinal LP, as only one out of six mice had an increased number of intracellular *L. monocytogenes* over time.

B. *L. monocytogenes* inefficiently invade and do not replicate inside DC isolated from the gut.

The proportion of GFP^+ P3 cells was higher than GFP^+ P4 cells in the large intestinal LP (Fig. 5.2C), and the proportion of GFP^+ P3 MLN cells increased from 48 to 72 hpi (Fig. 4.1E). Therefore, it is possible that a migratory GFP^+CD11c^+ cell may migrate from the intestinal LP to the MLN during infection. Therefore, throughout the remainder of this study we focused on the interaction of *L. monocytogenes* with P3 cells in the gut, which had a phenotype consistent with DC. We used a more sophisticated gating scheme to identify both $CD103^-$ cDC (blue gate) and $CD103^+$ cDC (red gate) in the intestinal LP and MLN during infection (Fig. 5.4A). As shown in Fig. 5.4B, approximately equal numbers of $CD103^-$ and $CD103^+$ DC were isolated from the large intestine LP 48 hpi. Next, the total number of GFP^+ (*L. monocytogenes*-associated) cells was determined in each DC subset using the same approach described in Fig. 5.2C. A similar number of GFP^+ $CD103^+$ and $CD103^-$ DC were found in the large intestine LP (Fig. 5.4C). In contrast, a significantly higher total number of $CD103^+$ DC were found in the MLN compared to $CD103^-$ DC 2 dpi (Fig. 5.4D), which is consistent with the migratory phenotype of $CD103^+$ DC from the gut to the MLN (Schulz et al., 2009). Despite a higher total number of $CD103^+$ DC in the MLN, *L. monocytogenes* did not preferentially associate with $CD103^+$ MLN DC (Fig. 5.4E). Overall, we found a higher number of GFP^+ DC in the MLN, but this was due strictly to the higher total number of DC in the MLN compared to the intestinal LP. In fact, the percentage of GFP^+ DC was similar (~0.5%) in both the intestinal LP and the MLN (~10 GFP^+ out of ~2,200 DC in the LP and ~200 GFP^+ out of ~45,000 DC in the MLN). More importantly, these data indicate that *L. monocytogenes* do not preferentially interact with $CD103^+$ DC, which we had originally hypothesized due to the expression of E-cadherin on these cells during colitis (Siddiqui et al., 2010).

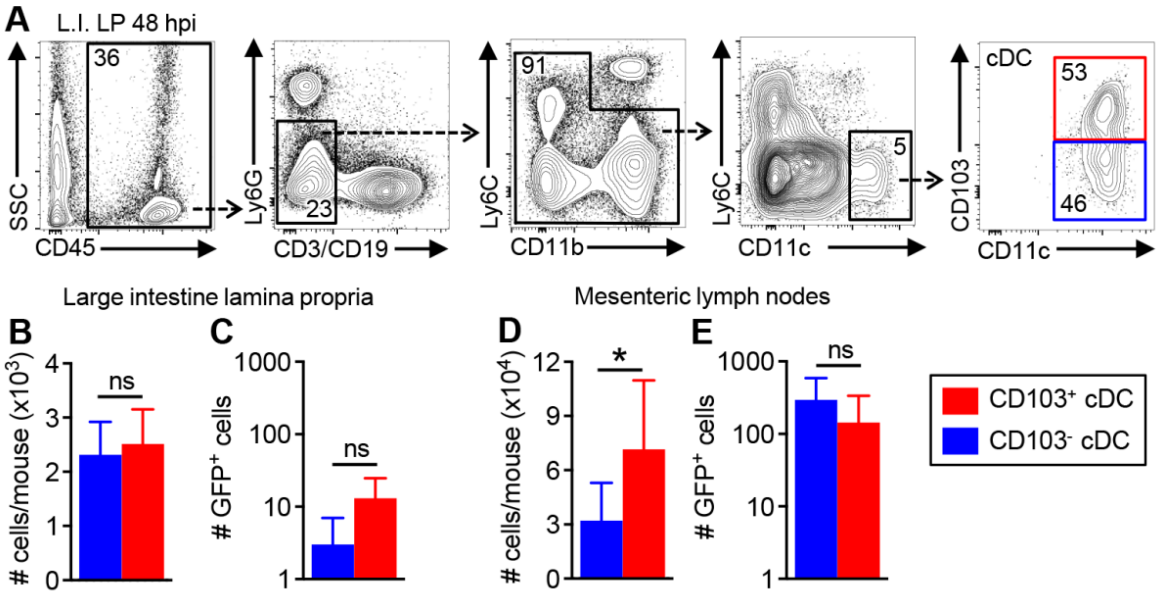

Figure 5.4: *L. monocytogenes* do not preferentially associate with CD103$^+$ DC in the gut.

BALB mice were fed 1-6x10^8 CFU of either *Lm* SD2710 (GFP$^+$ InlA^m) or *Lm* SD2001 (InlA^m + empty vector). **(A)** Gating scheme used to identify conventional CD103$^-$ and CD103$^+$ dendritic cells (cDC) isolated from the large intestine lamina propria (LP) 48 hours after infection. **(B & D)** Mean total number (±SD) of dendritic cells isolated from either the large intestine LP 48 hpi (n=6) (panel B) or the MLN 60-72 (n=7) (panel D) of each mouse. **(C & E)** The total number of GFP$^+$ (*Lm*-associated) cells in each DC subset isolated from either the intestinal LP 48 hpi **(C)** or MLN 60-72 hpi **(E)**.

In an effort to recover cell-associated *L. monocytogenes* from either CD103$^-$ or CD103$^+$ DC *ex vivo*, these cells were sorted from the large intestine LP 2 dpi, lysed, and then plated for CFU. However, due to low total number of *L. monocytogenes*-associated DC in an individual mouse we were unable to make any strong conclusions as we were near the limit of detection. Thus, we used an alternative, bulk approach to determine if any of the myeloid cells sorted from infected mice were found with either cell-associated or intracellular *L. monocytogenes.* As depicted in Fig. 5.5A, myeloid cells were sorted from the large intestine LP and MLN 2 dpi and then cultured *in vitro* with or without gentamicin for four hours to allow for growth amplification of any cell-associated *L. monocytogenes.* To establish a baseline growth of *L. monocytogenes* isolated *ex vivo,* serial dilutions of *Listeria*-infected MLN digests (containing mainly extracellular bacteria*;* Fig. 3.3) were cultured for four hours. The number of *L. monocytogenes* increased ~24-fold during this four-hour period in tissue-culture medium without gentamicin (data not shown). This indicates that the number of cell-associated *L. monocytogenes* recovered after this four hour amplification period *in vitro* would be approximately 24-fold higher than the number of bacteria directly *ex vivo*. The same gating scheme was used to sort myeloid cells from the large intestine LP (Fig. 5.5B) and the MLN (Fig. 5.5D) 48 hpi as done above when sorting myeloid cells from uninfected mice (Fig. 5.3). After being cultured four hours without gentamicin, a similar average number of cell-associated *L. monocytogenes* was recovered from myeloid cells isolated from the intestinal LP (Fig. 5.5C) and the MLN (Fig. 5.5E). However, when half of the cells sorted from the same mice were cultured in the presence of gentamicin, no intracellular (gentamicin-resistant) CFU were recovered from the intestinal LP cells (Fig. 5.5C). Likewise, only one out of four mice had recoverable intracellular CFU from myeloid cells sorted from the MLN 2 dpi (Fig. 5.5E). Together, these data confirm that a minor number of *L. monocytogenes* are associated with myeloid cells in the gut or MLN during infection, but it is extremely rare to isolate intracellular CFU from these cells.

One major caveat of isolating myeloid cells from mice 2 dpi is the possibility that the cells are activated, and thus, are more efficient at limiting the escape of *L. monocytogenes* from the phagocyte vacuole. This is supported by the idea that we successfully established infection of these cells after they were sorted from uninfected mice and subsequently infected *in vitro* (Fig. 5.3). Next, we evaluated whether CD103$^-$ or CD103$^+$ DC, which would have been included in the bulk myeloid population, supported the intracellular growth of *L. monocytogenes*. As depicted in Fig. 5.6A and 5.6B,

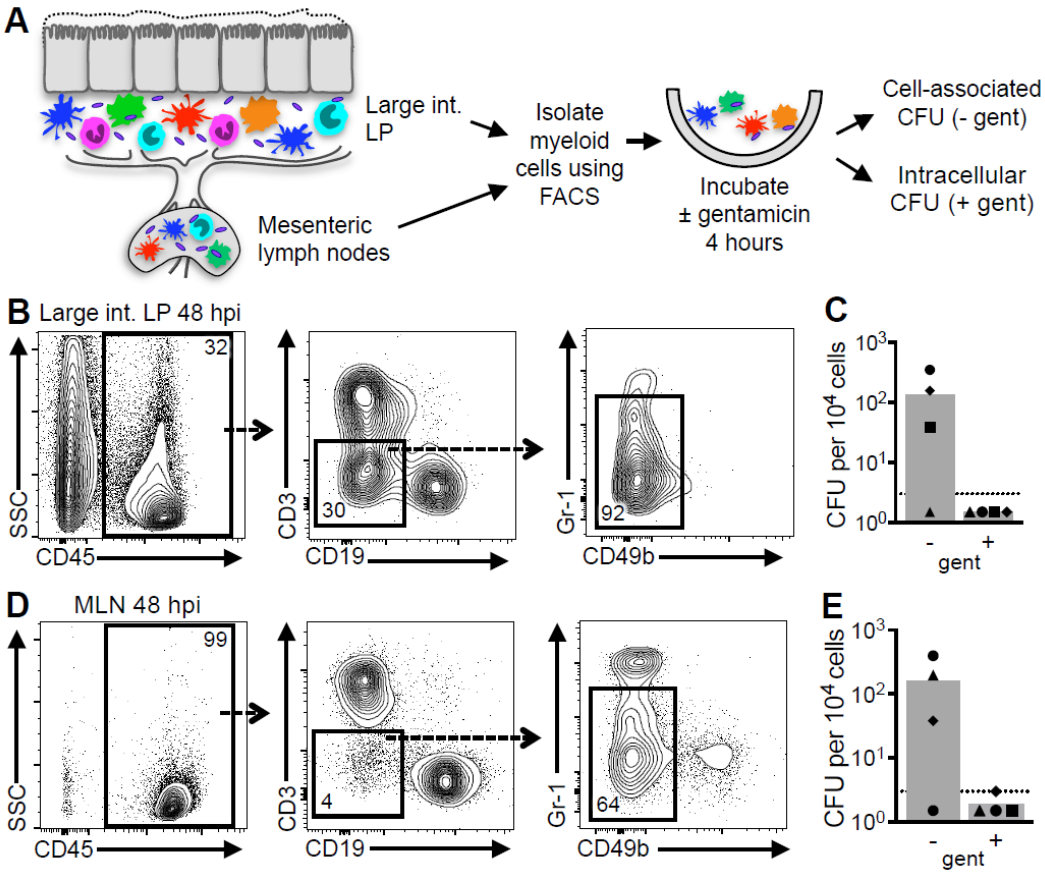

Figure 5.5: Myeloid cells isolated from the gut 2 dpi are not associated with intracellular *L. monocytogenes*.

(A) Schematic of experimental design in which BALB mice were infected with 10^8 *Lm* SD2001 and the large intestine LP and MLN were isolated 2 dpi. An average of $2x10^4$ sorted myeloid cells ($CD45^+CD3^-CD19^-DX5^-Gr\text{-}1^-$) were cultured in each well for four hours with or without gentamicin to determine intracellular or cell-associated *Lm,* respectively. **(B)** Gating scheme used to sort myeloid-derived cells from either the lamina propria or MLN 2 dpi. **(C)** Mean total number of cell-associated (- gent) or intracellular (+ gent) *Lm* recovered from myeloid cells after being cultured four hours in vitro with or without gentamicin. Symbols represent cells from the same mouse cultured with or without gentamicin (n=4). Data pooled from two separate experiments.

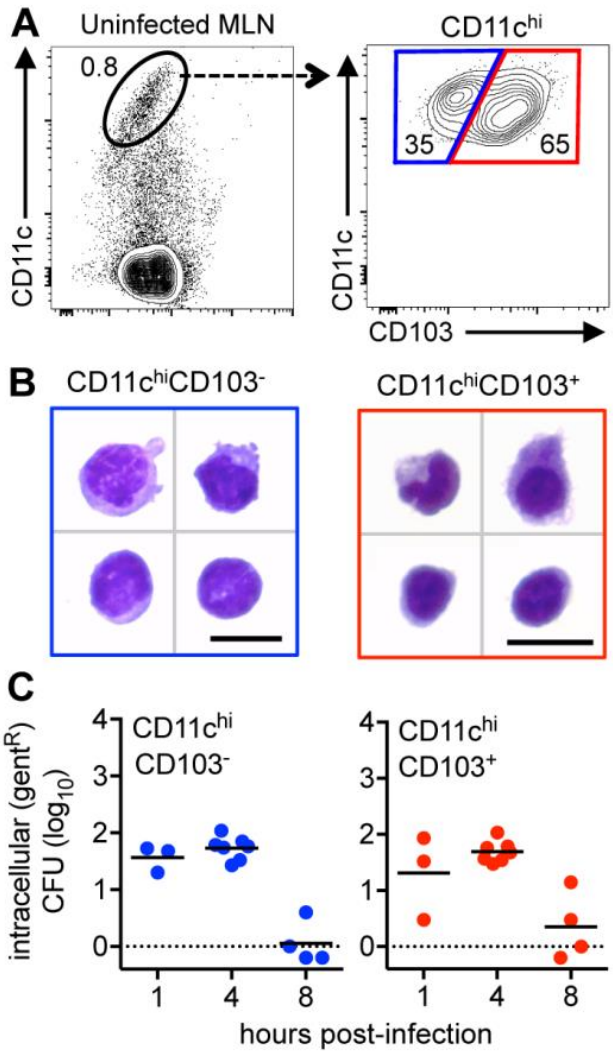

Figure 5.6: Dendritic cells isolated from the MLN do not support the growth of *L. monocytogenes.*

(A) CD11c^{hi}CD103^{-} (blue gate) or CD11c^{hi}CD103^{+} (red gate) cells were sorted from the MLN of uninfected BALB mice. **(B)** DiffQuik staining of each DC subset after sorting. Scale bars, 10 μm. **(C)** 1-2 x 10^4 sorted cells were infected *in vitro* with *Lm* for one hour at a MOI of 10 and horizontal lines indicate mean number of intracellular CFU recovered from each DC subset 1, 4, or 8 hours after infection. Symbols represent cells sorted from an individual mouse. Sorted cells from each mouse were used for two time points; pooled data from two separate experiments is shown (n=3; 1 hpi and 4 hpi; n=4, 4 hpi and 8 hpi).

$CD11c^{hi}CD103^{-}$ cDC (blue gate) and $CD11c^{hi}CD103^{+}$ cDC (red gate) were sorted from the MLN of uninfected mice. DiffQuik staining of sorted cells indicated that both DC subsets had similar morphologies, with the exception that $CD103^{+}$ cells were smaller than the $CD103^{-}$ cells (Fig. 5.6C), which is consistent with a previous report characterizing these DC subsets from the intestinal LP (Bogunovic et al., 2009). One hour after infection, similar numbers of intracellular *L. monocytogenes* were recovered from both $CD103^{-}$ and $CD103^{+}$ cDC (Fig. 5.6C). The number of intracellular *L. monocytogenes* did not significantly increase from one to four hpi (two-fold or less), suggesting that neither cDC subset efficiently supported bacterial growth (Fig. 5.6C). Likewise, the number of intracellular decreased from four to eight hpi, which suggested that *L. monocytogenes* was unable to replicate inside either cDC subset sorted from the MLN. Our data indicate that a minor fraction of $CD103^{-}$ and $CD103^{+}$ cDC are associated with *L. monocytogenes in vivo,* but there is no evidence to suggest that these cells serve as a growth niche for *L. monocytogenes.*

C. GM-CSF-derived $CD11c^{+}$ cells vary in their ability to support the intracellular growth of *L. monocytogenes*.

Our data suggest that DC isolated from the gut do not support the intracellular life cycle of *L. monocytogenes* contrary to the growth of *L. monocytogenes* in $CD11c^{+}$ cells cultured *in vitro* using GM-CSF (Westcott et al., 2007). This suggests that the process of culturing bone marrow-derived cells in the presence of GM-CSF generates a cell type permissive to *L. monocytogenes* replication. Therefore, we decided to better characterize the ability of *L. monocytogenes* to replicate in DC-like cells cultured *in vitro* in an effort to explain our findings with *ex vivo* DC.

In the study by Westcott et al., $CD11c^{+}$ cells were enriched from cells cultured using GM-CSF and then allowed to adhere to glass coverslips before infections. It is known that $CD11c^{+}$ cells in GM-CSF cultures are typically loosely attached or floating cells, whereas, the attached have more macrophage-like features. Likewise, our *ex vivo* DC infections were conducted in round-bottom wells, which could be one reason why we observed inefficient infection of these cells. Therefore, we next tested whether cell adherence was required for *L. monocytogenes* to invade and replicate in GM-CSF-derived $CD11c^{+}$ cells. Bone marrow cells were cultured for eight days in the presence of GM-CSF and then transferred to low-attachment 24-well plates with or without glass coverslips and infected the following day. At this time point, approximately 80% of the

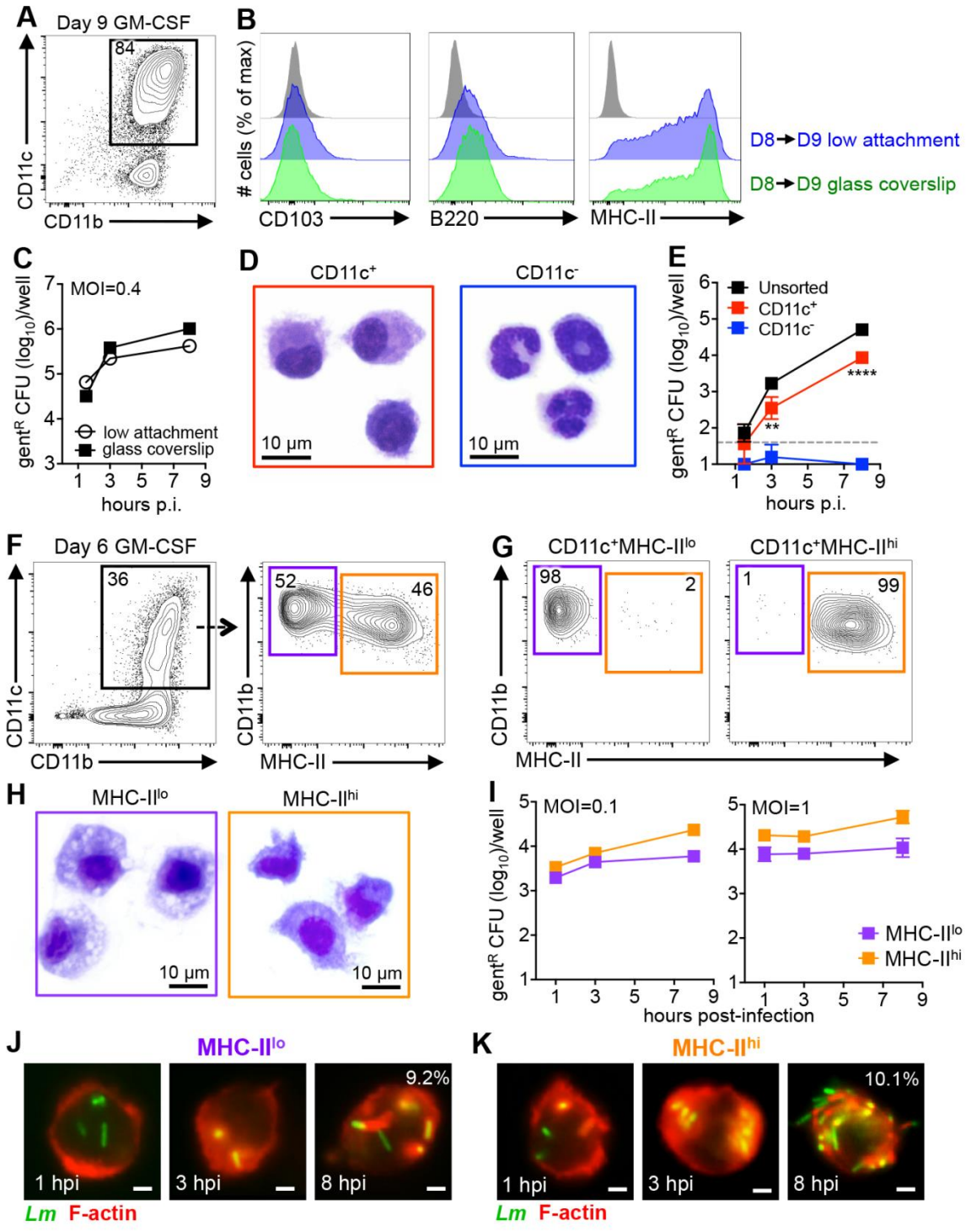
A
Day 9 GM-CSF
84
CD11c
CD11b
B
cells (% of max)
CD103
B220
MHC-II
D8→D9 low attachment
D8→D9 glass coverslip
C
MOI=0.4
gentR CFU (log10)/well
low attachment
glass coverslip
hours p.i.
D
CD11c+
CD11c-
10 µm
10 µm
E
Unsorted
CD11c+
CD11c-
gentR CFU (log10)/well
****
**
hours p.i.
F
Day 6 GM-CSF
36
52
46
CD11c
CD11b
CD11b
MHC-II
G
CD11c+MHC-IIlo
CD11c+MHC-IIhi
98
2
1
99
CD11b
MHC-II
H
MHC-IIlo
MHC-IIhi
10 µm
10 µm
I
MOI=0.1
MOI=1
gentR CFU (log10)/well
MHC-IIlo
MHC-IIhi
hours post-infection
J
MHC-IIlo
9.2%
1 hpi
3 hpi
8 hpi
Lm F-actin
K
MHC-IIhi
10.1%
1 hpi
3 hpi
8 hpi
Lm F-actin

Figure 5.7: GM-CSF-derived CD11c$^+$ cells vary in their ability to support *L. monocytogenes* growth.

(A) Bone marrow cells were cultured in 3% J558 supernatant (GM-CSF) for 8 days before being transferred to flat bottom low-attachment dishes with or without glass coverslips overnight. (**B)** Histograms depict expression of CD103, B220, and MHC-II on CD11c$^+$ cells cultured as described in "A". Gray histogram is negative gating control. **(C)** Mean (±SD) number of intracellular (gent-resistant) *Lm* SD2000 from triplicate wells with 5x10^5 cells at various time points after a one hour infection. Data from one of two separate experiments is shown. **(D)** DiffQuik staining of sorted CD11c$^+$ and CD11c$^-$ cells that were sorted on day 8 and then cultured in low attachment wells overnight. **(E)** Mean (±SD) number of intracellular *Lm* SD2000 from triplicate wells with 2.5x10^5 of the cell type indicted in the figure legend at various time points after a one hour infection (MOI=0.03) in low attachment wells. Statistical significance was determined using unpaired t tests. **(F)** Gating scheme to identify CD11c$^+$MHC-II^{lo} (purple gate) or CD11c$^+$MHC-II^{hi} (orange gate) cells after 6 days in GM-CSF. **(G)** Post sort analysis and **(H)** DiffQuik staining of each cell population. **(I)** Mean (±SD) number of intracellular (gent-resistant) *Lm* SD2000 from triplicate wells with 1x10^5 cells in 96-well low attachment plates at various time points after a 30 min. infection. Data from one of two separate experiments is shown. **(J-K)** Representative images of either CD11c$^+$MHC-II^{lo} (J) or CD11c$^+$MHC-II^{hi} (K) stained with Texas Red-conjugated phalloidin at various time points after a 30 min. infection with GFP$^+$ *Lm* SD2710 (MOI=0.2). Percentages at 8 hpi indicate the proportion of total cells associated with *Lm* that had actin tails. Scale bars, 2 μm.

cells expressed intermediate to high levels of CD11c regardless of whether the cells were transferred to glass coverslips the last day of culture (Fig. 5.7A, data not shown). In addition, attachment to glass did not alter the expression levels of CD103, B220, or MHC-II (Fig. 5.7B). Similar numbers of intracellular bacteria were recovered one hour after infection with *L. monocytogenes*, suggesting that adherence to glass did not significantly alter initial uptake or survival of *L. monocytogenes* (Fig. 5.7C). Furthermore, *L. monocytogenes* grew at a similar rate up to 8 hpi in cells attached to glass and non-adherent cells (Fig. 5.7C), which was comparable to a previous study using adherent cells (Westcott et al., 2007). Our data clearly indicate that adherence to glass did not enhance the ability of *L. monocytogenes* to invade or replicate in $CD11c^+$ cells generated using GM-CSF.

It is known that cells cultured in GM-CSF are heterogeneous and that ~20% of the cells were $CD11c^-$ on day nine (Fig. 5.7A). Therefore, it was possible that the small proportion of $CD11c^-$ cells in these cultures could account for the intracellular growth we observed in unsorted cells. To test this, $CD11c^+$ and $CD11c^-$ cells were sorted on day eight and then cultured overnight in low-attachment plates prior to infection. As shown in Fig. 5.7D, the $CD11c^+$ cells had a round mononuclear morphology with a relatively large cytoplasmic to nucleus ratio. Whereas, the $CD11c^-$ cells had characteristic monocytic kidney-shaped nuclei, and a minor proportion of the cells had lobular nuclei characteristic of the granulocytes that develop in GM-CSF cultures (Na et al., 2016) (Fig. 5.7D). As shown in Fig. 5.7E, the $CD11c^+$, but not the $CD11c^-$ cells supported the intracellular growth of *L. monocytogenes,* which increased approximately 100-fold over eight hours. This indicates that the increase in intracellular CFU over time in the unsorted (bulk) GM-CSF cultures was due to the growth of *L. monocytogenes* inside $CD11c^+$ cells.

Helft *et al*. recently demonstrated that GM-CSF-derived cells consist of heterogeneous populations with distinct ontogenies (Helft et al., 2015). In that report, the $CD11c^+MHC\text{-}II^+$ population included cells that expressed markers of true macrophages and DC (Helft et al., 2015). However, MHC-II expression on day 6 of culture could distinguish between $CD11c^+$ macrophage-like cells ($MHC\text{-}II^{lo}$) and $CD11c^+$ DC-like cells ($MHC\text{-}II^{hi}$) (Helft et al., 2015). As reported by Helft et al., we observed similar proportions of $CD11c^+$ cells on day six that were $MHC\text{-}II^{lo}$ and $MHC\text{-}II^{hi}$ (Fig. 5.7F). Next, we sorted $CD11c^+MHC\text{-}II^{lo}$ and $CD11c^+MHC\text{-}II^{hi}$ cells to determine their relative ability to support *L. monocytogenes* growth (Fig. 5.7G). The $CD11c^+MHC\text{-}II^{lo}$ cells had a macrophage-like

morphology with a large cytoplasm and phagocytic vacuoles, whereas, the CD11c^{+}MHC-II^{hi} cells had relatively larger nuclei with a more dendritic-like morphology (Fig. 5.7H). Similar numbers of *L. monocytogenes* were recovered from both cell populations one hpi, but the number of *L. monocytogenes* slightly increased over time in the MHC-II^{hi} cells (Fig. 5.7I). In contrast, the MHC-II^{lo} cells did not have a net increase in intracellular CFU over time, suggesting that *L. monocytogenes* survived, but did not efficiently replicate in the cytosol of these cells (Fig.5.7I).

Interestingly, the rate of intracellular growth in both MHC-II^{hi} and MHC-II^{lo} cells was much slower than what was observed in the CD11c^{+} cells on day nine (Fig. 5.7E). Despite the use of a 10-fold higher MOI of 1, which resulted in increased uptake of *L. monocytogenes* within an hour, the rate of intracellular growth in both cell types was not enhanced (Fig. 5.7I). To confirm that *L. monocytogenes* were able to escape the phagocytic vacuole and replicate in the cytosol, we visualized infected cells under the microscope after labeling F-actin. As shown in the representative images in Fig. 5.7J,K, GFP^{+} *L. monocytogenes* were associated with both cell types one hpi. At 3 hpi, both cell types were associated with *L. monocytogenes* surrounded by actin clouds, indicative of *L. monocytogenes* in a phagocytic vacuole or that recently invaded the cytosol (Fig. 5.7J,K). At 8 hpi, *L. monocytogenes* were found in association with actin tails, which were indicative of bacteria that had escaped from the phagocytic vacuole (Fig. 5.7J,K). As suggested by the growth curves, a slightly higher percentage of *L. monocytogenes*-associated MHC-II^{hi} cells harbored *L. monocytogenes* that had actin tails (~10%; Fig. 5.7K) compared to the MHC-II^{lo} cells (~9%; Fig. 5.7J). Likewise, a slightly higher number of bacteria per cell were found in the cytosol of MHC-II^{hi} compared to MHC-II^{lo} cells 8 hpi (data not shown). Together, our data suggest that the efficiency of *L. monocytogenes* growth inside CD11c^{+} cells was dependent on how long the cells were cultured *in vitro*, as prolonged culture in GM-CSF was correlated with enhanced growth of *L. monocytogenes.* However, it was also clear that GM-CSF-derived CD11c^{+} cells did not recapitulate our findings using DC isolated from the MLN, which did not support *L. monocytogenes* growth.

D. CD103^{+}CD11c^{+} generated using FLT3-L do not efficiently support the intracellular replication of *L. monocytogenes.*

Next, we used a different method to culture DC to induce the development of CD103^{+} DC, which were not generated using GM-CSF (Fig. 5.7B). Activation of Flt-3 is

important for the differentiation of DC progenitors into conventional DC, and a recent methodology has been described to generate $CD103^+$ *in vitro* using FLT3L (Mayer et al., 2014). Nearly all of the cells recovered using this method were $CD11c^+MHC\text{-}II^+$ on day 16, and approximately two-thirds of the cells were $CD103^+$ (Fig. 5.8A). Microscopic examination of FLT3-L-cultured cells on day 16 (Fig. 5.8B) indicated a morphology in between the GM-CSF-cultured $CD11c^+$ cells on day nine and the GM-CSF-cultured $MHC\text{-}II^{hi}$ cells on day six in regards to overall diameter and nuclear shape. Although *L. monocytogenes* was taken up efficiently by these cells within 30 minutes, there was less than a 10-fold increase in intracellular CFU over eight hours (Fig. 5.8C). This suggests that $CD11c^+CD103^+$ cells do not efficiently support the intracellular growth of *L. monocytogenes*. Lastly, we questioned whether prolonged cultured in FLT3-L enhanced the ability of *L. monocytogenes* to grow in these cells, as observed when using GM-CSF. Therefore, bone marrow cells were cultured for six days in FLT3-L, in which ~30-35% of the cells at this time were $CD11c^+$, whereas ~7-10% of the cells were $CD11c^{int}B220^+$ plasmacytoid DC (Fig. 5.8D). Although these cells had only been cultured for six days, the majority (~80%) of cells that expressed a conventional DC phenotype ($CD11c^+B220^-$) co-expressed MHC-II and CD103 (Fig. 5.8D). To determine if any of the cells using this culture method supported the intracellular growth of *L. monocytogenes,* we infected them in bulk. As shown in Fig. 5.8E, *L. monocytogenes* invaded these cells in a dose-dependent manner within 30 minutes, but the number of intracellular CFU did not increase over time. To confirm that *L. monocytogenes* were able to invade these cells, we performed differential in/out staining one hour after infection with GFP^+ *L. monocytogenes.* As shown in the representative images in Fig. 5.8F, nearly 60% of the cells had only internalized *L. monocytogenes,* whereas 13% of the cells had both internalized and adherent bacteria. This approach indicated that ~70% of cells cultured using FLT3-L on day six internalized *L. monocytogenes*. However, analysis of these cells at 8 hpi indicated that only 1.5% of cells counted harbored *L. monocytogenes* that was associated with actin tails, while most (~90%) of the cells appeared uninfected (Fig. 5.8G). Together, these data suggests that *L. monocytogenes* were able to efficiently invade cells cultured using FLT3-L for six days, but it was extremely rare to find *L. monocytogenes* replicating in the cytosol of these cells. Overall, these data suggest that prolonged exposure to FLT3-L also triggered a permissive intracellular niche for *L. monocytogenes* as observed with cells cultured in GM-CSF.

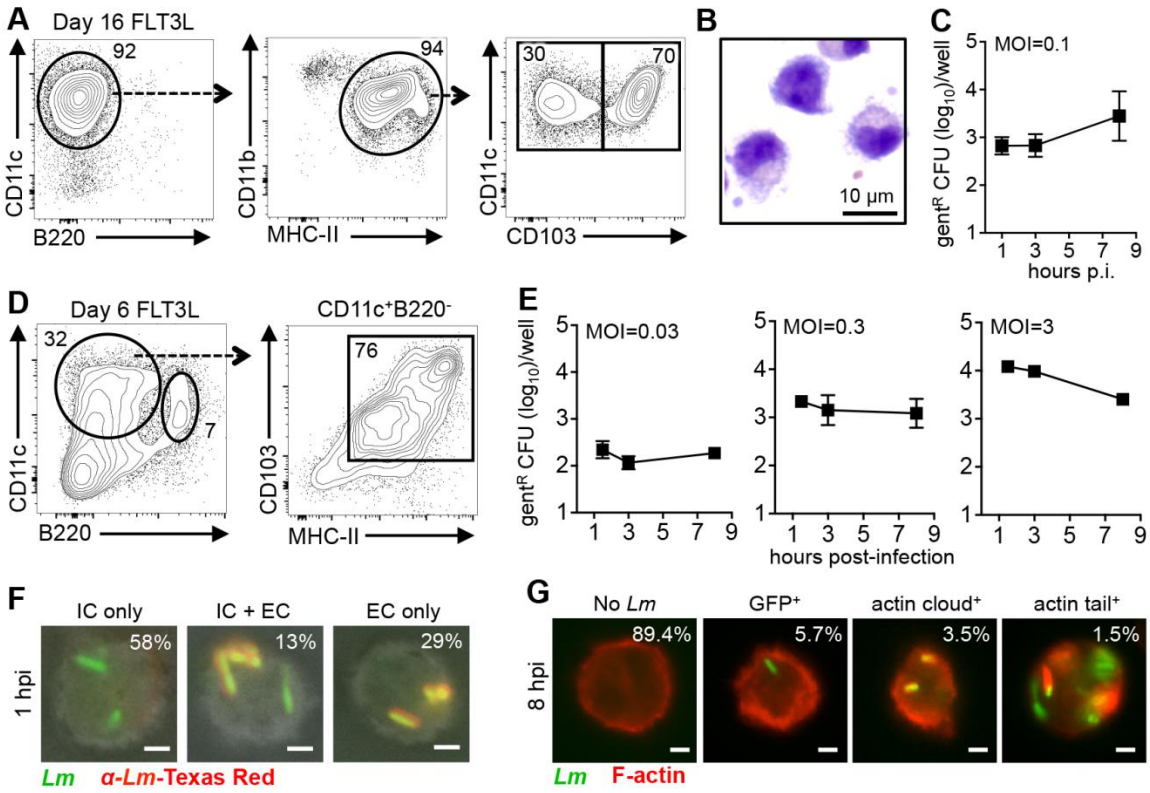
A
Day 16 FLT3L
92
94
30
70
CD11c
B220
CD11b
MHC-II
CD11c
CD103
B
10 µm
C
MOI=0.1
gentR CFU (log10)/well
hours p.i.
D
Day 6 FLT3L
CD11c+B220-
32
7
76
CD11c
B220
CD103
MHC-II
E
MOI=0.03
MOI=0.3
MOI=3
gentR CFU (log10)/well
hours post-infection
F
IC only
IC + EC
EC only
1 hpi
58%
13%
29%
Lm
α-Lm-Texas Red
G
No Lm
GFP+
actin cloud+
actin tail+
8 hpi
89.4%
5.7%
3.5%
1.5%
Lm
F-actin

Figure 5.8: CD103$^+$CD11c$^+$ generated using FLT3-L do not efficiently support the intracellular replication of *L. monocytogenes.*

(A) Gating scheme depicting the phenotype of BM cells that were cultured for 16 days in 12.5% FLT3-L supernatant with 0.75% GM-CSF. **(B)** DiffQuik staining of cells cultured for 16 days in FLT3-L. **(C)** Mean (±SD) number of intracellular (gent-resistant) *Lm* recovered from triplicate wells with 1x10^5 cells from day 16 FLT3-L cultures in 96-well low attachment plates after a 30 min. infection. **(D)** Gating scheme used to identify cell populations that resulted after BM cells were cultured in 20% FLT3-L for six days. **(E)** Mean (±SD) number of intracellular (gent-resistant) *Lm* recovered from triplicate wells with 1x10^5 cells from day six FLT3-L cultures in 96-well low attachment plates after a 30 min. infection. **(F-G)** Day six FLT3-L cells were infected with GFP$^+$ *Lm* SD2710 for 30 min. at a MOI of 1, washed 3 times, and then cultured in media containing gentamicin at least 20 min. **(F)** Representative images of cells that were spun onto slides 1 hpi and then stained with *Lm* antiserum that was detected using a Texas-Red secondary without membrane permeabilization. Internalized *Lm* are green only while extracellular bacteria appear yellow after merging green and red channels. Percentages indicate the percentage of *Lm*$^+$ cells that either had only intracellular *Lm* (IC only), intracellular and extracellular *Lm* (IC + EC), or only extracellular *Lm* (EC only). A total of ~300 cells were counted.**(G)** Representative images of cells that were spun onto slides and then stained with Texas Red-conjugated phalloidin 8 hpi. Percentages indicate the proportion of total cells counted (~400) that were either uninfected (No *Lm*), *Lm* not associated with F-actin (GFP$^+$ *Lm)*, *Lm* associated with actin clouds, or *Lm* associated with actin tails. Scale bars, 2 μm. In panels C and E, data representative of 2-3 separate experiments is shown.

IV. Discussion

There is little data describing the intracellular fate of *L. monocytogenes* in bona fide DC. Therefore, in this study, we focused on the growth of *L. monocytogenes* in DC, which were associated with *L. monocytogenes* in the intestinal LP and MLN during foodborne infection. However, we were unable to establish productive infection of DC isolated *ex vivo.* Infection of bone marrow-derived cells that phenotypically resembled *in vivo* DC indicated that these cells significantly vary in their ability to support *L. monocytogenes* growth over time depending on the culture method. Our data suggest that the minor proportion of DC associated with *L. monocytogenes* in the gut and MLN do not serve as an intracellular growth niche for *L. monocytogenes in vivo.* A summary of our findings using various types of DC is depicted in the cartoon shown in Fig. 5.9.

The role of DC during *L. monocytogenes* infection have been primarily limited to the interaction of *L. monocytogenes* with DC in the spleen following intravenous infection. A cohort of studies published around the same time demonstrated that the ablation DC reduced colonization of the spleen, but also, *L. monocytogenes*-infected DC were important for mediating local immune cell activation and effective T cell responses in the spleen (Campisi et al., 2011; Edelson et al., 2011; Kang et al., 2008; Kapadia et al., 2011; Mitchell et al., 2011; Neuenhahn et al., 2006). The role of DC in establishing infection of the spleen is intriguing, as it suggests that these cells may serve as an important intracellular growth niche for *L. monocytogenes.* However, rather than supporting intracellular growth, the underling mechanism is thought to be due to the translocation of *L. monocytogenes* by $CD8\alpha^+$ DC from the splenic red pulp into the periarteriolar lymphoid sheath of the white pulp, in which *L. monocytogenes* subsequently replicated in other cell types and also likely extracellularly (Aoshi et al., 2009; Edelson et al., 2011; Neuenhahn et al., 2006). Therefore, the role of DC *in vivo*, at least in the spleen during systemic *L. monocytogenes* infection, appears to be related to initial uptake of *L. monocytogenes* and not necessarily a productive intracellular niche for *L. monocytogenes*.

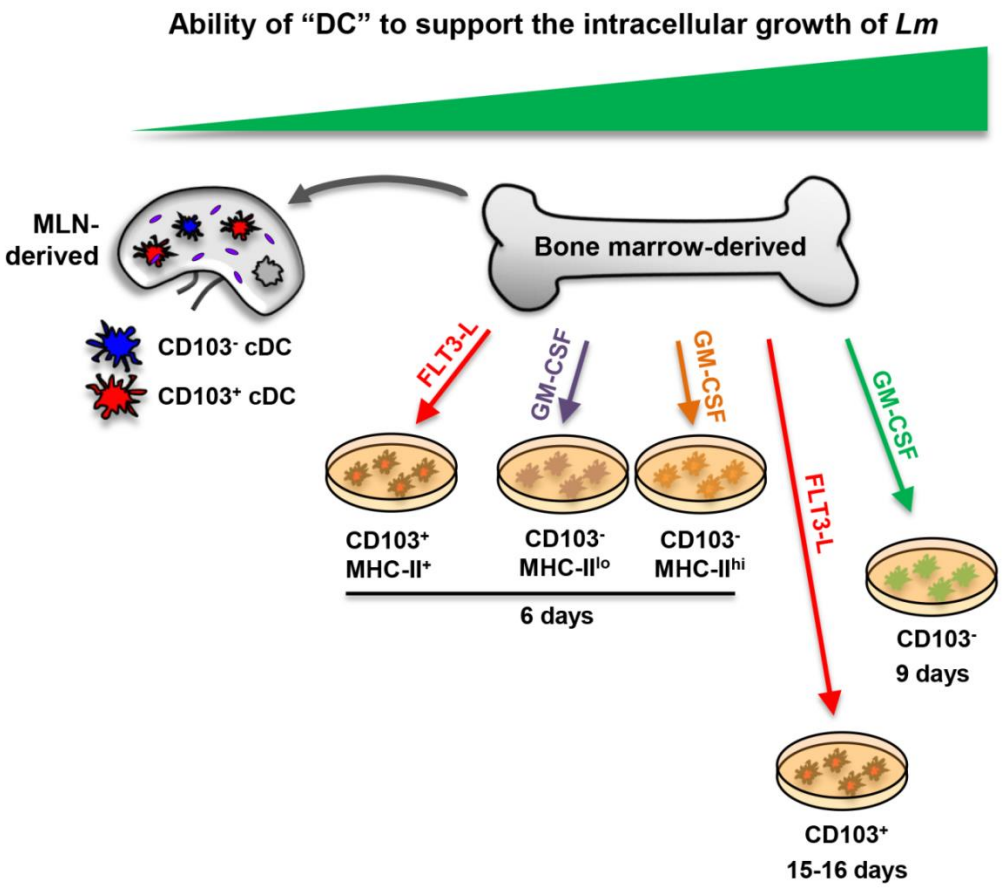

Figure 5.9: Comparison of *L. monocytogenes* growth inside *ex vivo* and cultured DC.

Cartoon depicting the relative ability of DC to support the intracellular growth of *Lm* after being isolated from the MLN or cultured *in vitro* using various methods. Intracellular growth rate of *Lm* is least efficient in DC on the left and growth rate increases in cells cultured from left to right.

When $CD11c^{hi}CD103^{-}$ and $CD11c^{hi}CD103^{+}$ DC were sorted from the MLN and infected *in vitro*, $CD103^{+}$ DC took up *L. monocytogenes* within an hour, but intracellular *L. monocytogenes* were undetectable 8 hpi. This result was consistent with microscopic findings by Pron *et al*. in which $OX\text{-}62^{+}$ (CD103) cells were found to be associated with *L. monocytogenes* in Peyer's patches and some in the MLN after a ligated loop infection in rats, but these cells did not appear to support *L. monocytogenes* growth by counting the number of bacteria per cell (Pron et al., 2001). In that study, the authors indicated that only a few *L. monocytogenes* were found associated with $OX\text{-}62^{+}$ DC, in contrast to other cell populations that were normally heavily infected (Pron et al., 2001). Hence, neither $CD103^{-}$ or $CD103^{+}$ DC in the gut appear to be the vital intracellular niche during foodborne *L. monocytogenes* infection as we had initially hypothesized.

The mechanism by which DC efficiently limit the intracellular growth of *L. monocytogenes* remains unclear. It is possible that *L. monocytogenes* are either unable to escape the phagocytic vacuole, or that *L. monocytogenes* do not efficiently replicate in the cytosol. Microscopic evaluation of cells cultured in FLT3-L indicated that at least one bacterium was internalized in ~70% of all cells within an hour (Fig. 5.8). However, at 8 hpi, ~90% of the cells appeared uninfected (Fig. 5.8), which suggests that *L. monocytogenes* were actively degraded in the phagocytic vacuole and not simply surviving in the cytosol. This observation is consistent with a previous report in which human monocyte-derived DC generated using GM-CSF for 7 days were able to efficiently retain *L. monocytogenes* in the phagocytic vacuole (Kolb-Maurer et al., 2000). There is some evidence to suggest the phagocytic vacuole of monocyte-derived $CD11c^{+}$ cells cultured using GM-CSF is more efficient at limiting the escape of *L. monocytogenes* compared to in M-CSF-derived cells (Westcott et al., 2010). This was thought to be due to the relatively higher pH of the phagocytic vacuole in GM-CSF-cultured cells (Westcott et al., 2010), and because LLO pore-forming activity is optimum at a low pH (Geoffroy et al., 1987), *L. monocytogenes* did not efficiently escape the phagocytic vacuole and were slowly degraded. Therefore, as we previously proposed in monocytes, it is possible that delayed or reduced acidification of the phagosome in DC efficiently limits the escape of *L. monocytogenes* from the phagocytes vacuole. Another study by Matsumura *et al.* proposed an alternative mechanism for why DC were relatively resistant against *L. monocytogenes* infection, which was due to the expression of Fascin-1, an actin-bundling protein that is not expressed by macrophages (Matsumura et al., 2013). Specifically, the expression of Fascin-1 induced the association of microtubule-

associated protein 1A/1B-light chain with *L. monocytogenes*, which was proposed to induce autophagy and killing of cytosolic *L. monocytogenes* (Matsumura et al., 2013). Therefore, multiple mechanisms may impair the ability of *L. monocytogenes* to productively infect DC in both the phagosomal and cytosolic compartment.

The variable rate of intracellular growth rate in different types of bone marrow-derived DC highlighted two main findings: (1) $CD11c^+$ cells differentiated in the presence of GM-CSF more efficiently supported the growth of *L. monocytogenes* compared to FLT3-L-cultured cells and (2) Prolonged growth of DC in either GM-CSF or FLT3-L resulted in a better intracellular niche for *L. monocytogenes.* First, the observation that *L. monocytogenes* grew more efficiently in GM-CSF-derived "DC" is not surprising given the fact that global gene expression profiling indicated that these cells are actually more similar to M-CSF-cultured macrophages and peritoneal macrophages than splenic DC (Mabbott et al., 2010). In contrast, it is clear that cells generated in FLT3-L cultures more closely resemble splenic DC in regards to their surface marker expression, dependence on IFN regulatory factor-8 for differentiation, production of inflammatory cytokines, and cross-presentation to CD8 T cells (Naik et al., 2005). In regards to the second raised question, there is no empirical evidence to explain why a prolonged culture period enhanced the intracellular growth rate of *L. monocytogenes.* One explanation could be the extended time period in which secreted cytokines remain in the culture medium, thereby leading to feedback regulation and possibly altered cellular functions (Lacey et al., 2012). It is also plausible that the function of these cells is altered over time *in vitro* due to the absence of unknown regulatory factors expressed by other types of immune cells or stromal cells *in vivo*. For these reasons, we would conclude that our results using FLT3-L-derived DC, especially when cultured only six days, most closely resemble true DC, and accordingly, reflected our findings using DC isolated from the MLN in terms of supporting *L. monocytogenes* growth over time. Collectively, our data indicate that *bona fide* DC do not support the intracellular replication of *L. monocytogenes.*

At the onset of this study, we found that myeloid cells isolated from the MLN supported the intracellular growth of *L. monocytogenes*. In contrast, myeloid cells isolated from the intestinal LP were less efficient at supporting *L. monocytogenes* growth over time. Therefore, we propose that an unidentified, non-DC myeloid cell type in the MLN, is likely to serve as the vital intracellular growth niche for *L. monocytogenes*. We would predict the most probable candidate cell type to be a macrophage-like cell. One underlying caveat with this hypothesis is that we were unable to recover intracellular

CFU from this same pool of myeloid cells isolated from the MLN 2 dpi (Fig. 5.5). However, one could argue that this approach may not be the best proxy to determine if these cells actually support intracellular growth over time due to the rare fraction of *L. monocytogenes*-associated cells that appear to be infected in the MLN at any given time (Jones et al., 2015). Therefore, future studies will focus on the identification of myeloid cells sorted from the MLN that are productively infected with *L. monocytogenes* using single-cell analyses such as flow cytometry and microscopy.

Chapter 6: Dissemination of *L. monocytogenes* from the gut to the MLN

I. Summary

The migration of foodborne pathogens beyond the intestinal mucosa is the first step in establishing systemic disease. In this study, we investigated the proposed mechanisms by which *L. monocytogenes* disseminate from the intestine to the MLN, which is one of the earliest bottlenecks of systemic *L. monocytogenes* infection. Previously, we found that *L. monocytogenes* were predominantly associated with Ly6C^{hi} monocytes that were recruited to the MLN during infection. Furthermore, monocytes isolated from the intestinal LP were also found in association with *L. monocytogenes.* Therefore, we tested whether monocytes recruited to the gut were important for transporting *L. monocytogenes* to the MLN. To do this, we compared the number of *L. monocytogenes* that reached the MLN between control and *ccr2*$^{-/-}$ mice, which have a defect in monocyte migration. However, we recovered nearly identical bacterial burdens from the MLN of both *ccr2*$^{-/-}$ and control mice. This suggests that monocytes are not required for *L. monocytogenes* to spread to the MLN, or that other routes can compensate for the lack of monocytes in *ccr2*$^{-/-}$ mice. We previously showed that the vast majority of *L. monocytogenes* recovered from the MLN 2 dpi were extracellular, and a large proportion of *L.* monocytogenes were extracellular in the intestinal LP. Thus, it is possible that extracellular *L. monocytogenes* migrate freely in lymphatic vessels that drain to the MLN. To confirm this possibility, we visualized afferent lymphatic vessels in the whole-mounted mesentery. Approximately one hour after injection of GFP^{+} *L. monocytogenes* into a ligated loop of the ileum, we found that *L. monocytogenes* were primarily extracellular in mesenteric lymphatic vessels. Overall, our findings suggest that multiple routes may be used by *L. monocytogenes* to spread from the gut to the MLN including both the migration of monocytes and extracellular trafficking of free *L. monocytogenes.*

II. Introduction

Tolerance to food-derived antigens and commensal bacteria in the gastrointestinal tract is crucial for maintaining homeostasis in the gut. Immune tolerance is mediated primarily by the migration of intestinal dendritic cells to the MLN and the subsequent presentation of either food or microbiota-derived antigens to lymph node-

resident T cells in the context of suppressive cytokines (Macpherson and Smith, 2006). It is also possible for T cell tolerization to occur in peripheral lymph nodes against gut-derived antigens that passage through the hepatic portal vein and the liver. However, foodborne enteric pathogens can utilize both hematogenous and lymphatic pathways to spread beyond the intestinal mucosa and cause systemic infections.

Studies using signature-tagged bacteria (Barnes et al., 2006; Lim et al., 2014; Melton-Witt et al., 2012) have been fundamental in modeling the dissemination of enteric pathogens by highlighting two routes of spread from the gut. Oral infection of guinea pigs with signature-tagged *L. monocytogenes* clones suggested a direct route of spread from the intestine to the liver, presumably via the portal vein, since those clones were not found in the spleen (Melton-Witt et al., 2012). Dissemination from the gut to the spleen and liver occurred through a lymphatic route via the MLN, as *L. monocytogenes* recovered from the spleen and liver were also found in the MLN (Melton-Witt et al., 2012). The MLN contained the highest percentage of bacterial clones of all other organs tested with approximately one in every 10^2 to 10^3 *L. monocytogenes* making it past this rate-limiting step from the MLN to the spleen (Melton-Witt et al., 2012). In addition to a physical route for trafficking beyond the intestine, the MLN can be a reservoir for other foodborne pathogens such as *Salmonella* Typhi that persisted throughout antibiotic treatment (Griffin et al., 2011). Therefore, it is important to understand how enteric pathogens spread to the MLN, which represent a reservoir for bacterial growth and a bottleneck for systemic disease.

Facultative intracellular pathogens such as *Salmonella* Typhimurium and *Yersinia pestis* are thought to migrate to tissue-draining lymph nodes extracellularly, but have also been associated with migratory dendritic cells and monocytes (Gonzalez et al., 2015; Kaiser et al., 2013; St John et al., 2014; Voedisch et al., 2009). The mechanism by which *L. monocytogenes* disseminate from the intestinal LP to the MLN has not been clearly defined. Pron *et al.* proposed that DC are capable of transporting intracellular *L. monocytogenes* from the small intestine Peyer's patches to the MLN. In that study, they found that *L. monocytogenes* were preferentially associated with OX-62^+ (CD103) cells in Peyer's patches early after infection and that OX-62^+ cells were the first to be infected in the MLN (Pron et al., 2001). It is important to mention that this study used wild type *L. monocytogenes* to inoculate a ligated section of the ileum in rats, a species which expresses E-cadherin that is not efficiently bound by wild type *L. monocytogenes* InlA (Pron et al., 2001). In contrast, our data suggests that the majority

of *L. monocytogenes* in the gut and MLN are extracellular after foodborne infection, and that the minor proportion of cell-associated *L. monocytogenes* were found with Ly6C^{hi} monocytes, and not DC.

Dogma would suggest that bloodborne monocytes always differentiate into macrophages after entering tissues. However, recent studies have demonstrated that monocyte subsets can enter peripheral tissues, take up antigen, and then deliver it to draining lymph nodes *without* differentiating into macrophages (Jakubzick et al., 2013; Rodero et al., 2015). Likewise, *Salmonella abortusovis*, a sheep adapted strain, was found to migrate primarily with monocytes and granulocytes in lymphatic fluid after infection of the oral mucosa (Bonneau et al., 2006). Therefore, we propose that either the flow of extracellular *L. monocytogenes*, or the migration of *L. monocytogenes* adhered to monocytes promotes spread of *L. monocytogenes* to the MLN. In this study, we examined both of these routes by inhibiting the egress of monocytes from the bone marrow and visualizing *L. monocytogenes* in afferent lymphatic vessels that drain the intestine.

III. Results

A. Recruitment of monocytes to the gut is not required for dissemination to the MLN

We previously showed that the majority of cell-associated *L. monocytogenes* in the MLN was found with Ly6C^{hi} monocytes 2 dpi (Jones and D'Orazio, 2017), which is one of earliest time points *L. monocytogenes* is consistently found in the MLN (Bou Ghanem et al., 2012). In addition, *L. monocytogenes* interacted with Ly6C^{hi} monocytes in the large intestinal lamina propria 2 dpi. *L. monocytogenes* inefficiently invaded monocytes sorted from the MLN, which suggested that most of the cell-associated *L. monocytogenes* were adhered to monocytes in the MLN. Therefore, it is possible that spread of *L. monocytogenes* from the gut to the MLN could be achieved by the migration of monocytes with adherent *L. monocytogenes.* To block the migration of inflammatory monocytes to the intestine during *L. monocytogenes* infection we obtained *ccr2*$^{-/-}$ mice, which have a defect in monocyte egress from the bone marrow. We hypothesized that *ccr2*$^{-/-}$ mice would have significantly lower bacterial burdens compared to wild type mice if inflammatory monocytes transported adherent *L. monocytogenes* from the gut to the MLN. However, c*cr2*$^{-/-}$ mice are only commercially available on the C57BL/6J (B6)

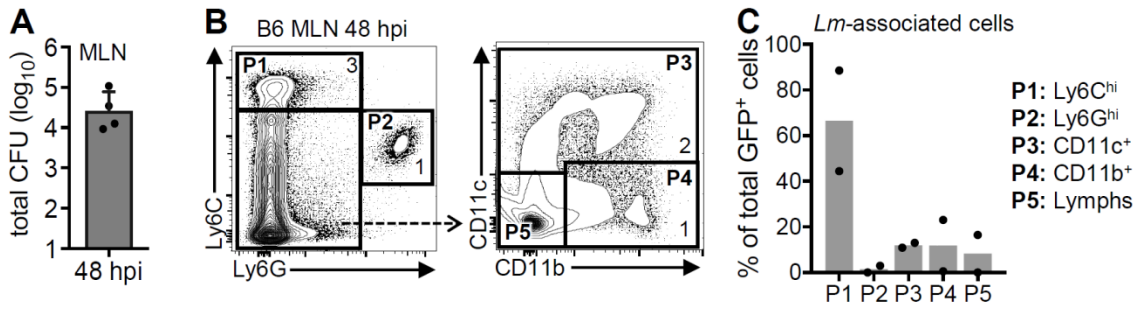

Figure 6.1: *L. monocytogenes* preferentially associate with Ly6C^{hi} cells in the MLN of C57BL/6J mice

Six to eight week-old female C57BL6J mice were fed 5x10^8 *Lm* SD2000 (vector control strain) or *Lm* SD2710. **(A)** Mean (±SD) number of *Lm* recovered from the MLN 2 dpi (n=4). **(B)** Gating scheme used to subset MLN populations (P1, P2, P3, P4, P5) 2 dpi as done previously in BALB mice (compare to Fig. 4.1). Numbers inside each gated population indicate the percentage of cells in each contour plot. **(C)** Average proportion of total GFP$^+$ cells in each population (n=2).

background, which are relatively resistant to foodborne *L. monocytogenes* infection compared to BALB mice (Bou Ghanem et al., 2012). Likewise, slightly lower bacterial burdens were found in the MLN of B6 mice 2 dpi (Fig. 6.1A) compared to BALB/cBy/J mice (~10^5 CFU). Therefore, we confirmed that the majority of cell-associated *L. monocytogenes* in the MLN were found with Ly6C^{hi} monocytes in B6 mice as we previously observed in BALB mice. To do this, B6 mice were fed GFP$^+$ *L. monocytogenes* and MLN cells were isolated 2 dpi and analyzed for GFP expression compared to MLN cells isolated from mice fed a vector control strain. Nearly the same percentage (2-3%) of MLN cells were Ly6C^{hi} in B6 mice as previously found in BALB mice 2 dpi (see Fig. 4.1A). Furthermore, the majority of GFP$^+$ cells isolated from the MLN were also Ly6C^{hi} P1 cells (Fig. 6.1). Together, this indicates that the recruitment of Ly6C^{hi} monocytes to the MLN is similar in both mouse strains, as well as their preferential association with *L. monocytogenes.*

Next, flow cytometry was used to confirm that the recruitment of Ly6C^{hi} monocytes to the MLN was inhibited in *ccr2*$^{-/-}$ compared to B6 mice (Fig. 6.2A). As expected, there was a significant reduction in the number of Ly6C^{hi}CD11b$^+$ cells in the MLN of *ccr2*$^{-/-}$ compared to B6 mice (Fig. 6.2B). This was consistent with previous studies in which recruitment the inflammatory monocytes to the spleen of *ccr2*$^{-/-}$ mice was impaired after intravenous *L. monocytogenes* infection (Serbina and Pamer, 2006). Lastly, there was no difference in the number of Ly6C$^{-/+}$CD11c$^+$CD64$^-$ dendritic cells or Ly6C$^{-/+}$CD64$^+$ macrophages (Fig. 6.2C), indicating the number of mononuclear phagocytes in the MLN was similar in both mouse strains during infection.

Two days after infection, the same number of CFU was recovered from the intestine and MLN of B6 and *ccr2*$^{-/-}$ mice (Fig. 6.2D,E). This indicates that trafficking of monocytes from the gut to the MLN is not required for *L. monocytogenes* dissemination. A significantly higher number of *L. monocytogenes* was recovered from the livers of *ccr2*$^{-/-}$ mice compared to B6 mice, but there was not a significant difference in the number of CFU recovered from the spleen (Fig. 6.2F). The biological significance of elevated bacterial burdens in the livers of *ccr2*$^{-/-}$ mice is unclear. It is possible that inflammatory monocytes are either important for limiting the hematogenous spread of *L. monocytogenes* from the intestine to the liver via the portal vein, or efficiently killing *L. monocytogenes* after spread to the liver.

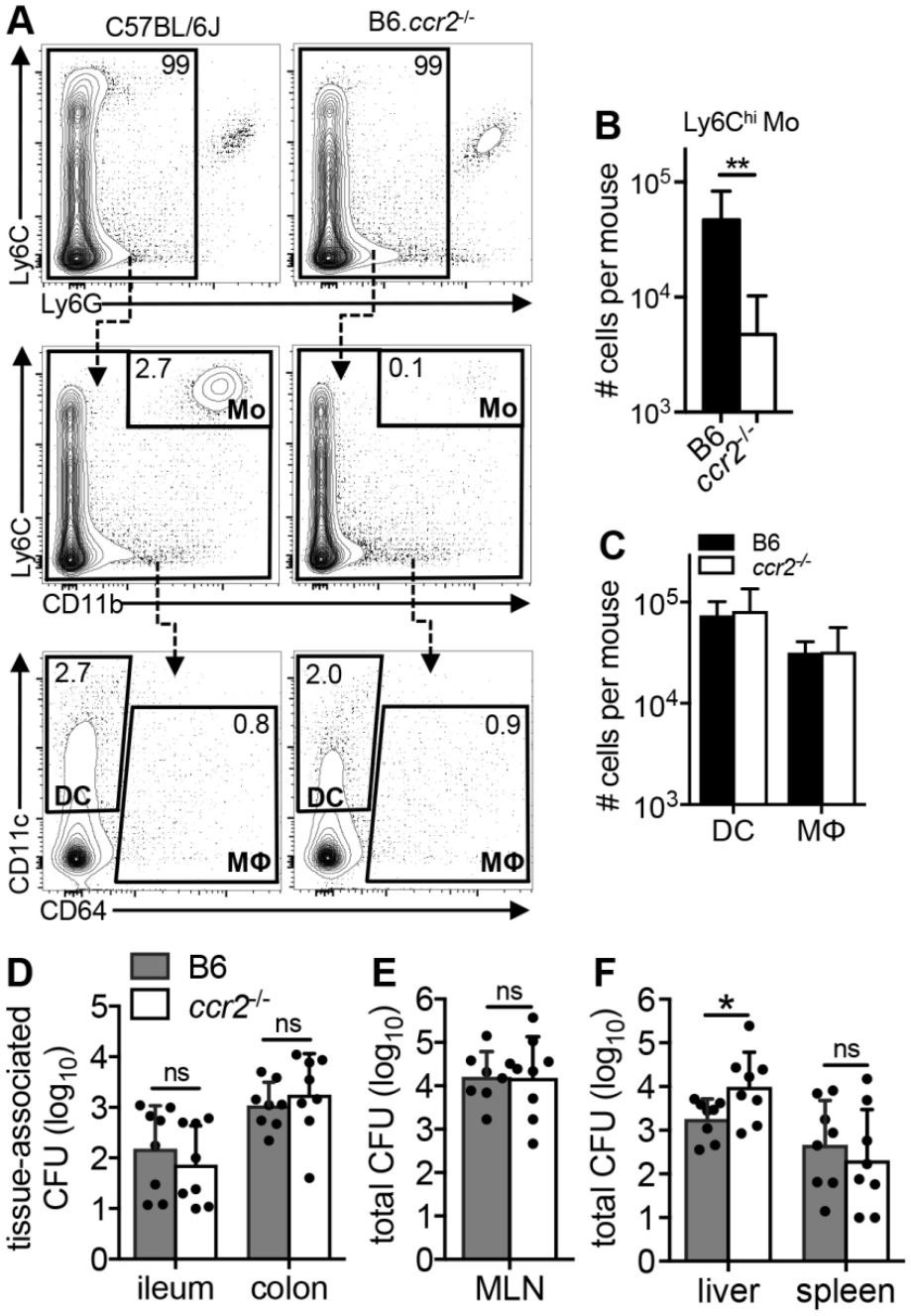
A
C57BL/6J
B6.ccr2-/-
99
99
Ly6C
Ly6G
2.7
Mo
0.1
Mo
Ly6C
CD11b
2.7
0.8
DC
MΦ
2.0
0.9
DC
MΦ
CD11c
CD64
B
Ly6Chi Mo
**
cells per mouse
10^5
10^4
10^3
B6
ccr2-/-
C
B6
ccr2-/-
cells per mouse
10^5
10^4
10^3
DC
MΦ
D
B6
ccr2-/-
tissue-associated CFU (log10)
ns
ns
ileum
colon
E
ns
total CFU (log10)
MLN
F
*
ns
total CFU (log10)
liver
spleen

Figure 6.2: Similar numbers of *L. monocytogenes* are recovered from the MLN of *ccr2*$^{-/-}$ and control mice

Seven to eight week-old female B6 or *ccr2*$^{-/-}$ mice were fed 3-4x10^{8} *Lm* SD2001. **(A)** Gating scheme used to determine the number of Ly6C^{hi} monocytes, CD11c^{+}CD64^{-} DC, and CD64^{+} macrophages in the MLN of each mouse. **(B)** Mean (±SD) total number of Ly6C^{hi}CD11b^{+} monocytes in the MLN of each mouse strain 2 dpi (n=8 of each strain). **(C)** Mean (±SD) total number of DC (CD11c^{+}CD64^{-}) and Ly6C$^{-/+}$CD64^{+} macrophages (Mϕ) in the MLN of each mouse strain 2 dpi (n=8 of each strain). **(D-F)** Mean (±SD) total number of *Lm* recovered from the **(D)** ileum and colon, **(E)** MLN, or **(F)** liver and spleen of each mouse strain 2 dpi. Symbols represent each mouse. Pooled data from two separate experiments is shown. Statistical significance was evaluated by Mann-Whitney analysis.

B. Extracellular *L. monocytogenes* primarily migrate in afferent mesenteric lymphatic vessels

We previously found that intracellular *L. monocytogenes* represented only a minor proportion of the total bacterial burden recovered from the MLN. Therefore, it is possible that monocytes play only a minor role in transporting *L. monocytogenes* to the MLN, whereas, spread to the MLN could be mediated primarily by trafficking of extracellular *L. monocytogenes*. To determine if extracellular *L. monocytogenes* could spread to the MLN, we directly visualized *L. monocytogenes* in afferent mesenteric lymphatic vessels using confocal microscopy (Fig. 6.3A). To synchronize intestinal infection and subsequent entry into lymphatic vessels, we used a ligated ileal loop infection in BALB mice (Fig. 6.3B, "1"). The series of steps depicted by the images in Fig. 6.3B describes the methodology used to whole-mount the mesentery and label lymphatic vessels and immune cells using α-podoplanin and α-CD45, respectively. Forty-five minutes after ileal loop infection with 10^8-10^9 GFP^+ *L. monocytogenes,* 10^3 to 10^4 CFU could be recovered from each mesenteric lymph node, confirming that this approach resulted in spread of *L. monocytogenes* to the MLN via lymphatic vessels. To visualize *L. monocytogenes* trafficking in lymphatic vessels, z-stack projections were created to visualize across the entire depth (z-axis) of each vessel. Lymphatic vessels imaged near the gut were densely filled with *L. monocytogenes*, which were predominantly non cell-associated (Fig. 6.4). To confirm that *L. monocytogenes* were localized in the lumen of lymphatic vessels, we used orthogonal views to visualize *L. monocytogenes* inside a vessel (Fig. 6.5A,B). This method convinced us that *L. monocytogenes* were located in the lumen of lymphatic vessels (Fig. 6.5B). Mesenteric lymphatic vessels predominantly contained extracellular *L. monocytogenes*, as it was rare to find $CD45^+$ cells in vessels (Fig. 6.6). However, the few $CD45^+$ cells that were in lymphatic vessels were often associated with *L. monocytogenes*, but it is unclear if these cells harbored intracellular bacteria, or *L. monocytogenes* that were adherent.

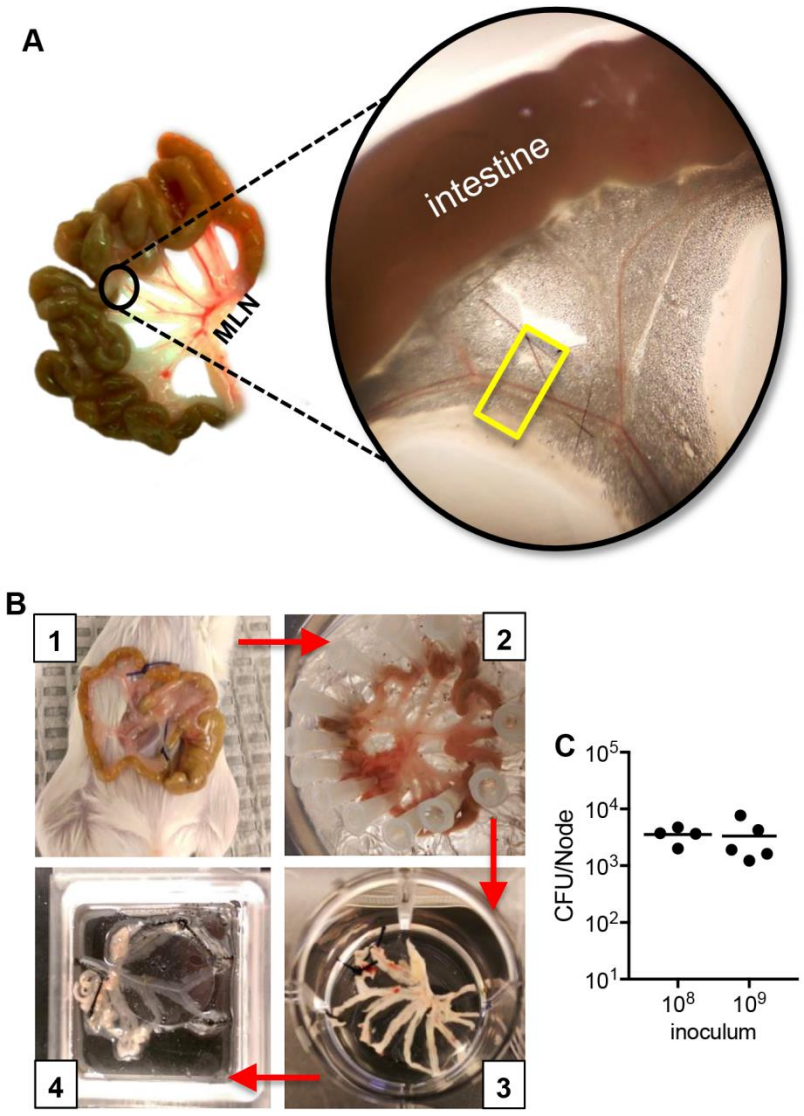
A
intestine
MLN
B
1
2
3
4
C
CFU/Node
10^5
10^4
10^3
10^2
10^1
10^8
10^9
inoculum

Figure 6.3: Description of ligated ileal loop infection and mesentery whole-mount protocol

(A) Macroscopic image of a mesentery plexus containing blood and lymphatic vessels adjacent to the small intestine. Yellow square indicates typical area of mesentery that was visualized using confocal microscopy after whole mount protocol. **(B)** Steps used to prepare the mesentery for analysis; (1) 10^8-10^9 GFP^+ *Lm* were injected into a 4 to 5-cm ligated ileal section in anesthetized mice. (2) Mice were euthanized 45 minutes later and the mesentery (still connected to the intestine) was stabilized with needles. The MLN were removed for CFU analysis and then the tissue was fixed overnight in 4% paraformaldehyde. (3) The mesentery was excised from the intestine using a scalpel, washed with PBS, permeabilized for four hours, blocked in BSA for two hours, and then stained overnight with CD45-eFluor450 and Podoplanin-eFluor660. (4) The next day, the tissue was washed with PBS for four hours and then transferred to a glass coverslip-bottom dish with liquid mounting medium and analyzed using confocal microscopy. **(C)** Mean number of CFU recovered from each mesenteric lymph node 45 minutes after ileal loop infection with 10^8 or 10^9 *Lm* SD2710. Horizontal bar indicates mean and symbols represent CFU found in each node from one mouse at each dose.

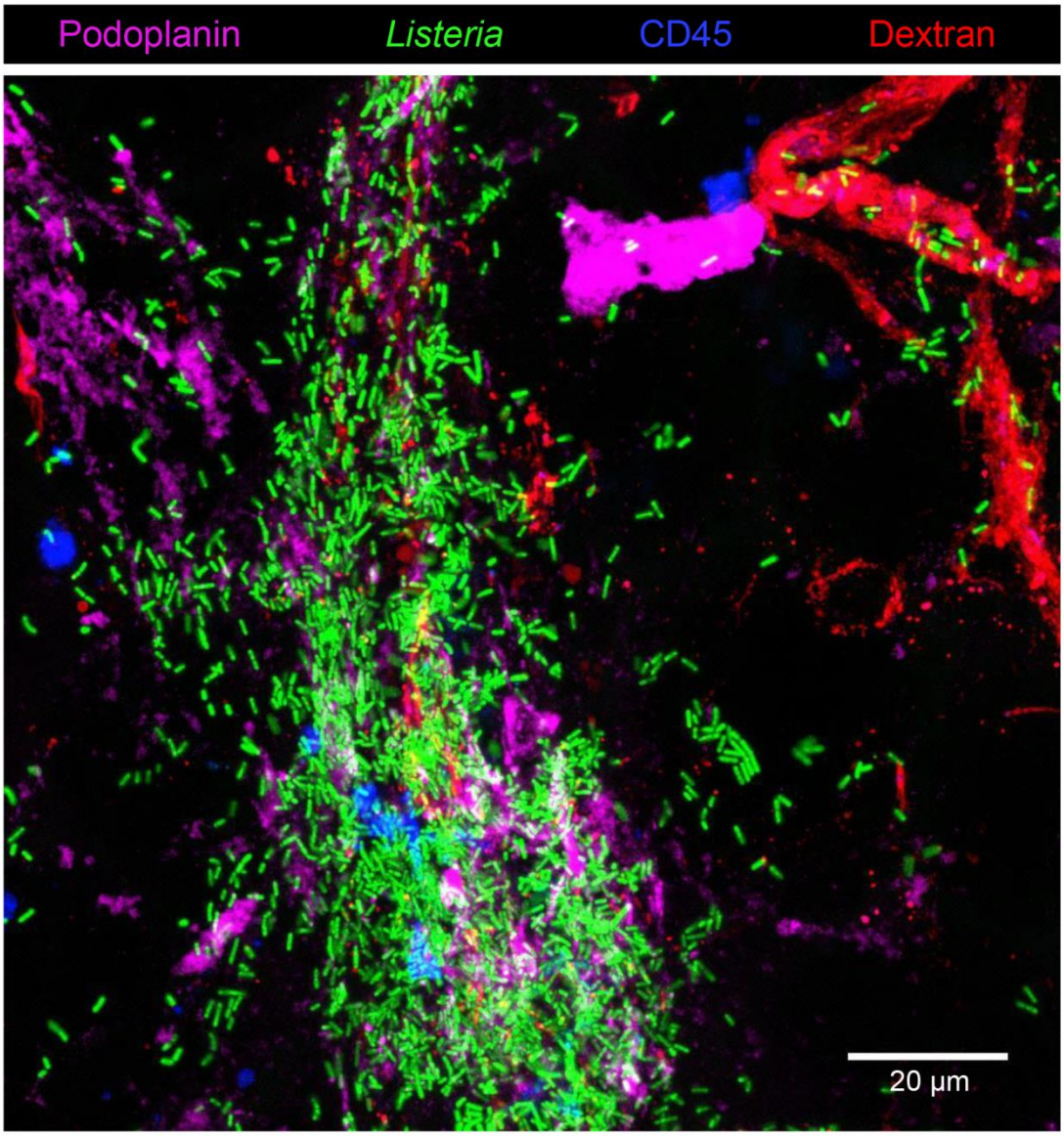

Figure 6.4: Extracellular *L. monocytogenes* are primarily found in afferent lymphatic vessels

Maximum z-stack projection of a lymphatic vessel (podoplanin$^+$) near the intestine that contained mainly non cell-associated GFP$^+$ *Lm*. Two minutes before euthanasia, Texas-Red-conjugated dextran was injected retro-orbitally to label blood vessels. Acquired using 63X objective.

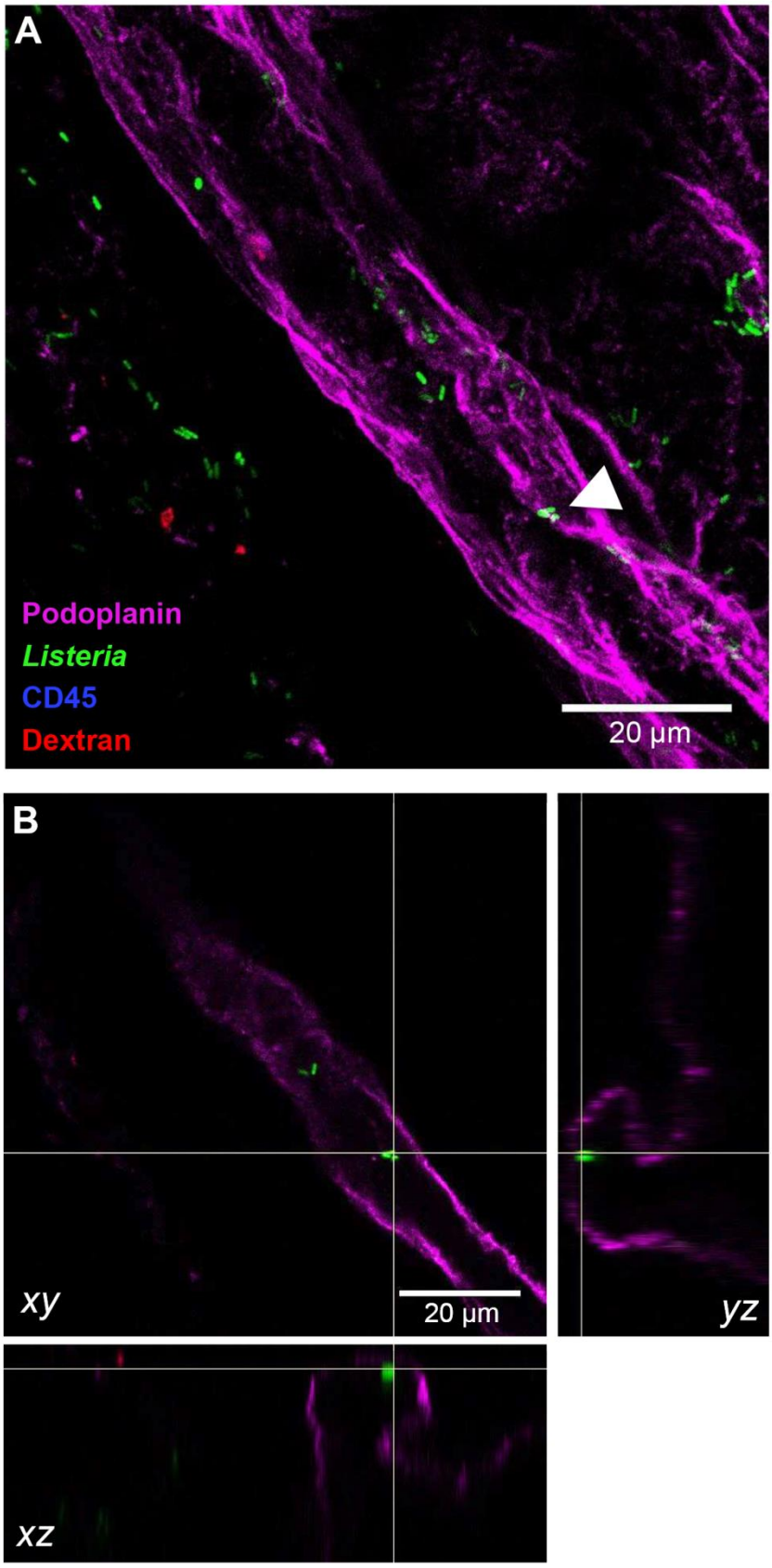
A
Podoplanin
Listeria
CD45
Dextran
20 µm
B
xy
20 µm
yz
xz

Figure 6.5: Orthogonal views of extracellular *L. monocytogenes* in the lumen of a lymphatic vessel.

(A) Maximum z-stack projection of a lymphatic vessel associated with extracellular *Lm.* White arrow head indicates the bacterium analyzed with orthogonal views below **(B)** Orthogonal views (xz, yz) of a single focal plane in the z-stack showing that the GFP^+ *Lm* is located near the luminal surface inside the vessel. Acquired using 63X objective.

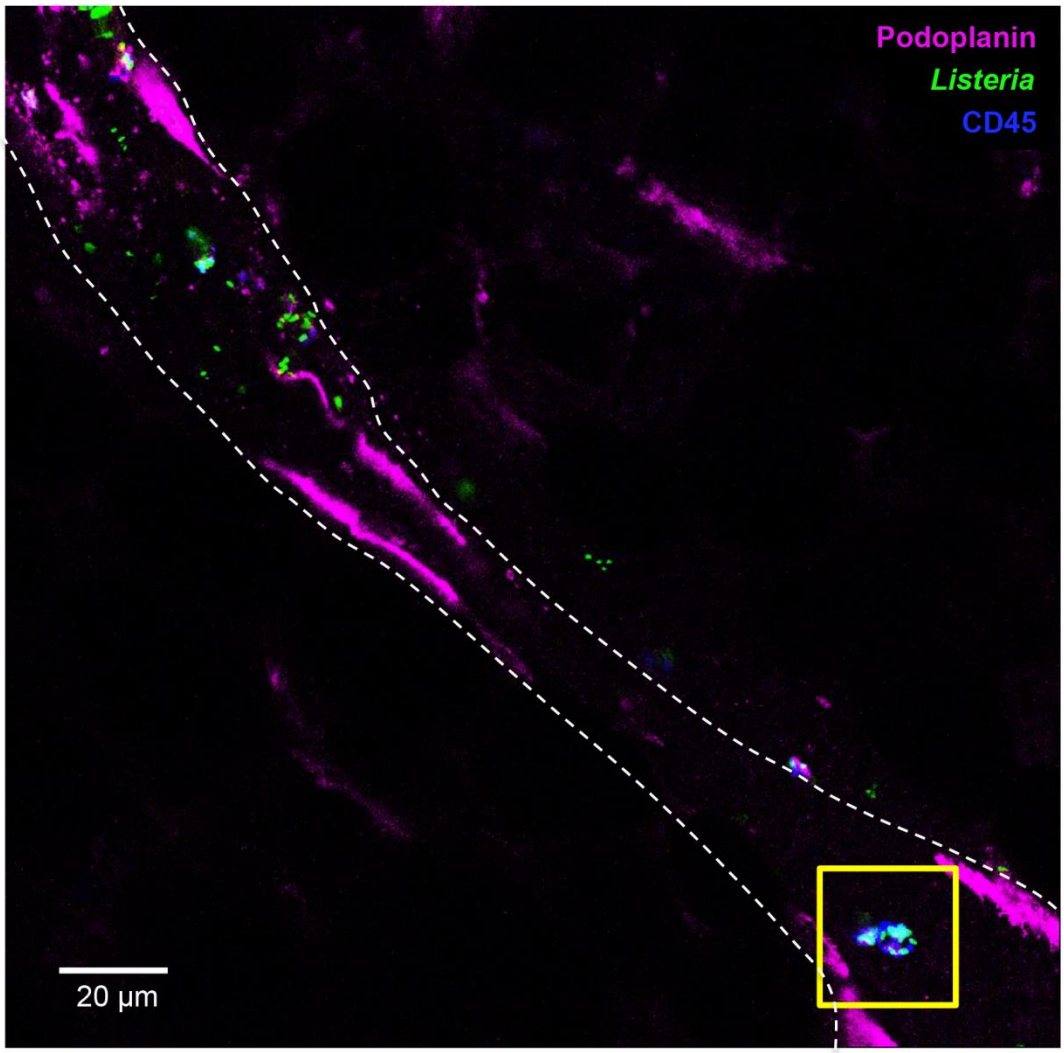

Figure 6.6: Cell-associated *Listeria* are rare in mesenteric lymphatic vessels

Cross-section of a lymphatic vessel containing extracellular *Lm* (near top-left of image) and a $CD45^+$ cell associated with ~10 GFP^+ *Lm* (yellow square). White dashed lines demarcate the vessel walls. Acquired using 63X objective.

Lastly, an intriguing finding that was evident at lower magnification was that *L. monocytogenes* was found in the adipose tissue that surrounds lymphatic vessels (Fig. 6.7). The implications for this observation are unclear, but it may suggest that *L. monocytogenes* can leak out of lymphatic vessels in the mesentery. Moreover, it is possible that the mesenteric adipose tissue serves as niche for bacterial persistence. Additional studies will be required to determine whether this phenomenon is due to either ligation of the gut tissue or the relatively high inoculum.

IV. Discussion

We propose that dissemination of *L. monocytogenes* from the gut to the MLN occurs by at least two major routes: adherence to monocytes and extracellular trafficking. In this study, we demonstrated that the migration of monocytes was not a required pathway since blocking the recruitment of monocytes to the gut did not reduce *L. monocytogenes* burdens in the MLN. Moreover, it is likely that monocyte-mediated transport of *L. monocytogenes* to the MLN is not the primary route used by *L. monocytogenes* to migrate in lymphatics, since *L. monocytogenes* were predominately extracellular in mesenteric lymphatic vessels. Hence, we propose that extracellular migration of *L. monocytogenes* is the primarily route of spread to the MLN.

There has been a recent surge in interest concerning the mesentery, particularly in regards to its modified structure and function during inflammatory bowel disease (Coffey and O'Leary, 2016; Li et al., 2016). It is now appreciated that lymphatic vessels in the mesentery are not simply conduits that drain lymphatic fluid from the gut the MLN. In fact, these vessels may be inherently leaky to some degree, releasing intestinal-derived antigens into the “swamp” of the mesenteric fat. These antigens are subsequently taken-up by a plethora of tissue-resident antigen-presenting cells localized in perinodal fat, which promote T cell responses (Kuan et al., 2015). In addition, some of these phagocytes can also be found intimately attached to lymphatic vessels, whose function appear akin to mononuclear phagocytes that reach dendrites into the lumen of the intestine (Niess et al., 2005). Accordingly, these phagocytes are localized around lymphatic vessels and have been observed to take-up antigens derived directly from the lumen of lymphatic collecting ducts (Kuan et al., 2015).

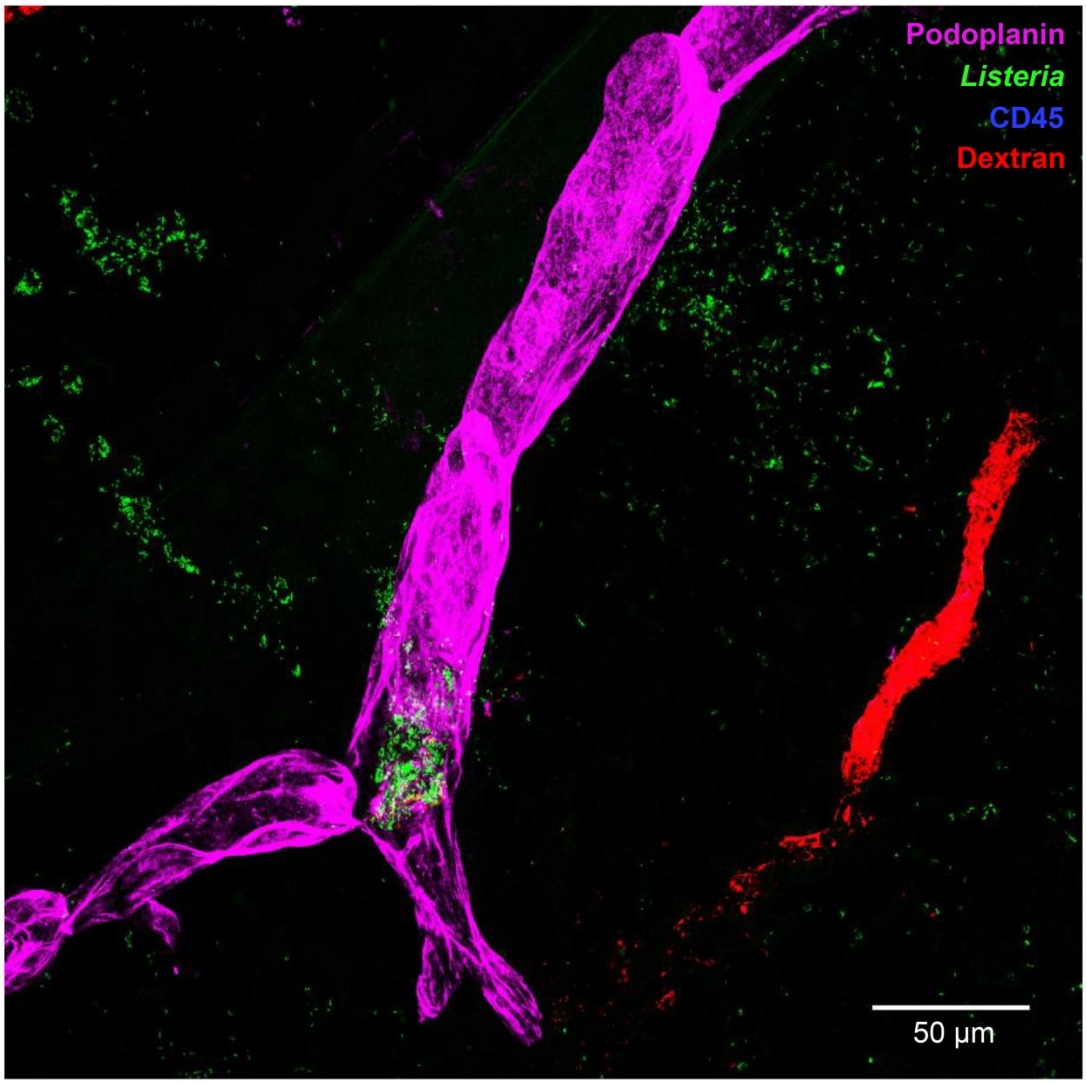

Figure 6.7: *L. monocytogenes* are found in the mesenteric adipose tissue after ileal loop infection

Maximum z-stack projection of a lymphatic vessel containing extracellular *Lm* as well as the *Lm* located in the surrounding adipose tissue. Acquired using 40X objective.

In addition, mononuclear phagocytes situated in the surrounding adipose tissue may have a role in taking-up antigens and controlling local immune responses in the mesentery. As evidenced in our images of the mesentery, we did not reliably observe such phagocytes, likely due to the relatively low expression of CD45 on tissue-resident phagocytes combined with our primary focus on immune cells found migrating inside lymphatic vessels. CD11b and MHC-II are expressed at high levels on these cells (Kuan et al., 2015), and future studies using these markers will allow us to better characterize these phagocytes in the mesentery that may be associated with *L. monocytogenes* in the mesenteric adipose tissue.

Permeable mesenteric lymphatic vessels may exacerbate inflammation of the mesentery during foodborne disease. Oral infection with *Yersinia pseudotuberculosis* triggered a complete remodeling of both mesenteric lymphatic vessels and neighboring adipose tissue (Fonseca et al., 2015). Acute infection with *Y. pseudotuberculosis* triggered excessive permeability of the lymphatic vessels, which impaired migration of DC to the MLN and disrupted normal immune responses for up to 10 weeks after initial infection (Fonseca et al., 2015). Interestingly, this inflammation of the mesentery was suggested to be largely mediated by the microbiota, since antibiotic treatment reversed these effects 4 weeks post-infection and since *Y. pseudotuberculosis* was undetectable after 3 weeks post-infection (Fonseca et al., 2015). We may find that this interesting phenomenon also occurs during foodborne *L. monocytogenes*.

Future directions include titrating down the inoculum used in the ligated ileal loop infection model and well as visualizing lymphatic vessels after foodborne infection with *L. monocytogenes.* We will determine if *L. monocytogenes* is still localized in the surrounding mesenteric fat, as well as determine if cell-associated *L. monocytogenes* are more abundant inside lymphatic vessels. Both of these findings have underlying caveats of using a high inoculum in pilot assays, which could have overwhelmed the natural permeability of lymphatic vessels in the gut, thereby leading to rapid invasion of lymphatic vessels by extracellular organisms. However, these studies were performed to confirm that the extracellular trafficking of *L. monocytogenes* was a possible route of spread from the intestinal LP to the MLN, which was confirmed using this approach. For this reason, we propose that *L. monocytogenes* can migrate extracellularly to the MLN during foodborne infection, but it is possible that other routes such as the migration of *L. monocytogenes* with DC and Ly6C^{hi} monocytes occur at a relatively higher frequency during natural infection.

Chapter 7: Discussion

The conclusions reached by the completion of these studies provide new perspectives into *L. monocytogenes* pathogenesis during foodborne infection as well as highlight the heterogeneity of mononuclear phagocytes in regards to their ability to support the intracellular growth of *L. monocytogenes.* The following implications of the completed studies will be compared to our initial hypotheses, current paradigms in the field, and their context in a proposed order of events that occurs during foodborne *L. monocytogenes* infection: **(I)** Extracellular *L. monocytogenes* drive early immune responses in the gut; **(II)** *L. monocytogenes* is found preferentially adhered to inflammatory cells, and not growing inside tissue-resident phagocytes in the MLN; and **(III)** Dissemination of *L. monocytogenes* to the MLN occurs by multiple mechanisms.

I. Extracellular *L. monocytogenes* drive early immune responses in the gut

One of the most common misconceptions that undermines the pathogenesis of facultative intracellular pathogens is rooted in the description of their life cycle. Simply put, facultative intracellular bacteria are typically extracellular in the environment but are also adapted to grow inside host cells. This assumption underestimates the complex environment that exist *in vivo* including the heterogeneity of innate immune cells, as well as the bottlenecks that must be successfully traversed to disseminate and cause systemic disease (Silva and Pestana, 2013). This misconception also biases immunologists studying the early immune recognition of such pathogens by focusing mainly on the recognition of either internalized organisms by intracellular sensors, or signals secreted by actively infected cells.

The use of *L. monocytogenes* as a tool to study adaptive immunity and T cell-mediated immune responses in the context of systemic infection overshadows our understanding of innate immunity against *L. monocytogenes*, especially during the natural route of infection. Therefore, the implication is that the detection of cytosolic *L. monocytogenes* primarily drives the innate immune response against *L. monocytogenes*, which presumably governs the efficacy of the adaptive immune response. Therefore, much work has focused on the detection of cytosolic *L. monocytogenes* by intracellular sensors, such as those that detect bacterial-derived nucleic acids including RIG-I, MDA5, and STING (Abdullah et al., 2012; Archer et al., 2014), bacterial peptidoglycan by NOD-like receptors (Warren et al., 2008), and NLRP3 and AIM2 inflammasome

activation (Kim et al., 2010). Much less is known about how *L. monocytogenes* drive the overall immune response following foodborne infection, which we found results in a large proportion of extracellular *L. monocytogenes* in the intestine, MLN, spleen, and liver. It is possible that the recognition of peptidoglycan on the surface of *L. monocytogenes* by TLR-2 is one of the first ways *L. monocytogenes* is detected by mononuclear phagocytes in the intestinal LP. The role for TLR-2 in mediating overall resistance to systemic *L. monocytogenes* infection is somewhat conflicting. Expression of TLR-2 was important for the overall survival of mice infected intravenously by controlling *L. monocytogenes* burdens in the liver and mediating the recruitment of inflammatory cells by inducing the secretion of TNF-α and IL-12 (Seki et al., 2002; Torres et al., 2004). Another study indicated that TLR-2-deficient mice were not more susceptible to intraperitoneal *L. monocytogenes*infection compared to control mice (Edelson and Unanue, 2002). However, it is clear from all three of these studies that MyD88-deficient mice are highly susceptible to systemic *L. monocytogenes* infection, which suggests that other TLR-mediated signaling events may be important. Intriguingly, MyD88 may also be important for the activation of inflammatory monocytes by promoting the secretion of TNF-α (Serbina et al., 2003a). Thus, it would be especially interesting to examine the role of TLR-2 during foodborne infection of mice given our findings that the majority of the bacterial burden is extracellular and the few cell-associated *L. monocytogenes* are found with Ly6C^{hi} monocytes that are bactericidal.

Multiple virulence genes originally identified for their role during the intracellular life cycle of *L. monocytogenes* moonlight as extracellular effectors. The secretion of extracellular LLO has been shown to induce apoptosis of lymphocytes (Carrero et al., 2004) as well as dendritic cells (Guzman et al., 1996), thereby inducing the death of cells without actively infecting them. Interestingly, it was shown that the C-terminal region of ActA, which is not involved in actin polymerization in the cytosol, promoted the aggregation of *L. monocytogenes* in the gut lumen and significantly enhanced the luminal persistence of *L. monocytogenes* (Travier et al., 2013). Overall, it obvious that *L. monocytogenes* have the capacity to persist *in vivo* extracellularly, and thus, this proportion of *L. monocytogenes* should not be discounted in either studies of pathogenesis or innate immunity. Likewise, it is not unreasonable to suggest that extracellular *L. monocytogenes*, which comprised the majority of the bacterial burden in the gut after foodborne infection, promote a unique innate immune response in the intestinal mucosa contrary to what occurs during systemic infection.

II. *L. monocytogenes* is found preferentially adhered to inflammatory cells, and not growing inside tissue-resident phagocytes in the MLN

The majority of cell-associated *L. monocytogenes* in the MLN were found with cells that were not permissive for *L. monocytogenes* growth including neutrophils and inflammatory monocytes. Thus, *L. monocytogenes* were not primarily found replicating in the cytosol of tissue-resident phagocytes, which is inconsistent with the prevailing notion of *L. monocytogenes* pathogenesis. This has implications for the overall immune response and the role of inflammatory cells during the gastrointestinal stage of infection. Our studies using CCR2-deficient mice indicated that the recruitment of Ly6C^{hi} monocytes to the intestine and MLN within 2 dpi had practically no effect on the overall bacterial burden. However, we would predict that the lack of CCR2^{+} inflammatory monocytes in the gut or MLN during infection would impede the clearance of *L. monocytogenes* over time, as evidenced in the spleen after i.v. infection due to the secretion of bactericidal effectors by these cells (Serbina et al., 2003b). Nevertheless, our data indicate that Ly6C^{hi} monocytes directly interact with *L. monocytogenes* soon after infection.

Ly6C^{hi} monocytes egress from the bone marrow and infiltrate inflamed tissues in a CCR2-dependent manner (Serbina and Pamer, 2006). Our data provide additional insight into the initial activation of Ly6C^{hi} monocytes in the bone marrow prior to recruitment to the MLN. Despite the role of CCR2 in egress from the bone marrow, the cellular source of CCR2 ligands (primarily being MCP-1 or CCL2) remains unclear. It has been proposed that cytosolic sensing of *L. monocytogenes* in an infected macrophage promotes MCP-1 secretion because MCP-1 was not detected in the spleen after infection with Δ*hly L. monocytogenes* (Serbina et al., 2003a). However, there is still no a priori reason to assume that a tissue-resident phagocyte must be heavily infected with *L. monocytogenes* in the intestine or MLN to recruit inflammatory monocytes. In fact, it is possible that intestinal epithelial cells promote the recruitment of inflammatory monocytes to the gut, as these cells can also secrete MCP-1 after *L. monocytogenes* infection *in vitro* (Jung et al., 1995). Lastly, it is possible that extracellular *L. monocytogenes,* which comprise the majority of the bacterial burden in the gut and MLN, directly induce monocytosis due to the expression of a monocytosis producing activity (Shum and Galsworthy, 1979).

Our Δ*lplA1* data suggest that intracellular growth of *L. monocytogenes* in an as yet unidentified cell type was not important for persistence in the intestine until 3 dpi. We know that only a minor proportion of *L. monocytogenes*-associated cells in the intestinal LP express a phenotype consistent with tissue-resident macrophages and DC, and we now have evidence that DC found *in vivo* do not support *L. monocytogenes* growth. Taken together with our findings using bulk myeloid cells isolated from the intestinal LP and MLN, we hypothesize that a relatively rare subset of mononuclear phagocytes with macrophage-like characteristics serve as the vital intracellular niche. Using a ligated ileal loop infection in rats, Pron *et al.* observed *L. monocytogenes* mainly inside mononuclear cells located in the follicular dome of Peyer's patches, and these cells were associated with foci of infection (Pron et al., 1998). It is noteworthy to mention that this finding was observed in the ileum of the small intestine, in which the cells described by Pron *et al.* would not be in the pool of myeloid cells we recovered from the large intestine, which lacks Peyer' patches. We typically focus on the large intestine due to the relatively higher bacterial burdens after foodborne infection compared to the small intestine. However, it may be worth our effort to determine the identify of phagocytes in Peyer's patches that support *L. monocytogenes* growth, as we actually observed a much greater defect for Δ*lpla1 L. monocytogenes* in the ileum compared to the colon, suggesting that indeed a host cell found in the ileum may serve an intracellular growth niche for *L. monocytogenes.*

III. Dissemination of *L. monocytogenes* to the MLN occurs by multiple mechanisms

The dissemination of facultative intracellular bacterial pathogens including *Salmonella enterica* Typhimurium, *Yersinia pseudotuberculosis*, and *Yersinia pestis* involve some degree of extracellular trafficking (Barnes et al., 2006; Gonzalez et al., 2015; Voedisch et al., 2009). It is now clear that *L. monocytogenes* can migrate freely in lymphatic vessels from the gut to the MLN. However, we need to reconcile our findings with what was described by Pron *et al.* previously (Pron et al., 2001). In that study, confocal microscopy was used to visualize *L. monocytogenes* in Peyer's patches and the MLN after a one hour ligated loop infection with wild type *L. monocytogenes*. The authors noted that OX-62^{+} cells (DC) were the primary cell type associated with *L. monocytogenes* in both the Peyer's patches and MLN, whereas, at later time points, *L. monocytogenes* could be found replicating in OX-62^{-} cells (Pron et al., 2001). However,

two main differences set this study apart from ours. First, a wild type strain of *L. monocytogenes* (EGD) was used, which does not interact with rat E-cadherin. A high affinity InlA interaction was required for *L. monocytogenes* to be transcytosed across the intestinal epithelium, in which *L. monocytogenes* was found extracellular in the intestinal LP within 45 minutes, which did not occur with *L. monocytogenes* Δ*inlA* (Nikitas et al., 2011). Therefore, *L. monocytogenes* EGD used by Pron *et al.* would be unable to invade the intestinal villi using this pathway, thereby forcing *L. monocytogenes* to be taken up primarily by M cells residing above Peyer's patches. This would result in subsequent preferential infection of OX-62$^+$ cells in Peyer's patch, which may have been able to migrate to the MLN in that model. In contrast, we used mouse-adapted *L. monocytogenes*, which would be expected to transcytose across the intestinal barrier using InlA and then reside extracellularly in the intestinal LP. The second major difference is that we directly visualized *L. monocytogenes* migrating inside lymphatic vessels in between the intestine and the MLN. Whereas, identification of *L. monocytogenes*-infected cells in the gut and the MLN is unable to definitively prove that cellular migration occurred.

Although we found that *L. monocytogenes* can traffic freely to the MLN, we have yet to investigate the relative contribution of other pathways such as the migration of monocytes or DC that may occur less frequently. Thus, we have yet to rule out the transport of *L. monocytogenes* by monocytes or DC, but we propose that extracellular trafficking of *L. monocytogenes* primarily occurs given the ratio of extracellular and intracellular *L. monocytogenes* in the MLN. Collectively, our data is consistent with a model in which extracellular *L. monocytogenes* disseminate to the MLN, in which subsequent intracellular replication in a rare myeloid cell type is important for colonization. Overall, our data implies that extracellular *L. monocytogenes* may drive early innate immune responses in the gut, which also promote systemic dissemination following foodborne infection of mice.

IV. Proposed events early after foodborne *L. monocytogenes* infection

At the onset of these studies, we hypothesized that a high affinity InlA-interaction enhanced the ability of *L. monocytogenes* to invade and replicate inside E-cadherin-expressing DC that also promoted migration to the MLN. However, throughout the completion of these studies, it became apparent that the events that actually occur during the gastrointestinal stage of infection are much too complicated to be mediated by a single cell type. In fact, DC sorted *ex vivo* did not support *L. monocytogenes* growth. Our data is now more consistent with a model in which extracellular *L. monocytogenes* comprise the majority of the bacterial burden in the MLN. Intracellular growth of *L. monocytogenes* is vital in some fashion, but is limited to a rare subset of myeloid cells, presumably macrophage-like, that we propose are important for increasing the pool of extracellular *L. monocytogenes* in the gut. Free *L. monocytogenes* efficiently migrate to the MLN and are mainly associated with inflammatory monocytes upon entering the MLN, which exhibit bactericidal activity. Lastly, dissemination of *L. monocytogenes* from the MLN to the systemic circulation via efferent lymphatic vessels remains to be investigated, but may also be mediated by either extracellular, or cell-associated *L. monocytogenes.* Figure 7.1 depicts these proposed events during the gastrointestinal stage of *L. monocytogenes* infection.

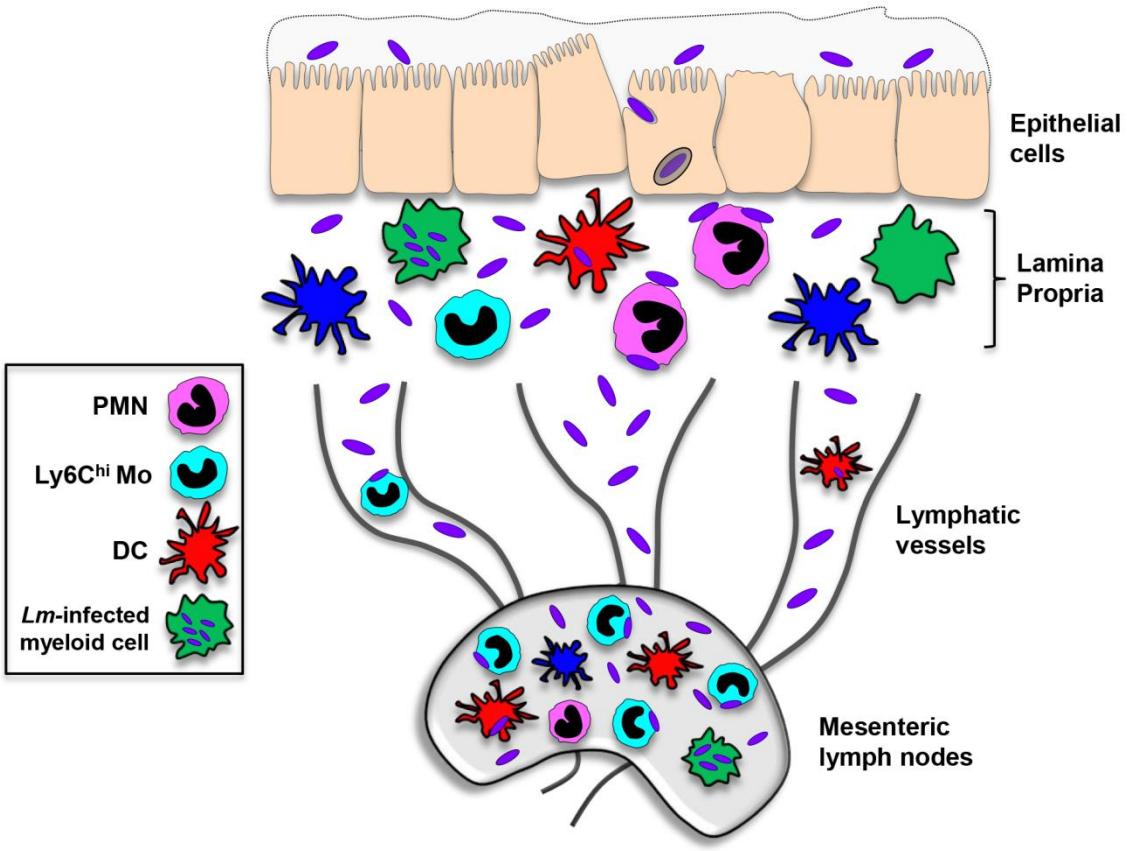

Figure 7.1: Overall proposed model of events that occur during foodborne *L. monocytogenes* infection

Cartoon depicting that extracellular *Lm* comprise the majority of the bacterial burden in the MLN 2-3 days after infection. Intracellular growth of *Lm* does occur, but is limited to a rare subset of myeloid cells (green cell), presumably macrophage-like, that are important for increasing the pool of extracellular *Lm* in the intestinal LP and the MLN. This extracellular pool of *Lm* in the gut can migrate freely to the MLN and is thought to be the primary route of spread. Two other potential routes to the MLN may occur including trafficking adhered to monocytes, or inside DC. Lastly, early after spread to the MLN, inflammatory monocytes closely associate with extracellular *Lm.*

APPENDIX I: List of Abbreviations

σ^B: sigma B

APC: allophycocyanin

B6: C57BL/6J

BALB: BALB/cBy/J

BHI: brain heart infusion

BM: bone marrow

BMMO: bone marrow-derived monocytes

BSA: bovine serum albumin

Cb: carbenicillin

CCL: C-C motif chemokine ligand

CCR: C-C motif chemokine receptor

cDC: conventional DC

CFU: colony-forming units

CHO: Chinese hamster ovary

Cm: chloramphenicol

cMoP: common monocyte progenitor

CNS: central nervous system

DC: dendritic cell

DMEM: Dulbecco's modified eagle medium

DNA: deoxyribonucleic acid

dpi: days post-infection

FSC: forward-scattered light in FACS

EDTA: ethylenediaminetetraacetic acid

ELISA: enzyme-linked immunosorbent assay

Ery: erythromycin

FACS: fluorescence-activated cell sorting

FBS: fetal bovine serum

Fc: fragment crystallizable region of immunoglobulin

FLT3-L: FMS-like tyrosine kinase 3 ligand

FMO: fluorescent minus one negative gating control

GFP: green fluorescent protein

GM-CSF: granulocyte-macrophage colony-stimulating factor

HBSS: Hanks' balanced salt solution

HEPES: 4-(2-Hydroxyethyl)-1-piperazineethanesulfonic acid

hpi: hours post-infection

IFN-γ: interferon gamma

IgG: immunoglobulin G

IMM: improved minimal medium

$InlA^m$: mouse-adapted InlA

iNOS: inducible nitric oxide synthase

i.v.: intravenous

Kan: kanamycin

L+G: LiCl and glycine

LiCl: lithium chloride

LIP-1: *Listeria* pathogenicity island 1

LLO: Listeriolysin O

LP: lamina propria

LPS: lipopolysaccharide

LPTXG: Amino acid motif, Leu-Pro-any-Thr-Gly

M cell: microfold cell

MCP-1: monocyte chemoattractant protein-1 (CCL2)

M-CSF: macrophage colony-stimulating factor

MFI: mean fluorescence intensity

MHC: Major histocompatibility complex

MLN: mesenteric lymph nodes

Mo: Monocyte

MOI: multiplicity of infection

NK: natural killer

NOD: nucleotide-binding oligomerization domain-like receptors

PBS: phosphate-buffered saline

pDC: plasmacytoid DC

PE: phycoerythrin

PMN: polymorphonuclear leukocyte

RNA: ribonucleic acid

RP-10: complete RPMI-based media with 10% FBS

SD: standard deviation

SSC: side-scattered light in FACS

TC: tissue culture

Tet: tetracycline

TipDC: TNF-α/iNOS-producing dendritic cells

TLR: toll-like receptor

TNF-α: tumor necrosis factor alpha

VGP: vegetable peptone broth

REFERENCES

Abdullah, Z., M. Schlee, S. Roth, M.A. Mraheil, W. Barchet, J. Bottcher, T. Hain, S. Geiger, Y. Hayakawa, J.H. Fritz, F. Civril, K.P. Hopfner, C. Kurts, J. Ruland, G. Hartmann, T. Chakraborty, and P.A. Knolle. 2012. RIG-I detects infection with live *Listeria* by sensing secreted bacterial nucleic acids. *The EMBO Journal* 31:4153-4164.

Alberti-Segui, C., K.R. Goeden, and D.E. Higgins. 2007. Differential function of *Listeria monocytogene*s listeriolysin O and phospholipases C in vacuolar dissolution following cell-to-cell spread. *Cellular Microbiology* 9:179-195.

Allerberger, F., and M. Wagner. 2010. Listeriosis: a resurgent foodborne infection. *Clin Microbiol Infect* 16:16-23.

Alonzo, F., 3rd, L.D. Bobo, D.J. Skiest, and N.E. Freitag. 2011. Evidence for subpopulations of *Listeria monocytogenes* with enhanced invasion of cardiac cells. *J Med Microbiol* 60:423-434.

Alvarez-Dominguez, C., E. Carrasco-Marin, and F. Leyva-Cobian. 1993. Role of complement component C1q in phagocytosis of *Listeria monocytogenes* by murine macrophage-like cell lines. *Infection and Immunity* 61:3664-3672.

Aoshi, T., J.A. Carrero, V. Konjufca, Y. Koide, E.R. Unanue, and M.J. Miller. 2009. The cellular niche of *Listeria monocytogenes* infection changes rapidly in the spleen. *European Journal of Immunology* 39:417-425.

Archer, K.A., J. Durack, and D.A. Portnoy. 2014. STING-dependent type I IFN production inhibits cell-mediated immunity to *Listeria monocytogenes*. *PLoS Pathogens* 10:e1003861.

Armstrong, R.W., and P.C. Fung. 1993. Brainstem encephalitis (rhombencephalitis) due to *Listeria monocytogenes*: case report and review. *Clinical infectious diseases : an official publication of the Infectious Diseases Society of America* 16:689-702.

Arnett, E., S. Vadia, C.C. Nackerman, S. Oghumu, A.R. Satoskar, K.R. McLeish, S.M. Uriarte, and S. Seveau. 2014. The pore-forming toxin listeriolysin O is degraded by neutrophil metalloproteinase-8 and fails to mediate *Listeria monocytogenes* intracellular survival in neutrophils. *Journal of Immunology* 192:234-244.

Asano, K., N. Takahashi, M. Ushiki, M. Monya, F. Aihara, E. Kuboki, S. Moriyama, M. Iida, H. Kitamura, C.H. Qiu, T. Watanabe, and M. Tanaka. 2015. Intestinal CD169(+) macrophages initiate mucosal inflammation by secreting CCL8 that recruits inflammatory monocytes. *Nature Communications* 6:7802.

Askenase, M.H., S.J. Han, A.L. Byrd, D. Morais da Fonseca, N. Bouladoux, C. Wilhelm, J.E. Konkel, T.W. Hand, N. Lacerda-Queiroz, X.Z. Su, G. Trinchieri, J.R. Grainger, and Y. Belkaid. 2015. Bone-marrow-resident NK cells prime monocytes for regulatory function during infection. *Immunity* 42:1130-1142.

Aureli, P., G.C. Fiorucci, D. Caroli, G. Marchiaro, O. Novara, L. Leone, and S. Salmaso. 2000. An outbreak of febrile gastroenteritis associated with corn contaminated by *Listeria monocytogenes*. *The New England Journal of Medicine* 342:1236-1241.

Bain, C.C., C.L. Scott, H. Uronen-Hansson, S. Gudjonsson, O. Jansson, O. Grip, M. Guilliams, B. Malissen, W.W. Agace, and A.M. Mowat. 2013. Resident and pro-inflammatory macrophages in the colon represent alternative context-dependent fates of the same Ly6Chi monocyte precursors. *Mucosal Immunology* 6:498-510.

Bakardjiev, A.I., J.A. Theriot, and D.A. Portnoy. 2006. *Listeria monocytogenes* traffics from maternal organs to the placenta and back. *PLoS Pathogens* 2:e66.

Baker, H., B. Deangelis, E.R. Baker, and S.H. Hutner. 1998. A practical assay of lipoate in biologic fluids and liver in health and disease. *Free Radic Biol Med* 25:473-479.

Balestrino, D., M.A. Hamon, L. Dortet, M.A. Nahori, J. Pizarro-Cerda, D. Alignani, O. Dussurget, P. Cossart, and A. Toledo-Arana. 2010. Single-cell techniques using chromosomally tagged fluorescent bacteria to study *Listeria monocytogenes* infection processes. *Applied and Environmental Microbiology* 76:3625-3636.

Barnes, P.D., M.A. Bergman, J. Mecsas, and R.R. Isberg. 2006. Yersinia pseudotuberculosis disseminates directly from a replicating bacterial pool in the intestine. *The Journal of Experimental Medicine* 203:1591-1601.

Becker, L.A., M.S. Cetin, R.W. Hutkins, and A.K. Benson. 1998. Identification of the gene encoding the alternative sigma factor sigmaB from *Listeria monocytogenes* and its role in osmotolerance. *Journal of Bacteriology* 180:4547-4554.

Becker, L.A., S.N. Evans, R.W. Hutkins, and A.K. Benson. 2000. Role of sigmaB in adaptation of *Listeria monocytogenes* to growth at low temperature. *Journal of Bacteriology* 182:7083-7087.

Begley, M., R.D. Sleator, C.G. Gahan, and C. Hill. 2005. Contribution of three bile-associated loci, bsh, pva, and btlB, to gastrointestinal persistence and bile tolerance of *Listeria monocytogenes*. *Infection and Immunity* 73:894-904.

Bergmann, S., P.M. Beard, B. Pasche, S. Lienenklaus, S. Weiss, C.G. Gahan, K. Schughart, and A. Lengeling. 2013. Influence of internalin A murinisation on host resistance to orally acquired listeriosis in mice. *BMC Microbiol* 13:90.

Bierne, H., and P. Cossart. 2002. InlB, a surface protein of *Listeria monocytogenes* that behaves as an invasin and a growth factor. *Journal of Cell Science* 115:3357-3367.

Biroum, N. 1977. Listericidal activity of non-stimulated and stimulated human macrophages in vitro. *Clinical and experimental immunology* 28:138-145.

Bogunovic, M., F. Ginhoux, J. Helft, L. Shang, D. Hashimoto, M. Greter, K. Liu, C. Jakubzick, M.A. Ingersoll, M. Leboeuf, E.R. Stanley, M. Nussenzweig, S.A. Lira, G.J. Randolph, and M. Merad. 2009. Origin of the lamina propria dendritic cell network. *Immunity* 31:513-525.

Bonneau, M., M. Epardaud, F. Payot, V. Niborski, M.I. Thoulouze, F. Bernex, B. Charley, S. Riffault, L.A. Guilloteau, and I. Schwartz-Cornil. 2006. Migratory monocytes and granulocytes are major lymphatic carriers of Salmonella from tissue to draining lymph node. *Journal of Leukocyte Biology* 79:268-276.

Bou Ghanem, E.N., G.S. Jones, T. Myers-Morlaes, P.N. Patil, A.N. Hidayatullah, and S.E.F. D'Orazio. 2012. InlA promotes dissemination of *Listeria monocytogenes* to the mesenteric lymph nodes during food borne infection of mice. *PLoS Pathogens* 8:e1003015.

Bou Ghanem, E.N., T. Myers-Morales, and S.E. D'Orazio. 2013a. A mouse model of foodborne *Listeria monocytogenes* infection. *Current Protocols in Microbiology* 31:9B 3 1-9B 3 16.

Bou Ghanem, E.N., T. Myers-Morales, G.S. Jones, and S.E.F. D'Orazio. 2013b. Oral transmission of *Listeria monocytogenes* in mice via ingestion of contaminated food. *J Vis Exp* 75:doi:3791/50381.

Brasel, K., T. De Smedt, J.L. Smith, and C.R. Maliszewski. 2000. Generation of murine dendritic cells from flt3-ligand-supplemented bone marrow cultures. *Blood* 96:3029-3039.

Braun, L., B. Ghebrehiwet, and P. Cossart. 2000. gC1q-R/p32, a C1q-binding protein, is a receptor for the InlB invasion protein of *Listeria monocytogenes*. *The EMBO Journal* 19:1458-1466.

Braun, L., H. Ohayon, and P. Cossart. 1998. The InIB protein of *Listeria monocytogenes* is sufficient to promote entry into mammalian cells. *Molecular Microbiology* 27:1077-1087.

Burkholder, K.M., and A.K. Bhunia. 2010. *Listeria monocytogenes* uses Listeria adhesion protein (LAP) to promote bacterial transepithelial translocation and induces expression of LAP receptor Hsp60. *Infection and Immunity* 78:5062-5073.

Burkholder, K.M., K.P. Kim, K.K. Mishra, S. Medina, B.K. Hahm, H. Kim, and A.K. Bhunia. 2009. Expression of LAP, a SecA2-dependent secretory protein, is induced under anaerobic environment. *Microbes Infect* 11:859-867.

Cabanes, D., P. Dehoux, O. Dussurget, L. Frangeul, and P. Cossart. 2002. Surface proteins and the pathogenic potential of *Listeria monocytogenes*. *Trends in Microbiology* 10:238-245.

Cabanes, D., S. Sousa, A. Cebria, M. Lecuit, F. Garcia-del Portillo, and P. Cossart. 2005. Gp96 is a receptor for a novel *Listeria monocytogenes* virulence factor, Vip, a surface protein. *The EMBO Journal* 24:2827-2838.

Campisi, L., S.M. Soudja, J. Cazareth, D. Bassand, A. Lazzari, F. Brau, E. Narni-Mancinelli, N. Glaichenhaus, F. Geissmann, and G. Lauvau. 2011. Splenic CD8alpha(+) dendritic cells undergo rapid programming by cytosolic bacteria and inflammation to induce protective CD8(+) T-cell memory. *European Journal of Immunology* 41:1594-1605.

Carlson, D.A., Young, K.L., Fischer, S.J., Ulrich, H. 2008. An Evaluation of the Stability and Plasma Pharmacokinetics of R-lipoic acid (RLA) and R-Dihydrolipoic acid (R-DHLA) Dosage Forms in Human Plasma from Healthy Volunteers. In Lipoic Acid: Energy Production, Antioxidant Activity & Health Effects. M.S. Patel, editor Taylor and Francis Publishers, London. 235-270.

Carr, K.D., A.N. Sieve, M. Indramohan, T.J. Break, S. Lee, and R.E. Berg. 2011. Specific depletion reveals a novel role for neutrophil-mediated protection in the liver during *Listeria monocytogenes* infection. *European Journal of Immunology* 41:2666-2676.

Carrero, J.A., B. Calderon, and E.R. Unanue. 2004. Listeriolysin O from *Listeria monocytogenes* is a lymphocyte apoptogenic molecule. *The Journal of Immunology* 172:4866-4874.

Cartwright, E.J., K.A. Jackson, S.D. Johnson, L.M. Graves, B.J. Silk, and B.E. Mahon. 2013. Listeriosis outbreaks and associated food vehicles, United States, 1998-2008. *Emerg Infect Dis* 19:1-9; quiz 184.

CDC. 2012. Multi-state outbreak of listeriosis linked to whole cantaloupe in Jenson Farms, Colorado. In: *http://www.cdc.gov/listeria/outbreaks/cantaloupes-jensen-farms/082712/index.html*

CDC. 2013. Vital signs: *Listeria* illnesses, deaths, and outbreaks--United States, 2009-2011. *MMWR Morb Mortal Wkly Rep* 62:448-452.

Cecchini, M.G., M.G. Dominguez, S. Mocci, A. Wetterwald, R. Felix, H. Fleisch, O. Chisholm, W. Hofstetter, J.W. Pollard, and E.R. Stanley. 1994. Role of colony stimulating factor-1 in the establishment and regulation of tissue macrophages during postnatal development of the mouse. *Development* 120:1357-1372.

Cepek, K.L., S.K. Shaw, C.M. Parker, G.J. Russell, J.S. Morrow, D.L. Rimm, and M.B. Brenner. 1994. Adhesion between epithelial cells and T lymphocytes mediated by E-cadherin and the alpha E beta 7 integrin. *Nature* 372:190-193.

Cerovic, V., C.C. Bain, A.M. Mowat, and S.W. Milling. 2014. Intestinal macrophages and dendritic cells: what's the difference? *Trends Immunol* 35:270-277.

Cerovic, V., S.A. Houston, C.L. Scott, A. Aumeunier, U. Yrlid, A.M. Mowat, and S.W. Milling. 2013. Intestinal CD103(-) dendritic cells migrate in lymph and prime effector T cells. *Mucosal Immunology* 6:104-113.

Chakraborty, T., M. Leimeister-Wachter, E. Domann, M. Hartl, W. Goebel, T. Nichterlein, and S. Notermans. 1992. Coordinate regulation of virulence genes in *Listeria monocytogenes* requires the product of the prfA gene. *Journal of Bacteriology* 174:568-574.

Chapuis, F., M. Rosenzwajg, M. Yagello, M. Ekman, P. Biberfeld, and J.C. Gluckman. 1997. Differentiation of human dendritic cells from monocytes in vitro. *European Journal of Immunology* 27:431-441.

Chaturongakul, S., S. Raengpradub, M. Wiedmann, and K.J. Boor. 2008. Modulation of stress and virulence in *Listeria monocytogenes*. *Trends in Microbiology* 16:388-396.

Chico-Calero, I., M. Suarez, B. Gonzalez-Zorn, M. Scortti, J. Slaghuis, W. Goebel, J.A. Vazquez-Boland, and C. European Listeria Genome. 2002. Hpt, a bacterial homolog of the microsomal glucose- 6-phosphate translocase, mediates rapid intracellular proliferation in Listeria. *Proceedings of the National Academy of Sciences of the United States of America* 99:431-436.

Chong, R., R. Swiss, G. Briones, K.L. Stone, E.E. Gulcicek, and H. Agaisse. 2009. Regulatory mimicry in *Listeria monocytogenes* actin-based motility. *Cell Host & Microbe* 6:268-278.

Coffey, J.C., and D.P. O'Leary. 2016. The mesentery: structure, function, and role in disease. *The Lancet. Gastroenterology & Hepatology* 1:238-247.

Conlan, J.W., and R.J. North. 1991. Neutrophil-mediated dissolution of infected host cells as a defense strategy against a facultative intracellular bacterium. *Journal of Experimental Medicine* 174:741-744.

Conlan, J.W., and R.J. North. 1994. Neutrophils are essential for early anti-*Listeria* defense in the liver, but not in the spleen or peritoneal cavity, as revealed by a granulocyte-depleting monoclonal antibody. *The Journal of Experimental Medicine* 179:259-268.

Cortez-Retamozo, V., M. Etzrodt, and M.J. Pittet. 2012. Regulation of macrophage and dendritic cell responses by their lineage precursors. *Journal of Innate Immunity* 4:411-423.

Cossart, P., J. Pizarro-Cerda, and M. Lecuit. 2003. Invasion of mammalian cells by *Listeria monocytogenes*: functional mimicry to subvert cellular functions. *Trends in Cell Biology* 13:23-31.

Cossart, P., M.F. Vicente, J. Mengaud, F. Baquero, J.C. Perez-Diaz, and P. Berche. 1989. Listeriolysin O is essential for virulence of *Listeria monocytogenes*: direct evidence obtained by gene complementation. *Infection and Immunity* 57:3629-3636.

Crispe, I.N. 2011. Liver antigen-presenting cells. *Journal of hepatology* 54:357-365.

D'Orazio, S.E. 2014. Animal models for oral transmission of *Listeria monocytogenes. Frontiers in Cellular and Infection Microbiology* 4:15.

Dalton, C.B., C.C. Austin, J. Sobel, P.S. Hayes, W.F. Bibb, L.M. Graves, B. Swaminathan, M.E. Proctor, and P.M. Griffin. 1997. An outbreak of gastroenteritis and fever due to *Listeria monocytogenes* in milk. *The New England Journal of Medicine* 336:100-105.

Davis, M.J., B. Gregorka, J.E. Gestwicki, and J.A. Swanson. 2012. Inducible renitence limits *Listeria monocytogenes* escape from vacuoles in macrophages. *Journal of Immunology* 189:4488-4495.

de Bruijn, M.F., W. van Vianen, R.E. Ploemacher, I.A. Bakker-Woudenberg, P.A. Campbell, W. van Ewijk, and P.J. Leenen. 1998. Bone marrow cellular composition in *Listeria monocytogenes* infected mice detected using ER-MP12 and ER-MP20 antibodies: a flow cytometric alternative to differential counting. *Journal of Immunological Methods* 217:27-39.

de las Heras, A., R.J. Cain, M.K. Bielecka, and J.A. Vazquez-Boland. 2011. Regulation of *Listeria* virulence: PrfA master and commander. *Current Opinion in Microbiology* 14:118-127.

del Rio, M.L., G. Bernhardt, J.I. Rodriguez-Barbosa, and R. Forster. 2010. Development and functional specialization of CD103+ dendritic cells. *Immunological Reviews* 234:268-281.

Disson, O., S. Grayo, E. Huillet, G. Nikitas, F. Langa-Vives, O. Dussurget, M. Ragon, A. Le Monnier, C. Babinet, P. Cossart, and M. Lecuit. 2008. Conjugated action of two species-specific invasion proteins for fetoplacental listeriosis. *Nature* 455:1114-1118.

Domann, E., J. Wehland, M. Rohde, S. Pistor, M. Hartl, W. Goebel, M. Leimeister-Wachter, M. Wuenscher, and T. Chakraborty. 1992. A novel bacterial virulence gene in *Listeria monocytogenes* required for host cell microfilament interaction with homology to the proline-rich region of vinculin. *The EMBO Journal* 11:1981-1990.

Dramsi, S., I. Biswas, E. Maguin, L. Braun, P. Mastroeni, and P. Cossart. 1995. Entry of *Listeria monocytogenes* into hepatocytes requires expression of inIB, a surface protein of the internalin multigene family. *Molecular Microbiology* 16:251-261.

Dramsi, S., F. Bourdichon, D. Cabanes, M. Lecuit, H. Fsihi, and P. Cossart. 2004. FbpA, a novel multifunctional Listeria monocytogenes virulence factor. *Molecular Microbiology* 53:639-649.

Dramsi, S., S. Levi, A. Triller, and P. Cossart. 1998. Entry of *Listeria monocytogenes* into neurons occurs by cell-to-cell spread: an in vitro study. *Infection and Immunity* 66:4461-4468.

Drevets, D.A., and P.A. Campbell. 1991. Roles of complement and complement receptor type 3 in phagocytosis of *Listeria monocytogenes* by inflammatory mouse peritoneal macrophages. *Infection and Immunity* 59:2645-2652.

Drevets, D.A., B.P. Canono, P.J. Leenen, and P.A. Campbell. 1994. Gentamicin kills intracellular *Listeria monocytogenes*. *Infection and Immunity* 62:2222-2228.

Drevets, D.A., M.J. Dillon, J.S. Schawang, N. Van Rooijen, J. Ehrchen, C. Sunderkotter, and P.J. Leenen. 2004. The Ly-6Chigh monocyte subpopulation transports *Listeria monocytogenes* into the brain during systemic infection of mice. *Journal of Immunology* 172:4418-4424.

Drevets, D.A., T.A. Jelinek, and N.E. Freitag. 2001. *Listeria monocytogenes*-infected phagocytes can initiate central nervous system infection in mice. *Infection and Immunity* 69:1344-1350.

Drevets, D.A., P.J. Leenen, and P.A. Campbell. 1993. Complement receptor type 3 (CD11b/CD18) involvement is essential for killing of *Listeria monocytogenes* by mouse macrophages. *Journal of Immunology* 151:5431-5439.

Drevets, D.A., R.T. Sawyer, T.A. Potter, and P.A. Campbell. 1995. *Listeria monocytogenes* infects human endothelial cells by two distinct mechanisms. *Infection and Immunity* 63:4268-4276.

Drevets, D.A., J.E. Schawang, V.K. Mandava, M.J. Dillon, and P.J. Leenen. 2010. Severe *Listeria monocytogenes* infection induces development of monocytes with distinct phenotypic and functional features. *Journal of Immunology* 185:2432-2441.

Dussurget, O., D. Cabanes, P. Dehoux, M. Lecuit, C. Buchrieser, P. Glaser, and P. Cossart. 2002. *Listeria monocytogenes* bile salt hydrolase is a PrfA-regulated virulence factor involved in the intestinal and hepatic phases of listeriosis. *Molecular Microbiology* 45:1095-1106.

Dykes, G.A., and K.M. Withers. 1999. Sub-lethal damage of *Listeria monocytogenes* after long-term chilled storage at 4 degrees C. *Lett Appl Microbiol* 28:45-48.

Edelson, B.T., T.R. Bradstreet, K. Hildner, J.A. Carrero, K.E. Frederick, W. Kc, R. Belizaire, T. Aoshi, R.D. Schreiber, M.J. Miller, T.L. Murphy, E.R. Unanue, and K.M. Murphy. 2011. CD8alpha(+) dendritic cells are an obligate cellular entry point for productive infection by *Listeria monocytogenes*. *Immunity* 35:236-248.

Edelson, B.T., and E.R. Unanue. 2002. MyD88-dependent but Toll-like receptor 2-independent innate immunity to *Listeria*: no role for either in macrophage listericidal activity. *Journal of Immunology* 169:3869-3875.

FAO/WHO. 2004. Risk assessment of *Listeria monocytogenes* in ready-to-eat foods. In Microbiological Risk Assessment Series No. 5.

Farber, J.M., and P.I. Peterkin. 1991. *Listeria monocytogenes*, a food-borne pathogen. *Microbiological Reviews* 55:476-511.

Farber, J.M., W.H. Ross, and J. Harwig. 1996. Health risk assessment of *Listeria monocytogenes* in Canada. *International Journal of Food Microbiology* 30:145-156.

Fogg, D.K., C. Sibon, C. Miled, S. Jung, P. Aucouturier, D.R. Littman, A. Cumano, and F. Geissmann. 2006. A clonogenic bone marrow progenitor specific for macrophages and dendritic cells. *Science* 311:83-87.

Fonseca, D.M., T.W. Hand, S.J. Han, M.Y. Gerner, A. Glatman Zaretsky, A.L. Byrd, O.J. Harrison, A.M. Ortiz, M. Quinones, G. Trinchieri, J.M. Brenchley, I.E. Brodsky, R.N. Germain, G.J. Randolph, and Y. Belkaid. 2015. Microbiota-Dependent Sequelae of Acute Infection Compromise Tissue-Specific Immunity. *Cell* 163:354-366.

Forster, R., A.C. Davalos-Misslitz, and A. Rot. 2008. CCR7 and its ligands: balancing immunity and tolerance. *Nature reviews. Immunology* 8:362-371.

Francke, A., J. Herold, S. Weinert, R.H. Strasser, and R.C. Braun-Dullaeus. 2011. Generation of mature murine monocytes from heterogeneous bone marrow and description of their properties. *The journal of histochemistry and cytochemistry : official journal of the Histochemistry Society* 59:813-825.

Freitag, N.E., G.C. Port, and M.D. Miner. 2009. *Listeria monocytogenes* - from saprophyte to intracellular pathogen. *Nat Rev Microbiol* 7:623-628.

Gaillard, J.L., P. Berche, C. Frehel, E. Gouin, and P. Cossart. 1991. Entry of *L. monocytogenes* into cells is mediated by internalin, a repeat protein reminiscent of surface antigens from gram-positive cocci. *Cell* 65:1127-1141.

Gaillard, J.L., P. Berche, J. Mounier, S. Richard, and P. Sansonetti. 1987. In vitro model of penetration and intracellular growth of *Listeria monocytogenes* in the human enterocyte-like cell line Caco-2. *Infection and Immunity* 55:2822-2829.

Gaillard, J.L., P. Berche, and P. Sansonetti. 1986. Transposon mutagenesis as a tool to study the role of hemolysin in the virulence of *Listeria monocytogenes*. *Infection and Immunity* 52:50-55.

Galsworthy, S.B., and D. Fewster. 1988. Comparison of responsiveness to the monocytosis-producing activity of *Listeria monocytogenes* in mice genetically susceptible or resistant to listeriosis. *Infection* 16 Suppl 2:S118-122.

Gautier, E.L., T. Shay, J. Miller, M. Greter, C. Jakubzick, S. Ivanov, J. Helft, A. Chow, K.G. Elpek, S. Gordonov, A.R. Mazloom, A. Ma'ayan, W.J. Chua, T.H. Hansen, S.J. Turley, M. Merad, G.J. Randolph, and C. Immunological Genome. 2012.

Gene-expression profiles and transcriptional regulatory pathways that underlie the identity and diversity of mouse tissue macrophages. *Nature Immunology* 13:1118-1128.

Geissmann, F., S. Jung, and D.R. Littman. 2003. Blood monocytes consist of two principal subsets with distinct migratory properties. *Immunity* 19:71-82.

Geng, Y., T. Kodama, and G.K. Hansson. 1994. Differential expression of scavenger receptor isoforms during monocyte-macrophage differentiation and foam cell formation. *Arteriosclerosis and Thrombosis : a Journal of Vascular Biology / American Heart Association* 14:798-806.

Geoffroy, C., J.L. Gaillard, J.E. Alouf, and P. Berche. 1987. Purification, characterization, and toxicity of the sulfhydryl-activated hemolysin listeriolysin O from *Listeria monocytogenes*. *Infection and Immunity* 55:1641-1646.

Glomski, I.J., A.L. Decatur, and D.A. Portnoy. 2003. *Listeria monocytogenes* mutants that fail to compartmentalize listerolysin O activity are cytotoxic, avirulent, and unable to evade host extracellular defenses. *Infection and Immunity* 71:6754-6765.

Glomski, I.J., M.M. Gedde, A.W. Tsang, J.A. Swanson, and D.A. Portnoy. 2002. The *Listeria monocytogenes* hemolysin has an acidic pH optimum to compartmentalize activity and prevent damage to infected host cells. *The Journal of Cell Biology* 156:1029-1038.

Gonzalez, R.J., M.C. Lane, N.J. Wagner, E.H. Weening, and V.L. Miller. 2015. Dissemination of a highly virulent pathogen: tracking the early events that define infection. *PLoS Pathogens* 11:e1004587.

Gouin, E., M.D. Welch, and P. Cossart. 2005. Actin-based motility of intracellular pathogens. *Current Opinion in Microbiology* 8:35-45.

Goulet, V., L.A. King, V. Vaillant, and H. de Valk. 2013. What is the incubation period for listeriosis? *BMC Infect Dis* 13:11.

Grainger, J.R., E.A. Wohlfert, I.J. Fuss, N. Bouladoux, M.H. Askenase, F. Legrand, L.Y. Koo, J.M. Brenchley, I.D. Fraser, and Y. Belkaid. 2013. Inflammatory monocytes regulate pathologic responses to commensals during acute gastrointestinal infection. *Nature Medicine* 19:713-721.

Grif, K., G. Patscheider, M.P. Dierich, and F. Allerberger. 2003. Incidence of fecal carriage of *Listeria monocytogenes* in three healthy volunteers: a one-year prospective stool survey. *European journal of clinical microbiology & infectious diseases : official publication of the European Society of Clinical Microbiology* 22:16-20.

Griffin, A.J., L.X. Li, S. Voedisch, O. Pabst, and S.J. McSorley. 2011. Dissemination of persistent intestinal bacteria via the mesenteric lymph nodes causes typhoid relapse. *Infection and Immunity* 79:1479-1488.

Guilliams, M., F. Ginhoux, C. Jakubzick, S.H. Naik, N. Onai, B.U. Schraml, E. Segura, R. Tussiwand, and S. Yona. 2014. Dendritic cells, monocytes and macrophages: a unified nomenclature based on ontogeny. *Nature reviews. Immunology* 14:571-578.

Guzman, C.A., E. Domann, M. Rohde, D. Bruder, A. Darji, S. Weiss, J. Wehland, T. Chakraborty, and K.N. Timmis. 1996. Apoptosis of mouse dendritic cells is triggered by listeriolysin, the major virulence determinant of *Listeria monocytogenes*. *Molecular Microbiology* 20:119-126.

Guzman, C.A., M. Rohde, T. Chakraborty, E. Domann, M. Hudel, J. Wehland, and K.N. Timmis. 1995. Interaction of *Listeria monocytogenes* with mouse dendritic cells. *Infection and Immunity* 63:3665-3673.

Hamon, M., H. Bierne, and P. Cossart. 2006. *Listeria monocytogenes*: a multifaceted model. *Nat Rev Microbiol* 4:423-434.
Hardy, J., K.P. Francis, M. DeBoer, P. Chu, K. Gibbs, and C.H. Contag. 2004. Extracellular replication of *Listeria monocytogenes* in the murine gall bladder. *Science* 303:851-853.
Helft, J., J. Bottcher, P. Chakravarty, S. Zelenay, J. Huotari, B.U. Schraml, D. Goubau, and C. Reis e Sousa. 2015. GM-CSF Mouse Bone Marrow Cultures Comprise a Heterogeneous Population of CD11c(+)MHCII(+) Macrophages and Dendritic Cells. *Immunity* 42:1197-1211.
Hettinger, J., D.M. Richards, J. Hansson, M.M. Barra, A.C. Joschko, J. Krijgsveld, and M. Feuerer. 2013. Origin of monocytes and macrophages in a committed progenitor. *Nature Immunology* 14:821-830.
Ho, J.L., K.N. Shands, G. Friedland, P. Eckind, and D.W. Fraser. 1986. An outbreak of type 4b *Listeria monocytogenes* infection involving patients from eight Boston hospitals. *Arch Intern Med* 146:520-524.
Horwitz, M.A., and F.R. Maxfield. 1984. Legionella pneumophila inhibits acidification of its phagosome in human monocytes. *The Journal of Cell Biology* 99:1936-1943.
Hume, D.A., K.M. Summers, and M. Rehli. 2016. Transcriptional Regulation and Macrophage Differentiation. *Microbiology Spectrum* 4:3
Inaba, K., M. Inaba, N. Romani, H. Aya, M. Deguchi, S. Ikehara, S. Muramatsu, and R.M. Steinman. 1992. Generation of large numbers of dendritic cells from mouse bone marrow cultures supplemented with granulocyte/macrophage colony-stimulating factor. *The Journal of Experimental Medicine* 176:1693-1702.
Ishiguro, T., M. Naito, T. Yamamoto, G. Hasegawa, F. Gejyo, M. Mitsuyama, H. Suzuki, and T. Kodama. 2001. Role of macrophage scavenger receptors in response to *Listeria monocytogenes* infection in mice. *The American Journal of Pathology* 158:179-188.
Jaensson, E., H. Uronen-Hansson, O. Pabst, B. Eksteen, J. Tian, J.L. Coombes, P.L. Berg, T. Davidsson, F. Powrie, B. Johansson-Lindbom, and W.W. Agace. 2008. Small intestinal CD103+ dendritic cells display unique functional properties that are conserved between mice and humans. *The Journal of Experimental Medicine* 205:2139-2149.
Jakubzick, C., E.L. Gautier, S.L. Gibbings, D.K. Sojka, A. Schlitzer, T.E. Johnson, S. Ivanov, Q. Duan, S. Bala, T. Condon, N. van Rooijen, J.R. Grainger, Y. Belkaid, A. Ma'ayan, D.W. Riches, W.M. Yokoyama, F. Ginhoux, P.M. Henson, and G.J. Randolph. 2013. Minimal differentiation of classical monocytes as they survey steady-state tissues and transport antigen to lymph nodes. *Immunity* 39:599-610.
Jang, M.H., M.N. Kweon, K. Iwatani, M. Yamamoto, K. Terahara, C. Sasakawa, T. Suzuki, T. Nochi, Y. Yokota, P.D. Rennert, T. Hiroi, H. Tamagawa, H. Iijima, J. Kunisawa, Y. Yuki, and H. Kiyono. 2004. Intestinal villous M cells: an antigen entry site in the mucosal epithelium. *Proceedings of the National Academy of Sciences of the United States of America* 101:6110-6115.
Jang, M.H., N. Sougawa, T. Tanaka, T. Hirata, T. Hiroi, K. Tohya, Z. Guo, E. Umemoto, Y. Ebisuno, B.G. Yang, J.Y. Seoh, M. Lipp, H. Kiyono, and M. Miyasaka. 2006. CCR7 is critically important for migration of dendritic cells in intestinal lamina propria to mesenteric lymph nodes. *Journal of Immunology* 176:803-810.
Jensen, V.B., J.T. Harty, and B.D. Jones. 1998. Interactions of the invasive pathogens *Salmonella typhimurium*, *Listeria monocytogenes*, and *Shigella flexneri* with M cells and murine Peyer's patches. *Infection and Immunity* 66:3758-3766.
Johansson-Lindbom, B., M. Svensson, O. Pabst, C. Palmqvist, G. Marquez, R. Forster, and W.W. Agace. 2005. Functional specialization of gut CD103+ dendritic cells in

the regulation of tissue-selective T cell homing. *The Journal of Experimental Medicine* 202:1063-1073.
Johansson, J., P. Mandin, A. Renzoni, C. Chiaruttini, M. Springer, and P. Cossart. 2002. An RNA thermosensor controls expression of virulence genes in *Listeria monocytogenes*. *Cell* 110:551-561.
Join-Lambert, O.F., S. Ezine, A. Le Monnier, F. Jaubert, M. Okabe, P. Berche, and S. Kayal. 2005. *Listeria monocytogenes*-infected bone marrow myeloid cells promote bacterial invasion of the central nervous system. *Cellular Microbiology* 7:167-180.
Jones, G.S., K.M. Bussell, T. Myers-Morales, A.M. Fieldhouse, E.N. Bou Ghanem, and S.E. D'Orazio. 2015. Intracellular *Listeria monocytogenes* comprises a minimal but vital fraction of the intestinal burden following foodborne infection. *Infection and Immunity* 83:3146-3156.
Jones, G.S., and S.E. D'Orazio. 2017. Monocytes Are the Predominant Cell Type Associated with *Listeria monocytogenes* in the Gut, but They Do Not Serve as an Intracellular Growth Niche. *Journal of Immunology* 198:2796-2804.
Jonquieres, R., J. Pizarro-Cerda, and P. Cossart. 2001. Synergy between the N- and C-terminal domains of InlB for efficient invasion of non-phagocytic cells by *Listeria monocytogenes*. *Molecular Microbiology* 42:955-965.
Jung, H.C., L. Eckmann, S.K. Yang, A. Panja, J. Fierer, E. Morzycka-Wroblewska, and M.F. Kagnoff. 1995. A distinct array of proinflammatory cytokines is expressed in human colon epithelial cells in response to bacterial invasion. *The Journal of Clinical Investigation* 95:55-65.
Kaiser, P., E. Slack, A.J. Grant, W.D. Hardt, and R.R. Regoes. 2013. Lymph node colonization dynamics after oral salmonella typhimurium infection in mice. *PLoS Pathogens* 9:e1003532.
Kang, S.J., H.E. Liang, B. Reizis, and R.M. Locksley. 2008. Regulation of hierarchical clustering and activation of innate immune cells by dendritic cells. *Immunity* 29:819-833.
Kapadia, D., A. Sadikovic, Y. Vanloubbeeck, D. Brockstedt, and L. Fong. 2011. Interplay between CD8alpha+ dendritic cells and monocytes in response to *Listeria monocytogenes* infection attenuates T cell responses. *PloS One* 6:e19376.
Kayaaslan, B.U., E. Akinci, S. Bilen, M.G. Gozel, D. Erdem, M.A. Cevik, and H. Bodur. 2009. Listerial rhombencephalitis in an immunocompetent young adult. *Int J Infect Dis* 13:e65-67.
Keeney, K.M., J.A. Stuckey, and M.X. O'Riordan. 2007. LplA1-dependent utilization of host lipoyl peptides enables *Listeria* cytosolic growth and virulence. *Molecular Microbiology* 66:758-770.
Khelef, N., M. Lecuit, H. Bierne, and P. Cossart. 2006. Species specificity of the *Listeria monocytogenes* InlB protein. *Cellular Microbiology* 8:457-470.
Kim, H., and A.K. Bhunia. 2013. Secreted *Listeria* adhesion protein (Lap) influences Lap-mediated *Listeria monocytogenes* paracellular translocation through epithelial barrier. *Gut Pathog* 5:16.
Kim, H., K.J. Boor, and H. Marquis. 2004. *Listeria monocytogenes* sigmaB contributes to invasion of human intestinal epithelial cells. *Infection and Immunity* 72:7374-7378.
Kim, S., F. Bauernfeind, A. Ablasser, G. Hartmann, K.A. Fitzgerald, E. Latz, and V. Hornung. 2010. *Listeria monocytogenes* is sensed by the NLRP3 and AIM2 inflammasome. *European Journal of Immunology* 40:1545-1551.

Kocks, C., E. Gouin, M. Tabouret, P. Berche, H. Ohayon, and P. Cossart. 1992. *L. monocytogenes*-induced actin assembly requires the actA gene product, a surface protein. *Cell* 68:521-531.

Kocks, C., R. Hellio, P. Gounon, H. Ohayon, and P. Cossart. 1993. Polarized distribution of *Listeria monocytogenes* surface protein ActA at the site of directional actin assembly. *Journal of Cell Science* 105 (Pt 3):699-710.

Kolb-Maurer, A., I. Gentschev, H.W. Fries, F. Fiedler, E.B. Brocker, E. Kampgen, and W. Goebel. 2000. *Listeria monocytogenes*-infected human dendritic cells: uptake and host cell response. *Infection and Immunity* 68:3680-3688.

Koscso, B., and M. Bogunovic. 2016. Analysis and Purification of Mouse Intestinal Dendritic Cell and Macrophage Subsets by Flow Cytometry. *Current Protocols in Immunology* 114:14 39 11-14 39 14.

Krawczyk-Balska, A., and J. Bielecki. 2005. *Listeria monocytogenes* listeriolysin O and phosphatidylinositol-specific phospholipase C affect adherence to epithelial cells. *Canadian Journal of Microbiology* 51:745-751.

Kuan, E.L., S. Ivanov, E.A. Bridenbaugh, G. Victora, W. Wang, E.W. Childs, A.M. Platt, C.V. Jakubzick, R.J. Mason, A.A. Gashev, M. Nussenzweig, M.A. Swartz, M.L. Dustin, D.C. Zawieja, and G.J. Randolph. 2015. Collecting lymphatic vessel permeability facilitates adipose tissue inflammation and distribution of antigen to lymph node-homing adipose tissue dendritic cells. *Journal of Immunology* 194:5200-5210.

Kurihara, T., G. Warr, J. Loy, and R. Bravo. 1997. Defects in macrophage recruitment and host defense in mice lacking the CCR2 chemokine receptor. *The Journal of Experimental Medicine* 186:1757-1762.

Lacey, D.C., A. Achuthan, A.J. Fleetwood, H. Dinh, J. Roiniotis, G.M. Scholz, M.W. Chang, S.K. Beckman, A.D. Cook, and J.A. Hamilton. 2012. Defining GM-CSF- and macrophage-CSF-dependent macrophage responses by in vitro models. *Journal of Immunology* 188:5752-5765.

Lauer, P., M.Y. Chow, M.J. Loessner, D.A. Portnoy, and R. Calendar. 2002. Construction, characterization, and use of two *Listeria monocytogenes* site-specific phage integration vectors. *Journal of Bacteriology* 184:4177-4186.

Lauvau, G., L. Chorro, E. Spaulding, and S.M. Soudja. 2014. Inflammatory monocyte effector mechanisms. *Cellular Immunology* 291:32-40.

Lecuit, M., S. Dramsi, C. Gottardi, M. Fedor-Chaiken, B. Gumbiner, and P. Cossart. 1999a. A single amino acid in E-cadherin responsible for host specificity towards the human pathogen *Listeria monocytogenes. The EMBO Journal* 18:3956-3963.

Lecuit, M., S. Dramsi, C. Gottardi, M. Fedor-Chaiken, B. Gumbiner, and P. Cossart. 1999b. A single amino acid in E-cadherin responsible for host specificity towards the human pathogen *Listeria monocytogenes*. *The EMBO Journal* 18:3956-3963.

Lecuit, M., H. Ohayon, L. Braun, J. Mengaud, and P. Cossart. 1997. Internalin of *Listeria monocytogenes* with an intact leucine-rich repeat region is sufficient to promote internalization. *Infection and Immunity* 65:5309-5319.

Lecuit, M., S. Vandormael-Pournin, J. Lefort, M. Huerre, P. Gounon, C. Dupuy, C. Babinet, and P. Cossart. 2001. A transgenic model for listeriosis: role of internalin in crossing the intestinal barrier. *Science* 292:1722-1725.

Leimeister-Wachter, M., C. Haffner, E. Domann, W. Goebel, and T. Chakraborty. 1990. Identification of a gene that positively regulates expression of listeriolysin, the major virulence factor of *Listeria monocytogenes*. *Proceedings of the National Academy of Sciences of the United States of America* 87:8336-8340.

Lelouard, H., M. Fallet, B. de Bovis, S. Meresse, and J.P. Gorvel. 2012. Peyer's patch dendritic cells sample antigens by extending dendrites through M cell-specific transcellular pores. *Gastroenterology* 142:592-601 e593.
Lelouard, H., S. Henri, B. De Bovis, B. Mugnier, A. Chollat-Namy, B. Malissen, S. Meresse, and J.P. Gorvel. 2010. Pathogenic bacteria and dead cells are internalized by a unique subset of Peyer's patch dendritic cells that express lysozyme. *Gastroenterology* 138:173-184 e171-173.
Li, Y., W. Zhu, L. Zuo, and B. Shen. 2016. The Role of the Mesentery in Crohn's Disease: The Contributions of Nerves, Vessels, Lymphatics, and Fat to the Pathogenesis and Disease Course. *Inflammatory Bowel Diseases* 22:1483-1495.
Lim, C.H., S. Voedisch, B. Wahl, S.F. Rouf, R. Geffers, M. Rhen, and O. Pabst. 2014. Independent bottlenecks characterize colonization of systemic compartments and gut lymphoid tissue by *Salmonella*. *PLoS Pathogens* 10:e1004270.
Lingnau, A., E. Domann, M. Hudel, M. Bock, T. Nichterlein, J. Wehland, and T. Chakraborty. 1995. Expression of the *Listeria monocytogenes* EGD *inlA* and *inlB* genes, whose products mediate bacterial entry into tissue culture cell lines, by PrfA-dependent and -independent mechanisms. *Infection and Immunity* 63:3896-3903.
Mabbott, N.A., J. Kenneth Baillie, D.A. Hume, and T.C. Freeman. 2010. Meta-analysis of lineage-specific gene expression signatures in mouse leukocyte populations. *Immunobiology* 215:724-736.
MacGowan, A.P., K. Bowker, J. McLauchlin, P.M. Bennett, and D.S. Reeves. 1994. The occurrence and seasonal changes in the isolation of *Listeria* spp. in shop bought food stuffs, human faeces, sewage and soil from urban sources. *International Journal of Food Microbiology* 21:325-334.
Macpherson, A.J., and K. Smith. 2006. Mesenteric lymph nodes at the center of immune anatomy. *The Journal of Experimental Medicine* 203:497-500.
Maijala, R., O. Lyytikainen, T. Autio, T. Aalto, L. Haavisto, and T. Honkanen-Buzalski. 2001. Exposure of *Listeria monocytogenes* within an epidemic caused by butter in Finland. *International Journal of Food Microbiology* 70:97-109.
Manz, M.G., D. Traver, T. Miyamoto, I.L. Weissman, and K. Akashi. 2001. Dendritic cell potentials of early lymphoid and myeloid progenitors. *Blood* 97:3333-3341.
Maraskovsky, E., K. Brasel, M. Teepe, E.R. Roux, S.D. Lyman, K. Shortman, and H.J. McKenna. 1996. Dramatic increase in the numbers of functionally mature dendritic cells in Flt3 ligand-treated mice: multiple dendritic cell subpopulations identified. *The Journal of Experimental Medicine* 184:1953-1962.
Marquis, H., V. Doshi, and D.A. Portnoy. 1995. The broad-range phospholipase C and a metalloprotease mediate listeriolysin O-independent escape of *Listeria monocytogenes* from a primary vacuole in human epithelial cells. *Infection and Immunity* 63:4531-4534.
Matsumura, F., Y. Yamakita, V. Starovoytov, and S. Yamashiro. 2013. Fascin confers resistance to *Listeria* infection in dendritic cells. *Journal of Immunology* 191:6156-6164.
Mayer, C.T., P. Ghorbani, A. Nandan, M. Dudek, C. Arnold-Schrauf, C. Hesse, L. Berod, P. Stuve, F. Puttur, M. Merad, and T. Sparwasser. 2014. Selective and efficient generation of functional Batf3-dependent CD103+ dendritic cells from mouse bone marrow. *Blood* 124:3081-3091.
McElroy, D.S., T.J. Ashley, and S.E.F. D'Orazio. 2009. Lymphocytes serve as a reservoir for *L. monocytogenes* growth during infection of mice. *Microb Pathog* 46:214-221.

McKenna, H.J., K.L. Stocking, R.E. Miller, K. Brasel, T. De Smedt, E. Maraskovsky, C.R. Maliszewski, D.H. Lynch, J. Smith, B. Pulendran, E.R. Roux, M. Teepe, S.D. Lyman, and J.J. Peschon. 2000. Mice lacking flt3 ligand have deficient hematopoiesis affecting hematopoietic progenitor cells, dendritic cells, and natural killer cells. *Blood* 95:3489-3497.

Melton-Witt, J.A., S.M. Rafelski, D.A. Portnoy, and A.I. Bakardjiev. 2012. Oral infection with signature-tagged *Listeria monocytogenes* reveals organ-specific growth and dissemination routes in guinea pigs. *Infection and Immunity* 80:720-732.

Menashe, O., E. Kaganskaya, T. Baasov, and S. Yaron. 2008. Aminoglycosides affect intracellular *Salmonella enterica* serovars typhimurium and virchow. *Antimicrobial Agents and Chemotherapy* 52:920-926.

Mengaud, J., J. Chenevert, C. Geoffroy, J.L. Gaillard, and P. Cossart. 1987. Identification of the structural gene encoding the SH-activated hemolysin of *Listeria monocytogenes*: listeriolysin O is homologous to streptolysin O and pneumolysin. *Infection and Immunity* 55:3225-3227.

Mengaud, J., H. Ohayon, P. Gounon, R.M. Mege, and P. Cossart. 1996. E-cadherin is the receptor for internalin, a surface protein required for entry of *L. monocytogenes* into epithelial cells. *Cell* 84:923-932.

Miller, J.C., B.D. Brown, T. Shay, E.L. Gautier, V. Jojic, A. Cohain, G. Pandey, M. Leboeuf, K.G. Elpek, J. Helft, D. Hashimoto, A. Chow, J. Price, M. Greter, M. Bogunovic, A. Bellemare-Pelletier, P.S. Frenette, G.J. Randolph, S.J. Turley, M. Merad, and C. Immunological Genome. 2012. Deciphering the transcriptional network of the dendritic cell lineage. *Nature Immunology* 13:888-899.

Milohanic, E., R. Jonquieres, P. Cossart, P. Berche, and J.L. Gaillard. 2001. The autolysin Ami contributes to the adhesion of *Listeria monocytogenes* to eukaryotic cells via its cell wall anchor. *Molecular Microbiology* 39:1212-1224.

Milohanic, E., B. Pron, P. Berche, and J.L. Gaillard. 2000. Identification of new loci involved in adhesion of *Listeria monocytogenes* to eukaryotic cells. European Listeria Genome Consortium. *Microbiology* 146 (Pt 3):731-739.

Mitchell, G., L. Ge, Q. Huang, C. Chen, S. Kianian, M.F. Roberts, R. Schekman, and D.A. Portnoy. 2015. Avoidance of autophagy mediated by PlcA or ActA is required for *Listeria monocytogenes* growth in macrophages. *Infection and Immunity*

Mitchell, L.M., K.L. Brzoza-Lewis, C.J. Henry, J.M. Grayson, M.M. Westcott, and E.M. Hiltbold. 2011. Distinct responses of splenic dendritic cell subsets to infection with *Listeria monocytogenes*: maturation phenotype, level of infection, and T cell priming capacity ex vivo. *Cellular Immunology* 268:79-86.

Monk, I.R., P.G. Casey, M. Cronin, C.G. Gahan, and C. Hill. 2008a. Development of multiple strain competitive index assays for *Listeria monocytogenes* using pIMC; a new site-specific integrative vector. *BMC Microbiol* 8:96.

Monk, I.R., C.G. Gahan, and C. Hill. 2008b. Tools for functional postgenomic analysis of *Listeria monocytogenes. Applied and environmental microbiology* 74:3921-3934.

Mullapudi, S., R.M. Siletzky, and S. Kathariou. 2008. Heavy-metal and benzalkonium chloride resistance of *Listeria monocytogenes* isolates from the environment of turkey-processing plants. *Applied and Environmental Microbiology* 74:1464-1468.

Murray, E., R. Webb, and M. Swann. 1926. A disease of rabbits characterized by large mononuclear leucocytosis, aused by a hitherto undescribed bacillus *Bacterium monocytogenes*. *J. Path. Bacteriol.* 29:407-439.

Myers, J.T., A.W. Tsang, and J.A. Swanson. 2003. Localized reactive oxygen and nitrogen intermediates inhibit escape of *Listeria monocytogenes* from vacuoles in activated macrophages. *Journal of Immunology* 171:5447-5453.

Na, Y.R., D. Jung, G.J. Gu, and S.H. Seok. 2016. GM-CSF Grown Bone Marrow Derived Cells Are Composed of Phenotypically Different Dendritic Cells and Macrophages. *Molecules and Cells* 39:734-741.

Nadon, C.A., B.M. Bowen, M. Wiedmann, and K.J. Boor. 2002. Sigma B contributes to PrfA-mediated virulence in *Listeria monocytogenes*. *Infection and Immunity* 70:3948-3952.

Naik, S.H., M. O'Keeffe, A. Proietto, H.H. Shortman, and L. Wu. 2010. CD8+, CD8-, and plasmacytoid dendritic cell generation in vitro using flt3 ligand. *Methods in Molecular Biology* 595:167-176.

Naik, S.H., A.I. Proietto, N.S. Wilson, A. Dakic, P. Schnorrer, M. Fuchsberger, M.H. Lahoud, M. O'Keeffe, Q.X. Shao, W.F. Chen, J.A. Villadangos, K. Shortman, and L. Wu. 2005. Cutting edge: generation of splenic CD8+ and CD8- dendritic cell equivalents in Fms-like tyrosine kinase 3 ligand bone marrow cultures. *Journal of Immunology* 174:6592-6597.

Naik, S.H., P. Sathe, H.Y. Park, D. Metcalf, A.I. Proietto, A. Dakic, S. Carotta, M. O'Keeffe, M. Bahlo, A. Papenfuss, J.Y. Kwak, L. Wu, and K. Shortman. 2007. Development of plasmacytoid and conventional dendritic cell subtypes from single precursor cells derived in vitro and in vivo. *Nature Immunology* 8:1217-1226.

Neuenhahn, M., K.M. Kerksiek, M. Nauerth, M.H. Suhre, M. Schiemann, F.E. Gebhardt, C. Stemberger, K. Panthel, S. Schroder, T. Chakraborty, S. Jung, H. Hochrein, H. Russmann, T. Brocker, and D.H. Busch. 2006. CD8alpha+ dendritic cells are required for efficient entry of *Listeria monocytogenes* into the spleen. *Immunity* 25:619-630.

NicAogain, K., and C.P. O'Byrne. 2016. The Role of Stress and Stress Adaptations in Determining the Fate of the Bacterial Pathogen *Listeria monocytogenes* in the Food Chain. *Frontiers in Microbiology* 7:1865.

Niess, J.H., S. Brand, X. Gu, L. Landsman, S. Jung, B.A. McCormick, J.M. Vyas, M. Boes, H.L. Ploegh, J.G. Fox, D.R. Littman, and H.C. Reinecker. 2005. CX3CR1-mediated dendritic cell access to the intestinal lumen and bacterial clearance. *Science* 307:254-258.

Nikitas, G., C. Deschamps, O. Disson, T. Niault, P. Cossart, and M. Lecuit. 2011. Transcytosis of *Listeria monocytogenes* across the intestinal barrier upon specific targeting of goblet cell accessible E-cadherin. *The Journal of Experimental Medicine* 208:2263-2277.

O'Riordan, M., M.A. Moors, and D.A. Portnoy. 2003. *Listeria* intracellular growth and virulence require host-derived lipoic acid. *Science* 302:462-464.

Onai, N., A. Obata-Onai, M.A. Schmid, T. Ohteki, D. Jarrossay, and M.G. Manz. 2007. Identification of clonogenic common Flt3+M-CSFR+ plasmacytoid and conventional dendritic cell progenitors in mouse bone marrow. *Nature Immunology* 8:1207-1216.

Ooi, S.T., and B. Lorber. 2005. Gastroenteritis due to *Listeria monocytogenes*. *Clinical infectious diseases : an official publication of the Infectious Diseases Society of America* 40:1327-1332.

Pamer, E.G. 2004. Immune responses to *Listeria monocytogenes*. *Nature reviews. Immunology* 4:812-823.

Pentecost, M., J. Kumaran, P. Ghosh, and M.R. Amieva. 2010. *Listeria monocytogenes* internalin B activates junctional endocytosis to accelerate intestinal invasion. *PLoS Pathogens* 6:e1000900.

Pentecost, M., G. Otto, J.A. Theriot, and M.R. Amieva. 2006. *Listeria monocytogenes* invades the epithelial junctions at sites of cell extrusion. *PLoS Pathogens* 2:e3.

Perelman, S.S., M.E. Abrams, J.L. Eitson, D. Chen, A. Jimenez, M. Mettlen, J.W. Schoggins, and N.M. Alto. 2016. Cell-Based Screen Identifies Human Interferon-Stimulated Regulators of *Listeria monocytogenes* Infection. *PLoS Pathogens* 12:e1006102.

Peterson, P.K., J. Verhoef, D. Schmeling, and P.G. Quie. 1977. Kinetics of phagocytosis and bacterial killing by human polymorphonuclear leukocytes and monocytes. *The Journal of Infectious Diseases* 136:502-509.

Phan-Thanh, L., and T. Gormon. 1997. A chemically defined minimal medium for the optimal culture of *Listeria*. *International journal of food microbiology* 35:91-95.

Pizarro-Cerda, J., A. Kuhbacher, and P. Cossart. 2012. Entry of *Listeria monocytogenes* in mammalian epithelial cells: an updated view. *Cold Spring Harbor Perspectives in Medicine* 2:

Pron, B., C. Boumaila, F. Jaubert, P. Berche, G. Milon, F. Geissmann, and J.L. Gaillard. 2001. Dendritic cells are early cellular targets of *Listeria monocytogenes* after intestinal delivery and are involved in bacterial spread in the host. *Cellular Microbiology* 3:331-340.

Pron, B., C. Boumaila, F. Jaubert, S. Sarnacki, J.P. Monnet, P. Berche, and J.L. Gaillard. 1998. Comprehensive study of the intestinal stage of listeriosis in a rat ligated ileal loop system. *Infection and Immunity* 66:747-755.

Qazi, S.N., S.E. Harrison, T. Self, P. Williams, and P.J. Hill. 2004. Real-time monitoring of intracellular *Staphylococcus aureus* replication. *Journal of Bacteriology* 186:1065-1077.

Quereda, J.J., O. Dussurget, M.A. Nahori, A. Ghozlane, S. Volant, M.A. Dillies, B. Regnault, S. Kennedy, S. Mondot, B. Villoing, P. Cossart, and J. Pizarro-Cerda. 2016. Bacteriocin from epidemic *Listeria* strains alters the host intestinal microbiota to favor infection. *Proceedings of the National Academy of Sciences of the United States of America* 113:5706-5711.

Rajabian, T., B. Gavicherla, M. Heisig, S. Muller-Altrock, W. Goebel, S.D. Gray-Owen, and K. Ireton. 2009. The bacterial virulence factor InlC perturbs apical cell junctions and promotes cell-to-cell spread of *Listeria*. *Nature Cell Biology* 11:1212-1218.

Randolph, G.J., V. Angeli, and M.A. Swartz. 2005. Dendritic-cell trafficking to lymph nodes through lymphatic vessels. *Nature Reviews. Immunology* 5:617-628.

Randolph, G.J., K. Inaba, D.F. Robbiani, R.M. Steinman, and W.A. Muller. 1999. Differentiation of phagocytic monocytes into lymph node dendritic cells in vivo. *Immunity* 11:753-761.

Raybourne, R.B., G. Roth, P.A. Deuster, E.M. Sternberg, and A. Singh. 2001. Uptake and killing of *Listeria monocytogenes* by normal human peripheral blood granulocytes and monocytes as measured by flow cytometry and cell sorting. *FEMS Immunology and Medical Microbiology* 31:219-225.

Reid, C.D., A. Stackpoole, A. Meager, and J. Tikerpae. 1992. Interactions of tumor necrosis factor with granulocyte-macrophage colony-stimulating factor and other cytokines in the regulation of dendritic cell growth in vitro from early bipotent CD34+ progenitors in human bone marrow. *Journal of Immunology* 149:2681-2688.

Reis, O., S. Sousa, A. Camejo, V. Villiers, E. Gouin, P. Cossart, and D. Cabanes. 2010. LapB, a novel *Listeria monocytogenes* LPXTG surface adhesin, required for entry into eukaryotic cells and virulence. *The Journal of Infectious Diseases* 202:551-562.

Renier, S., M. Hebraud, and M. Desvaux. 2011. Molecular biology of surface colonization by *Listeria monocytogenes*: an additional facet of an opportunistic Gram-positive foodborne pathogen. *Environmental Microbiology* 13:835-850.
Reniere, M.L., A.T. Whiteley, K.L. Hamilton, S.M. John, P. Lauer, R.G. Brennan, and D.A. Portnoy. 2015. Glutathione activates virulence gene expression of an intracellular pathogen. *Nature* 517:170-173.
Resendiz-Albor, A.A., R. Esquivel, R. Lopez-Revilla, L. Verdin, and L. Moreno-Fierros. 2005. Striking phenotypic and functional differences in lamina propria lymphocytes from the large and small intestine of mice. *Life Sciences* 76:2783-2803.
Rodero, M.P., L. Poupel, P.L. Loyher, P. Hamon, F. Licata, C. Pessel, D.A. Hume, C. Combadiere, and A. Boissonnas. 2015. Immune surveillance of the lung by migrating tissue monocytes. *eLife* 4:e07847.
Rogers, H.W., and E.R. Unanue. 1993. Neutrophils are involved in acute, nonspecific resistance to *Listeria monocytogenes* in mice. *Infection and Immunity* 61:5090-5096.
Rydstrom, A., and M.J. Wick. 2010. *Salmonella* inhibits monocyte differentiation into CD11c hi MHC-II hi cells in a MyD88-dependent fashion. *Journal of Leukocyte Biology* 87:823-832.
Saklani-Jusforgues, H., E. Fontan, and P.L. Goossens. 2000. Effect of acid-adaptation on *Listeria monocytogenes* survival and translocation in a murine intragastric infection model. *FEMS Microbiol Lett* 193:155-159.
Sallusto, F., and A. Lanzavecchia. 1994. Efficient presentation of soluble antigen by cultured human dendritic cells is maintained by granulocyte/macrophage colony-stimulating factor plus interleukin 4 and downregulated by tumor necrosis factor alpha. *The Journal of Experimental Medicine* 179:1109-1118.
Sansonetti, P.J., and A. Phalipon. 1999. M cells as ports of entry for enteroinvasive pathogens: mechanisms of interaction, consequences for the disease process. *Semin Immunol* 11:193-203.
Sawyer, R.T., D.A. Drevets, P.A. Campbell, and T.A. Potter. 1996. Internalin A can mediate phagocytosis of *Listeria monocytogenes* by mouse macrophage cell lines. *Journal of Leukocyte Biology* 60:603-610.
Scallan, E., R.M. Hoekstra, F.J. Angulo, R.V. Tauxe, M.A. Widdowson, S.L. Roy, J.L. Jones, and P.M. Griffin. 2011. Foodborne illness acquired in the United States--major pathogens. *Emerg Infect Dis* 17:7-15.
Scheicher, C., M. Mehlig, R. Zecher, and K. Reske. 1992. Dendritic cells from mouse bone marrow: in vitro differentiation using low doses of recombinant granulocyte-macrophage colony-stimulating factor. *Journal of Immunological Methods* 154:253-264.
Schreurs, M.W., A.A. Eggert, A.J. de Boer, C.G. Figdor, and G.J. Adema. 1999. Generation and functional characterization of mouse monocyte-derived dendritic cells. *European Journal of Immunology* 29:2835-2841.
Schulz, O., E. Jaensson, E.K. Persson, X. Liu, T. Worbs, W.W. Agace, and O. Pabst. 2009. Intestinal CD103+, but not CX3CR1+, antigen sampling cells migrate in lymph and serve classical dendritic cell functions. *The Journal of Experimental Medicine* 206:3101-3114.
Seita, J., and I.L. Weissman. 2010. Hematopoietic stem cell: self-renewal versus differentiation. *Wiley Interdisciplinary Reviews. Systems Biology and Medicine* 2:640-653.
Seki, E., H. Tsutsui, N.M. Tsuji, N. Hayashi, K. Adachi, H. Nakano, S. Futatsugi-Yumikura, O. Takeuchi, K. Hoshino, S. Akira, J. Fujimoto, and K. Nakanishi.

2002. Critical roles of myeloid differentiation factor 88-dependent proinflammatory cytokine release in early phase clearance of *Listeria monocytogenes* in mice. *Journal of Immunology* 169:3863-3868.
Serbina, N.V., W. Kuziel, R. Flavell, S. Akira, B. Rollins, and E.G. Pamer. 2003a. Sequential MyD88-independent and -dependent activation of innate immune responses to intracellular bacterial infection. *Immunity* 19:891-901.
Serbina, N.V., and E.G. Pamer. 2006. Monocyte emigration from bone marrow during bacterial infection requires signals mediated by chemokine receptor CCR2. *Nature Immunology* 7:311-317.
Serbina, N.V., T.P. Salazar-Mather, C.A. Biron, W.A. Kuziel, and E.G. Pamer. 2003b. TNF/iNOS-producing dendritic cells mediate innate immune defense against bacterial infection. *Immunity* 19:59-70.
Seveau, S., J. Pizarro-Cerda, and P. Cossart. 2007. Molecular mechanisms exploited by *Listeria monocytogenes* during host cell invasion. *Microbes Infect* 9:1167-1175.
Shaughnessy, L.M., and J.A. Swanson. 2007. The role of the activated macrophage in clearing *Listeria monocytogenes* infection. *Frontiers in bioscience : a journal and virtual library* 12:2683-2692.
Shen, Y., M. Naujokas, M. Park, and K. Ireton. 2000. InIB-dependent internalization of *Listeria* is mediated by the Met receptor tyrosine kinase. *Cell* 103:501-510.
Shi, C., T.M. Hohl, I. Leiner, M.J. Equinda, X. Fan, and E.G. Pamer. 2011. Ly6G+ neutrophils are dispensable for defense against systemic *Listeria monocytogenes* infection. *Journal of Immunology* 187:5293-5298.
Shi, C., P. Velazquez, T.M. Hohl, I. Leiner, M.L. Dustin, and E.G. Pamer. 2010. Monocyte trafficking to hepatic sites of bacterial infection is chemokine independent and directed by focal intercellular adhesion molecule-1 expression. *Journal of Immunology* 184:6266-6274.
Shum, D.T., and S.B. Galsworthy. 1979. Stimulation of monocyte precursors in vivo by an extract from Listeria monocytogenes. *Canadian Journal of Microbiology* 25:698-705.
Siddiqui, K.R., S. Laffont, and F. Powrie. 2010. E-cadherin marks a subset of inflammatory dendritic cells that promote T cell-mediated colitis. *Immunity* 32:557-567.
Silva, M.T., and N.T. Pestana. 2013. The *in vivo* extracellular life of facultative intracellular bacterial parasites: role in pathogenesis. *Immunobiology* 218:325-337.
Sleator, R.D., H.H. Wemekamp-Kamphuis, C.G. Gahan, T. Abee, and C. Hill. 2005. A PrfA-regulated bile exclusion system (BilE) is a novel virulence factor in *Listeria monocytogenes*. *Molecular Microbiology* 55:1183-1195.
Smith, G.A., H. Marquis, S. Jones, N.C. Johnston, D.A. Portnoy, and H. Goldfine. 1995a. The two distinct phospholipases C of *Listeria monocytogenes* have overlapping roles in escape from a vacuole and cell-to-cell spread. *Infection and Immunity* 63:4231-4237.
Smith, G.A., D.A. Portnoy, and J.A. Theriot. 1995b. Asymmetric distribution of the *Listeria monocytogenes* ActA protein is required and sufficient to direct actin-based motility. *Molecular Microbiology* 17:945-951.
Smith, K., and P. Youngman. 1992. Use of a new integrational vector to investigate compartment-specific expression of *Bacillus subtilis spoIIM* gene. *Biochimie* 74:705-711.
Smith, M.A., K. Takeuchi, G. Anderson, G.O. Ware, H.M. McClure, R.B. Raybourne, N. Mytle, and M.P. Doyle. 2008. Dose-response model for *Listeria monocytogenes*-induced stillbirths in nonhuman primates. *Infection and Immunity* 76:726-731.

Somers, E.B., and A.C. Wong. 2004. Efficacy of two cleaning and sanitizing combinations on Listeria monocytogenes biofilms formed at low temperature on a variety of materials in the presence of ready-to-eat meat residue. *Journal of Food Protection* 67:2218-2229.

Specian, R.D., and M.G. Oliver. 1991. Functional biology of intestinal goblet cells. *Am J Physiol* 260:C183-193.

St John, A.L., W.X. Ang, M.N. Huang, C.A. Kunder, E.W. Chan, M.D. Gunn, and S.N. Abraham. 2014. S1P-Dependent trafficking of intracellular yersinia pestis through lymph nodes establishes Buboes and systemic infection. *Immunity* 41:440-450.

Strawn, L.K., E.D. Fortes, E.A. Bihn, K.K. Nightingale, Y.T. Grohn, R.W. Worobo, M. Wiedmann, and P.W. Bergholz. 2013. Landscape and meteorological factors affecting prevalence of three food-borne pathogens in fruit and vegetable farms. *Applied and Environmental Microbiology* 79:588-600.

Stritzker, J., J. Janda, C. Schoen, M. Taupp, S. Pilgrim, I. Gentschev, P. Schreier, G. Geginat, and W. Goebel. 2004. Growth, virulence, and immunogenicity of *Listeria monocytogenes* aro mutants. *Infection and Immunity* 72:5622-5629.

Stritzker, J., C. Schoen, and W. Goebel. 2005. Enhanced synthesis of internalin A in aro mutants of *Listeria monocytogenes* indicates posttranscriptional control of the inlAB mRNA. *Journal of Bacteriology* 187:2836-2845.

Suarez, M., B. Gonzalez-Zorn, Y. Vega, I. Chico-Calero, and J.A. Vazquez-Boland. 2001. A role for ActA in epithelial cell invasion by *Listeria monocytogenes*. *Cellular Microbiology* 3:853-864.

Sue, D., D. Fink, M. Wiedmann, and K.J. Boor. 2004. sigmaB-dependent gene induction and expression in *Listeria monocytogenes* during osmotic and acid stress conditions simulating the intestinal environment. *Microbiology* 150:3843-3855.

Sun, Z., D. Unutmaz, Y.R. Zou, M.J. Sunshine, A. Pierani, S. Brenner-Morton, R.E. Mebius, and D.R. Littman. 2000. Requirement for RORgamma in thymocyte survival and lymphoid organ development. *Science* 288:2369-2373.

Sunderkotter, C., T. Nikolic, M.J. Dillon, N. Van Rooijen, M. Stehling, D.A. Drevets, and P.J. Leenen. 2004. Subpopulations of mouse blood monocytes differ in maturation stage and inflammatory response. *Journal of Immunology* 172:4410-4417.

Tamoutounour, S., S. Henri, H. Lelouard, B. de Bovis, C. de Haar, C.J. van der Woude, A.M. Woltman, Y. Reyal, D. Bonnet, D. Sichien, C.C. Bain, A.M. Mowat, C. Reis e Sousa, L.F. Poulin, B. Malissen, and M. Guilliams. 2012. CD64 distinguishes macrophages from dendritic cells in the gut and reveals the Th1-inducing role of mesenteric lymph node macrophages during colitis. *European Journal of Immunology* 42:3150-3166.

Tattoli, I., M.T. Sorbara, C. Yang, S.A. Tooze, D.J. Philpott, and S.E. Girardin. 2013. *Listeria* phospholipases subvert host autophagic defenses by stalling pre-autophagosomal structures. *The EMBO journal* 32:3066-3078.

Thomas, G., R. Tacke, C.C. Hedrick, and R.N. Hanna. 2015. Nonclassical patrolling monocyte function in the vasculature. *Arteriosclerosis, Thrombosis, and Vascular Biology* 35:1306-1316.

Tilney, L.G., and D.A. Portnoy. 1989. Actin filaments and the growth, movement, and spread of the intracellular bacterial parasite, *Listeria monocytogenes*. *The Journal of Cell Biology* 109:1597-1608.

Toledo-Arana, A., O. Dussurget, G. Nikitas, N. Sesto, H. Guet-Revillet, D. Balestrino, E. Loh, J. Gripenland, T. Tiensuu, K. Vaitkevicius, M. Barthelemy, M. Vergassola, M.A. Nahori, G. Soubigou, B. Regnault, J.Y. Coppee, M. Lecuit, J. Johansson,

and P. Cossart. 2009. The *Listeria* transcriptional landscape from saprophytism to virulence. *Nature* 459:950-956.
Torres, D., M. Barrier, F. Bihl, V.J. Quesniaux, I. Maillet, S. Akira, B. Ryffel, and F. Erard. 2004. Toll-like receptor 2 is required for optimal control of *Listeria monocytogenes* infection. *Infection and Immunity* 72:2131-2139.
Traver, D., K. Akashi, M. Manz, M. Merad, T. Miyamoto, E.G. Engleman, and I.L. Weissman. 2000. Development of CD8alpha-positive dendritic cells from a common myeloid progenitor. *Science* 290:2152-2154.
Travier, L., S. Guadagnini, E. Gouin, A. Dufour, V. Chenal-Francisque, P. Cossart, J.C. Olivo-Marin, J.M. Ghigo, O. Disson, and M. Lecuit. 2013. ActA promotes *Listeria monocytogenes* aggregation, intestinal colonization and carriage. *PLoS Pathogens* 9:e1003131.
Tsai, Y.H., O. Disson, H. Bierne, and M. Lecuit. 2013. Murinization of internalin extends its receptor repertoire, altering *Listeria monocytogenes* cell tropism and host responses. *PLoS Pathogens* 9:e1003381.
Vadia, S., E. Arnett, A.C. Haghighat, E.M. Wilson-Kubalek, R.K. Tweten, and S. Seveau. 2011. The pore-forming toxin listeriolysin O mediates a novel entry pathway of *L. monocytogenes* into human hepatocytes. *PLoS Pathogens* 7:e1002356.
Vallon-Eberhard, A., L. Landsman, N. Yogev, B. Verrier, and S. Jung. 2006. Transepithelial pathogen uptake into the small intestinal lamina propria. *Journal of Immunology* 176:2465-2469.
van der Veen, S., R. Moezelaar, T. Abee, and M.H. Wells-Bennik. 2008. The growth limits of a large number of *Listeria monocytogenes* strains at combinations of stresses show serotype--and niche-specific traits. *J Appl Microbiol* 105:1246-1258.
Vivant, A.L., D. Garmyn, and P. Piveteau. 2013. L*isteria monocytogenes*, a down-to-earth pathogen. *Frontiers in Cellular and Infection Microbiology* 3:87.
Voedisch, S., C. Koenecke, S. David, H. Herbrand, R. Forster, M. Rhen, and O. Pabst. 2009. Mesenteric lymph nodes confine dendritic cell-mediated dissemination of *Salmonella enterica* serovar Typhimurium and limit systemic disease in mice. *Infection and Immunity* 77:3170-3180.
Vremec, D., G.J. Lieschke, A.R. Dunn, L. Robb, D. Metcalf, and K. Shortman. 1997. The influence of granulocyte/macrophage colony-stimulating factor on dendritic cell levels in mouse lymphoid organs. *European journal of immunology* 27:40-44.
Wampler, J.L., K.P. Kim, Z. Jaradat, and A.K. Bhunia. 2004. Heat shock protein 60 acts as a receptor for the *Listeria* adhesion protein in Caco-2 cells. *Infection and Immunity* 72:931-936.
Wang, L., and M. Lin. 2007. Identification of IspC, an 86-kilodalton protein target of humoral immune response to infection with *Listeria monocytogenes* serotype 4b, as a novel surface autolysin. *Journal of Bacteriology* 189:2046-2054.
Warren, S.E., D.P. Mao, A.E. Rodriguez, E.A. Miao, and A. Aderem. 2008. Multiple Nod-like receptors activate caspase 1 during *Listeria monocytogenes* infection. *Journal of Immunology* 180:7558-7564.
Watkins, J., and K.P. Sleath. 1981. Isolation and enumeration of *Listeria monocytogenes* from Sewage, Sewage Sludge and River Water. *The Journal of applied Bacteriology* 50:1-9.
Welch, M.D., A. Iwamatsu, and T.J. Mitchison. 1997. Actin polymerization is induced by Arp2/3 protein complex at the surface of *Listeria monocytogenes*. *Nature* 385:265-269.

Weller, D., M. Wiedmann, and L.K. Strawn. 2015. Irrigation Is Significantly Associated with an Increased Prevalence of *Listeria monocytogenes* in Produce Production Environments in New York State. *Journal of food protection* 78:1132-1141.

Welshimer, H.J., and J. Donker-Voet. 1971. *Listeria monocytogenes* in nature. *Applied Microbiology* 21:516-519.

Westcott, M.M., C.J. Henry, J.E. Amis, and E.M. Hiltbold. 2010. Dendritic cells inhibit the progression of *Listeria monocytogenes* intracellular infection by retaining bacteria in major histocompatibility complex class II-rich phagosomes and by limiting cytosolic growth. *Infection and Immunity* 78:2956-2965.

Westcott, M.M., C.J. Henry, A.S. Cook, K.W. Grant, and E.M. Hiltbold. 2007. Differential susceptibility of bone marrow-derived dendritic cells and macrophages to productive infection with *Listeria monocytogenes*. *Cellular Microbiology* 9:1397-1411.

Wiedmann, M., T.J. Arvik, R.J. Hurley, and K.J. Boor. 1998. General stress transcription factor sigmaB and its role in acid tolerance and virulence of *Listeria monocytogenes*. *Journal of Bacteriology* 180:3650-3656.

Wolfram, L., A. Fischbeck, I. Frey-Wagner, K.A. Wojtal, S. Lang, M. Fried, S.R. Vavricka, M. Hausmann, and G. Rogler. 2013. Regulation of the expression of chaperone gp96 in macrophages and dendritic cells. *PloS One* 8:e76350.

Wollert, T., B. Pasche, M. Rochon, S. Deppenmeier, J. van den Heuvel, A.D. Gruber, D.W. Heinz, A. Lengeling, and W.D. Schubert. 2007. Extending the host range of *Listeria monocytogenes* by rational protein design. *Cell* 129:891-902.

Xayarath, B., and N.E. Freitag. 2012. Optimizing the balance between host and environmental survival skills: lessons learned from *Listeria monocytogenes*. *Future Microbiol* 7:839-852.

Yona, S., K.W. Kim, Y. Wolf, A. Mildner, D. Varol, M. Breker, D. Strauss-Ayali, S. Viukov, M. Guilliams, A. Misharin, D.A. Hume, H. Perlman, B. Malissen, E. Zelzer, and S. Jung. 2013. Fate mapping reveals origins and dynamics of monocytes and tissue macrophages under homeostasis. *Immunity* 38:79-91.

Yoshikawa, Y., M. Ogawa, T. Hain, M. Yoshida, M. Fukumatsu, M. Kim, H. Mimuro, I. Nakagawa, T. Yanagawa, T. Ishii, A. Kakizuka, E. Sztul, T. Chakraborty, and C. Sasakawa. 2009. *Listeria monocytogenes* ActA-mediated escape from autophagic recognition. *Nature Cell Biology* 11:1233-1240.

Zapata, H.J., A. Bose, W. Javaid, and D. Blair. 2009. Listerial Rhomboencephalitis: Not Just for the Weakened Immune System. *Clin. Microb. Newsletter* 31:108-110.

Zigmond, E., C. Varol, J. Farache, E. Elmaliah, A.T. Satpathy, G. Friedlander, M. Mack, N. Shpigel, I.G. Boneca, K.M. Murphy, G. Shakhar, Z. Halpern, and S. Jung. 2012. Ly6C hi monocytes in the inflamed colon give rise to proinflammatory effector cells and migratory antigen-presenting cells. *Immunity* 37:1076-1090.

VITA

The author, Grant Steven Jones, received elementary and secondary education in Henderson, Kentucky, graduating from Henderson County Senior High School May 2008. He entered the University of Kentucky August 2008, and was awarded a Bachelor of Science in Biology with Departmental Honors and a Minor in Music Performance in May 2012.

He was accepted into the Integrated Biomedical Sciences program in the College of Medicine at the University of Kentucky August 2012, and joined the laboratory of Dr. Sarah D'Orazio in the Department of Microbiology, Immunology, & Molecular Genetics to complete his doctoral training.

He served as student representative in the Microbiology Educational Policies and Practices Committee from June 2015 to October 2016, as well as on student committees that organize the departmental retreat from 2014-2017. Throughout his training as a graduate student he has been awarded first place in a three-minute thesis competition and travel awards at two different scientific conferences.

He is an author on the following peer-reviewed publications: Bou Ghanem et al. (2012) PLoS Pathogens; Jones, G.S. and D'Orazio, S.E.F. (2013) Current Protocols in Microbiology; Bou Ghanem et al. (2013) Journal of Visualized Experiments; Jutras et al (2013) Journal of Bacteriology; Jones et al. (2015). Infection and Immunity; and Jones et al. (2017) Journal of Immunology.